FACULDADE DE ENGENHARIA DA UNIVERSIDADE DO PORTO
Departamento de Engenharia Electrotécnica e de Computadores

Topology Aware Channel Assignment in Single-radio Stub Wireless Mesh Networks

Tânia Cláudia dos Santos Pinto Calçada

Dissertação submetida para satisfação parcial dos
requisitos do grau de doutor
em
Engenharia Electrotécnica e de Computadores

Dissertação realizada sob a supervisão do
Professor Doutor Manuel Alberto Pereira Ricardo,
do Departamento de Engenharia Electrotécnica e de Computadores
da Faculdade de Engenharia da Universidade do Porto

Porto, Agosto de 2012

Abstract

Stub Wireless Mesh Networks (WMN) are multi-hop networks composed by wireless routers and connected to an infra-structured network through a set of gateway nodes. Stub WMN have multiple applications such as extending Internet coverage, providing last mile smart grid networks, or deploying wireless infrastructure for surveillance purposes. These applications of WMN have different requirements regarding throughput, delay and equipment costs. If the cost of the equipment is a relevant requirement, the number of wireless interface cards may have to be limited to assist the reduction of the cost, however, the capacity of the network must be addressed. Radio interference causes a reduction of the WMN capacity and of its performance but the usage of multiple channels may help mitigating this problem.

This work addresses the problem of channel assignment in stub WMN using the CSMA/CA access method and formed by multiple gateways, and by nodes having a single radio interface available to form the WMN. The problem consists in centrally deciding in which channel each WMN node shall operate so that the WMN becomes connected and the network performance is optimal. We argue that the problem can be solved by using solely the network topology information, instead of using also traffic information as done by state of the art works. In order to prove this claim a large set of experiments were conducted involving the simulation of thousands of network topologies.

The main contribution of this thesis is a centralized joint routing and channel assignment algorithm for single-radio WMN (TILIA) used to improve the performance of single-radio WMN using multiple channels. We improve the performance of multi-channel WMN by controlling solely the channel in which each node operates. This performance gain is obtained by enhancing the gateway neighborhood, in particular by increasing its size and avoiding hidden nodes on links around the gateway, while keeping the load balanced between channels. TILIA uses a breadth-first tree growing technique but, instead of growing a single tree, TILIA grows a forest of trees each of which rooted at a different gateway and operating on a different radio channel.

Resumo

As *stub WMN* são redes de múltiplos saltos compostas por *routers* sem fios ligados a uma rede infraestruturada através de um conjunto de portais. As *stub WMN* têm várias aplicações, tais como a extensão de cobertura da Internet sem fios, a parte de acesso de redes elétricas inteligentes, ou infraestrutura sem fios para sistemas de vigilância. Estas aplicações para *stub WMN* têm diferentes requisitos no que toca a custos de equipamento, tempos de resposta e débitos suportados. Se o custo do equipamento for requisito relevante, o número de interfaces de rede sem fios poderá ser limitado para promover a redução de custos, mesmo assim, a capacidade da rede deve ser considerada. As rádio-interferências provocam uma redução da capacidade e do desempenho das *stub WMN*, mas o uso de múltiplos canais rádio pode ajudar a atenuar este problema.

Este trabalho aborda o problema da atribuição de canais em *stub WMN* que utilizam CSMA/CA como método de acesso e que são formadas por vários portais e por nós dispondo de apenas uma interface de rede sem fios para formar a *stub WMN*. O problema consiste em decidir centralmente em que canal rádio deve funcionar cada nó da rede de modo a que a *stub WMN* se mantenha ligada e que tenha um desempenho ótimo. Defendemos que o problema pode ser resolvido usando apenas as informações de topologia de rede, em vez de usar também as informações de tráfego como tem sido feito por trabalhos existentes no estado da arte. Para provar esta afirmação foi realizado um grande conjunto de experiências envolvendo a simulação de milhares de topologias de rede.

A principal contribuição desta tese é um algoritmo centralizado de estabelecimento de rotas e de atribuição de canais rádio para *stub WMN* (TILIA) destinado a melhorar o desempenho das *stub WMN* que usam múltiplos canais e uma única interface de rede sem fios em cada nó. Melhoramos o desempenho das *stub WMN* controlando apenas o canal em que cada nó opera. Este ganho no desempenho é obtido através do melhoramento da vizinhança dos portais, em particular através do aumento do número de nós nessa vizinhança e evitando nós escondidos nas ligações em torno dos portais, enquanto se mantém a carga equilibrada entre os canais. O TILIA usa a técnica de procura em largura para formação de árvores em grafos mas em vez de formar uma única árvore, o TILIA forma uma floresta de árvores enraizadas em cada um dos portais e funcionando em diferentes canais rádio.

Acknowledgements

First and foremost I would like to than my advisor Prof. Manuel Ricardo. I has been an honor be his student. I appreciate all his contributions of time, ideas, and funding to make my work productive and stimulating. The joy and enthusiasm he has for research was contagious and motivational for me, even during tough times in the PhD pursuit. Throughout all the difficulties I had, Prof. Manuel Ricardo was always understanding and guided me with patience, humanity, kindness and wisdom.

I am also thankful to INESC TEC, where I have been extremely lucky to reside for the past nine years and interact with such brilliant and insightful researchers. I truly enjoyed working with many people at INESC TEC and I would like to thank them for their support and friendship and also for the interesting discussions we had about so many different topics and in particular about the work in this dissertation (in alphabetical order): Ana Viana, António Pinto, Bruno Marques, Carlos Pinho, Fernando Pereira, Filipe Abrantes, Filipe Ribeiro, Filipe Sousa, Filipe Teixeira, Gustavo Carneiro, Gustavo Martins, Helder Fontes, Hermes del Monego, Jaime Cardoso, Jaime Dias, Mohammad Abdellatif, Jorge Mamede, Prof. José Ruela, Nuno Salta ("requiescat in pace"), Paula Viana, Pedro Fortuna, Pedro Pinto, Pedro Silva, Renata Rodrigues, Ricardo Duarte, Ricardo Morla, Rui Campos, Saravanan Kandasamy. Apologies to anyone I forget.

Thanks to Faculdade de Engenharia da Universidade do Porto for providing excellent education and accepting me as student. This work was funded by the Portuguese government through Fundação para a Ciência e Tecnologia grant SFRH / BD/13444/2003 and by SitMe project from QREN–ON.2 program.

On a more personal note, I would like to leave a warm word of thanks to my family and friends for their encouragement and moral support. To my mother, Filomena, for her patience and wisdom, and for being my foundation stone; to my father and grand parents for all their love; they transmitted to me the love of learning. To my sister Safira for her love, admiration and support. To my parents-in-law for their readiness and support.

My beloved husband, Victor Calçada, and my wonderful children Maria, Sofia and Miguel deserve very special loving words, for being such incredible and kind human beings, who stood by my side and coped with my moody behavior during the writing of my thesis in the last months and suffering with those absences during the weekends and evenings of the last year. This journey would have been much harder without them in my life.

Tânia Pinto Calçada

"Life is like riding a bicycle.
To keep your balance you must keep moving."
Albert Einstein

Contents

List of Figures

List of Tables

Chapter 1

Introduction

This thesis is framed in the general field of wireless networks, in particular those networks operating based on the IEEE 802.11 standard [1]. With the fast growth of the Internet and the increasing demand for network connectivity anywhere and anytime, wireless access networks based on the IEEE 802.11 standard are assuming a prominent role. IEEE 802.11 access points are being massively deployed around the world in organization buildings, cities, homes, and vehicles, as a mean to provide wireless Internet access to people using laptops, mobile phones, and to other devices such as smart meters, vehicles, cameras, sensors, or industrial equipment. However, IEEE 802.11 has a limited radio range. The coverage of large geographical areas with this technology can only be achieved by deploying a large number of Access Points (APs). If wires are used to connect the APs to the infrastructure, the deployment of large IEEE 802.11 networks can be expensive and complex and, in some cases, it can even be impossible to execute due to the construction works required.

Wireless Mesh Networks (WMN) is one of the key technologies that will dominate wireless networking in the next decade [2]. WMN will help to realize the Always Best Connected [3] concept with simplicity and low cost. Their wireless multi-hop nature and their capability for self-organization significantly reduces the complexity of network deployment and maintenance and helps reducing the

operational costs. The multi-hop term refers to the fact that data from a source needs to travel through several other intermediate nodes, via wireless links, before it reaches the destination. There are multiple definitions of WMNs. For R. Bruno et al. in [4], WMN are built on a mix of fixed and mobile nodes interconnected via wireless links to form a multi-hop ad hoc network that extends wired infra-structured networks, coexisting with them. For Akyildiz et al. [2], a WMN consists of mesh routers and mesh clients, where mesh routers have minimal mobility and form the backbone of WMNs that provides network access for both mesh and conventional clients. In this thesis, a WMN is assumed to be a stub WMN which is composed by a set of fixed wireless routers multi-hop connected to each other, and some of these wireless routers are also wired connected to the infra-structured network acting as gateway nodes.

Early WMNs can be traced back to the DARPA Packet Radio Network (PRNet) project in 1972 [5] and to Mobile Ad-hoc Networks (MANETs) [6]. After almost a decade of research into ad hoc networking, MANET technology had not yet affected the way of using wireless networks because most of the ongoing research on mobile ad hoc networks was driven by either Departments of Defense requirements (large-scale military applications with thousands of ad hoc nodes) or specialized civilian applications (disaster recovery, planetary exploration, etc) [4]. To turn MANETs into a commodity, some changes to the original MANET definition were required. By relaxing one of the main constraints of MANETs, "the network is made of user's devices only and no infrastructure exists," the research community moved to a more pragmatic "opportunistic ad hoc networking" in which multi-hop ad hoc networks are not isolated self-configured networks, but rather emerge as a flexible and low-cost extension of wired infrastructure networks, coexisting with them [7, 8, 9]. WMNs are the new class of networks that emerged from this view in the early years of the 21 century [10].

Current research challenges on WMNs address all the layers of the communications stack and study the critical factors of WMN design including the following [2] : (1) to improve the WMN capacity using novel radio techniques on the physical layer or through cross-layer solutions that explore the existence of multiple channels;

(2) to improve the scalability of WMNs by redesigning scalable protocols from the Medium Access Control (MAC) to the application layers; (3) to provide security on WMNs by adapting existing security schemes designed for single hop or for ad-hoc networks; (4) to integrate WMNs with existing networks by supporting legacy nodes and providing network management using new tools that easy their deployment and maintenance.

WMN have a wide range of applications [2]: broadband home networking, community and neighborhood networking, enterprise networking, metropolitan area networks, transportation systems, building automation, health and medical systems, security surveillance systems, spontaneous (Emergency and Disaster) networking, and P2P communications. These applications have different constraints regarding costs, capacity, reliability, security, ease of use, and interoperability with legacy systems.

1.1 Problem characterization

1.1.1 Motivation

This work addresses three scenarios where WMN can be used: extend the Internet coverage, form the last mile of smart grid networks, and form the last mile of surveillance systems. In these scenarios, there are a set of gateways connected with wires to a infra-structured network, a set of WMN nodes that connect to the gateways through multiple wireless links, and a set of devices that are receiving or generating data flows towards the infra-structured network and that are connected to the WMN nodes through a single hop.

Internet coverage extension to areas where infra-structured connections to IEEE 802.11 access points are difficult to deploy or expensive. When providing coverage to homes or to rural areas on developing countries, the deployment cost is a relevant constraint and a low cost solution should be envisioned. WMNs can be used to achieve this goal as represented in Fig. 1.1 which is similar to the scenario addressed by IEEE 802.11s [1]. In this scenario, WMN nodes named Mesh Access Points (MAPs) are expected to have two

wireless cards with independent radio interfaces running the standard MAC 802.11 protocol. One radio interface operates as an access point giving Internet access to end-users which may be people or smart objects; the other radio interface is used to interconnect the MAP to others MAPs in order to form a multi-hop wireless network. WMNs connect to the infra-structured wire network via special nodes acting as gateways to the Internet.

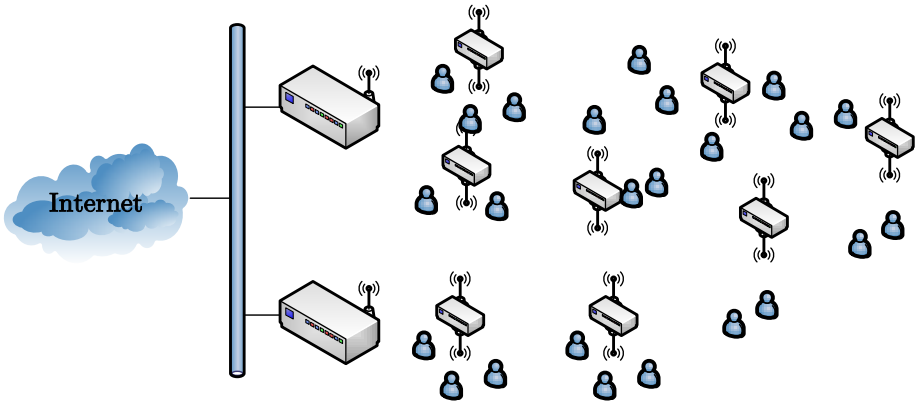

Figure 1.1: WMN scenario deployed to extend Internet access.

Last mile smart grid networks aim to connect thousands of smart meters installed in homes and business places to a distribution point of gas, electrical energy or watter suppliers. In order to provide national wide deployment, thousands of distribution points must be equipped and, therefore, a low cost solution should be envisioned. WMNs can be used to meet this goal as represented in Fig. 1.2. In this scenario WMN nodes are expected to have two wireless cards with independent radio interfaces running the standard MAC 802.11 protocol. One radio interface operates as an access point to connect the smart meters to the smart grid. The second radio interface is used to interconnect the WMN node to other WMN nodes in order to form a multi-hop wireless network. Special nodes located at the supplier distribution points act as gateways to connect the WMN to the supplier infrastructure.

Last mile surveillance systems aim to connect hundreds of cameras or other sensors installed in buildings or parking lots to the security office. The usage of wires on this scenario can be costly

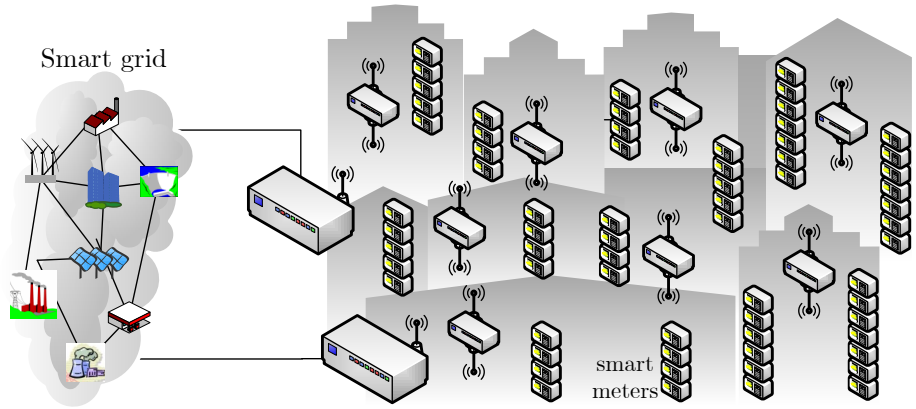

Figure 1.2: WMN used as the last mile of smart grid networks.

and complex. WMNs can be used to achieve this goal as represented in Fig. 1.3. In this scenario, WMN nodes are expected to have attached a couple of cameras and one radio interface card running the standard MAC 802.11 protocol. Each WMN node connects to other WMN nodes on the neighborhood through the radio card, forming a multi-hop network. It is assumed that this WMN is connected to multiple gateways which are aggregation points located at each corridor, hall, or floor wired connected to the security office.

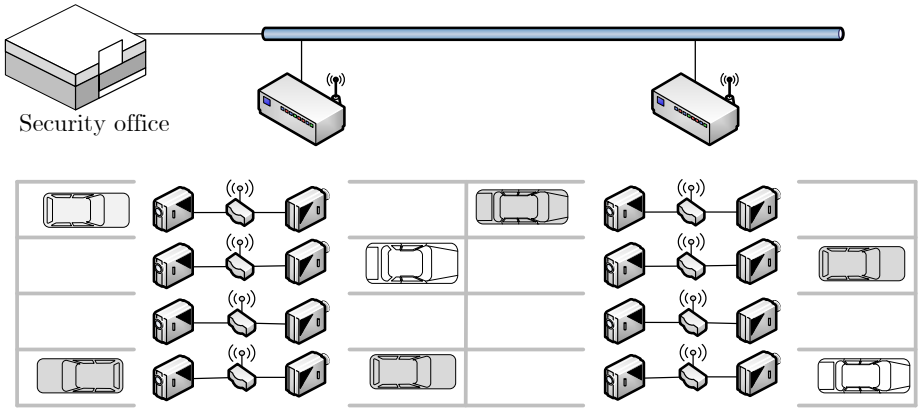

Figure 1.3: WMN used as the last mile of surveillance systems.

The three scenarios highlighted above have two main constraints in common: the demand for broadband which must be distributed fairly to all the nodes involved, and the low cost of the WMN node.

The demand for fair broadband is obvious on the Internet coverage extension scenario. In this case, the number of users accessing the Internet through each gateway is assumed to be around a few tens as in the mesh networks defined by the IEEE 802.11s standard

[1]. On the smart grid scenario, despite the low data rates required by each smart meter, the broadband capacity of the WMN becomes an issue due to the large number of smart meters connected to each WMN node. In this scenario, small delays may also become a critical constraint in order to allow real time actions. On the surveillance scenario the video cameras generate large amounts of data which need to be delivered to the gateways.

The low cost constraint comes from the low budget assumed on the Internet coverage extension scenario, and from the huge number of equipments assumed for the smart grids and surveillance scenarios. In order to meet the MAP equipment low cost constraint, three characteristics are assumed: (1) the number of wireless interface cards on each WMN node available to connect to other WMN nodes is limited to one turning the scenarios into a single-radio WMN; (2) the wireless interface cards are standard equipment and therefore modifications to their hardware or firmware are not welcome; (3) the memory and processing capabilities of WMNs nodes are low, therefore a centralized approach to meet the broadband constraint is preferable.

1.1.2 Problem description

This work addresses the problem of channel assignment in stub WMN formed by multiple gateways and mesh nodes using a single radio interface to communicate with other mesh nodes. **The problem consists in centrally deciding the channel each WMN node shall operate so that the WMN becomes connected and the network performance is optimal.**

Network capacity increases with the number of channels in use [11, 12] for the particular case of WMNs. As the number of active nodes in a wireless network increases, the number of frames that can be transmitted by each node falls down since these nodes are sharing a common wireless medium of finite capacity [13].

Centralized approaches are a natural solution for stub WMNs, where there are gateways that can be used as a central entity. Moreover, centralized approaches may be more efficient, easier to upgrade, and contribute to the low cost of WMN nodes.

1.1.3 Related work

The objective of most of the channel assignment strategies for WMNs studied in the past few years [14, 15] was to minimize the overall network interference which is calculated based on topology and traffic information. Most of the approaches address the scenario of WMNs with multi-radio nodes [16, 17, 18] which are not suitable for the single-radio scenario we aim to address. The single-radio approaches found can be classified as dynamic or static. Dynamic approaches are mostly MAC layer protocols that stand on channel switching [19, 20, 21] which are difficult to implement with currently deployed 802.11 hardware. The static approaches found are three: (1) a distributed routing protocol [22] that uses traffic information to balance the load between channels disregarding the reduction of interference, (2) a centralized tree-based multi-channel scheme [23] designed for data collection applications in dense wireless sensor networks that assumes the existence of a single gateway, and (3) a couple of algorithms [24] designed to realize a component based channel assignment strategy that do not address stub networks.

1.2 Thesis

Our thesis is that by assigning channels to WMN nodes using solely the network topology information, it is possible to improve the performance of stub WMN that use the CSMA/CA access method and are formed by single radio interface nodes.

1.2.1 Main contribuitions

The main contribution of this thesis is the Topology aware Algorithm for Channel Assignment on Single-radio Stub WMN (TILIA). TILIA is a centralized joint routing and channel assignment algorithm used to improve the performance of a multi-channel WMN by controlling solely the channel in which each node operates. TILIA enhances the gateways neighborhood by increasing their size and avoiding hidden nodes on links around the gateways, while keeping the load balanced between channels. TILIA uses a breadth-first tree growing

technique but, instead of growing a single tree, TILIA grows a forest of trees each of which rooted at a different gateway and operating on a different radio channel; all the trees grow simultaneously and their union spans the network. Experimental evaluations based in ns-2 simulations show that the gains of TILIA are visible on packet loss, HTML page loss, and packet delay, respectively with gains of 45%, 33%, and 29% when compared with a state-of-the-art proposal [22], and with gains of 88%, 69% and 72% when compared with random channel assignment.

The second contribution of this thesis is the composed topology metric *tmet* used to select the forest with best topology characteristics. The accuracy of the proposed topology metric is over 94%.

The third contribution of this thesis is the identification and ranking of topology metrics. In order to prove that the performance of the WMN depends of its topology characteristics, firstly it is essential to identify the relevant topology characteristics and the metrics that better describe them. Secondly, it is fundamental to rank the impact that the network topology characteristics have on the performance of a WMN. We believe we have been able to propose a meaningful set of metrics and rank them.

1.2.2 Publications related to the thesis

This research work resulted in a set publications which are listed below by order of relevance.

i Tânia Calçada and Manuel Ricardo. Topology Aware Channel Assignment for Single-radio Stub WMN. Submitted to *IEEE Transactions on Mobile Computing*, July 2012. [25]

ii Tânia Calçada and Manuel Ricardo. Characterization of network topology impact on the performance single-radio wireless mesh networks. Accepted in *Telecommunication Systems*, July 2012. [26]

iii Tânia Calçada, Paulo Cortez, and Manuel Ricardo. Using data mining to study the impact of topology characteristics on the performance of wireless mesh networks. In *IEEE Wireless Communications and Networking Conference (WCNC'12)*, Paris, France, April 2012. [27]

iv Tânia Calçada and Manuel Ricardo. The impact of network topology on the performance of multi-channel single-radio mesh networks. In *Proceedings of the Networking and Electronic Commerce Research Conference (NAEC'11)*, Riva del Garda, Italy, October 2011. [28]

v Filipe Teixeira, Tânia Calçada, and Manuel Ricardo. Protocol for channel assignment in single-radio mesh networks. In *Proceedings of the Conference on Mobile Networks and Management (MONAMI'11)*, Aveiro, Portugal, September 2011 [29, 30]

vi Filipe Teixeira, Tânia Calçada and Manuel Ricardo. Single-radio Stub Wireless Mesh Networks - Architecture for a Channel Assignment Subsystem. In *Proceedings of the Networking and Electronic Commerce Research Conference (NAEC'12)*, Riva del Garda, Italy, October 2012. [31]

vii Tania Calçada and Manuel Ricardo. Extending the coverage of a 4G telecom network using hybrid ad-hoc networks: a case study. *Proceedings of the Mediterranean Ad Hoc Networking Workshop*, 2005. and also in *International Federation for Information Processing Digital Library; Challenges in Ad Hoc Networking*, 2006. [7, 8]

viii Susana Sargento, Tânia Calçada, João P. Barraca, Sérgio Crisóstomo, João Girão, M Natkaniec, Norber Vicari, Francisco Galera, Manuel Ricardo, and A. Glowacz. Mobile ad-hoc networks integration in the daidalos architecture. In *Proceedings of the IST Mobile & Wireless Communications Summit*, Dresden, Germany, June 2005. [9]

The research work conducted in this PhD had two main parts. In the first part we addressed the problem of integrating the ad-hoc networks with infra-structured networks. This subject was of great relevance when the beyond 3G networks were discussed. In [7] (publication vii) we proposed a solution to integrate a gateway discovery protocol with an ad-hoc network based on the AODV [32] protocol. Our work, described in [9] (publication viii), is the integration of ad-hoc networks into the general network architecture developed in the IST Daidalos project. Our contribution to this architecture was an efficient unicast routing and mobility mechanism capable of enabling the mobility of users inside and between ad-hoc networks.

In the second part of the PhD research work we addressed the problem of improving the capacity of stub WMNs consisting of nodes equipped with a single radio standard 802.11 interface, by statically assigning channels to nodes. This problem was firstly raised by the early drafts of IEEE 802.11s [33] which did not include multi channel specification. We posed the hypothesis of using solely the topology information about the WMN to solve the problem, instead of using also traffic information as done by state of the art works. To prove this hypothesis we conducted an extended set of experiments in which we simulated thousands of different network topologies. The first experiments, on a set of 18 arbitrary network topologies, were reported in [28] (publication iv) and then detailed in [26] (publication ii). This first study was essential to identify which topology characteristics have impact on the WMNs performance. The quantification of the impact that a given topology metric has on the WMNs performance was published in [27] (publication iii); these results were obtained using data mining techniques applied to the simulation results of 7000 random network topologies. The results of this work gave us confidence to move forward and to formalize the channel assignment problem using solely the WMN topology information. As this problem was shown to be NP-hard, an algorithm was designed, implemented and evaluated, being the results are reported in [25] (publication i). In [29] (publication v) we presented results of research conducted on a real testbed; with the proposed protocol, we proved that (1) it was possible to efficiently gather the topology information of a WMN in which nodes may be operating in different radio channels, and (2) it is possible to reconfigure the radio channel of WMN nodes according to decisions taken centrally by a network manager. The work in [31] (publication vi) proposes an architecture to integrate the protocol proposed in [29] (publication v) and the TILIA algorithm [27].

1.3 Outline of the dissertation

This dissertation is organized in 6 chapters. Chapter 2 presents the state-of-the art on the IEEE 802.11 MAC, the capacity of WMNs,

the interference models, the solutions for multi-channel WMNs, and the approaches that relate topology characteristics and network performance. Chapter 3 identifies the set of topology characteristics that have impact on the WMNs performance. Chapter 4 evaluates the impact of these characteristics on the network performance using data mining techniques. Chapter 5 formulates formally the channel assignment problem and presents and evaluates an algorithm to solve the problem. Finally, Chapter 6 draws the main conclusions and discusses future work.

Chapter 2

Wireless networks based on CSMA/CA

This chapter introduces existing work related to CSMA/CA based wireless networks. In the first part of the chapter (Section 2.1, Section 2.2, and Section 2.3) we describe the operation of the medium access control protocols of the IEEE 802.11 standard focusing on the CSMA/CA; we also identify the studies that establish the boundaries of capacity of WMNs and the interference models that are used in these studies. In the second part of the chapter (Section 2.4), we present a survey of existing channel assignment methods, particularly those addressing single-radio WMNs; we classify these methods according to their requirements and mode of operation. In the third part of the chapter (Section 2.5), we present a survey that characterizes the relevant topology characteristics of WMNs that can be related to the network performance. Section 2.6 summarizes the chapter.

2.1 IEEE 802.11 medium access control protocols

A wireless channel is a broadcast medium. When a node transmits a packet onto the radio channel, the packet reaches all the nodes in the

transmission range of the sender. If a node receives multiple packets on the same channel at the same time, it cannot properly decode the packets because of interference. In this case, we say that packets have "collided" at the receiver. The major goal of wireless MAC is to ensure that when a node is transmitting, all other interfering nodes are silent.

IEEE 802.11 specifies two MAC protocols: the Point Coordination Function (PCF) and the Distributed Coordination Function (DCF) [1]. PCF can only work in infra-structured networks. DCF is the MAC protocol of interest for this work, and it is based on the Carrier Sense Multiple Access with Collision Avoidance (CSMA/CA) access method.

The basic idea of CSMA/CA to check whether the channel is busy or idle before transmitting a packet. A node implementing CSMA/CA listens to the channel and measures the signal level on the channel. The node transmits a packet only when the signal level on the channel is sufficiently low for a given time duration, implicitly assuming that no other transmission is taking place in the region. CSMA/CA blocks a node from initiating a transmission if another nearby node is transmitting and in its basic form it does not address the well-known hidden terminal problem. Consider the scenario in Figure 2.1(a). When node A is transmitting a packet to node B, node C may not sense the channel as busy. Thus, node C can start transmitting a packet, which results in a collision at node B as shown in Figure 2.1(b)

The hidden terminal problem can be particially avoided by let a node reserving the channel before transmitting a packet. This 4-way handshake mechanism is illustrated in Figure 2.2 where a station can reserve the medium for a period of time using the control frames RTS (Request-To-Send), CTS (Clear-To-Send). In topology of Figure 2.1(a), suppose node A has a packet to send to B. Before transmitting the data packet, node A sends RTS to B, which contains the duration of time node A needs to reserve. When node B receives RTS, it replies back by sending a CTS packet, which also includes the duration of time the channel needs to be reserved. All other nodes that receive RTS or CTS defer transmission for the duration specified in the packets. Each node maintains the Network

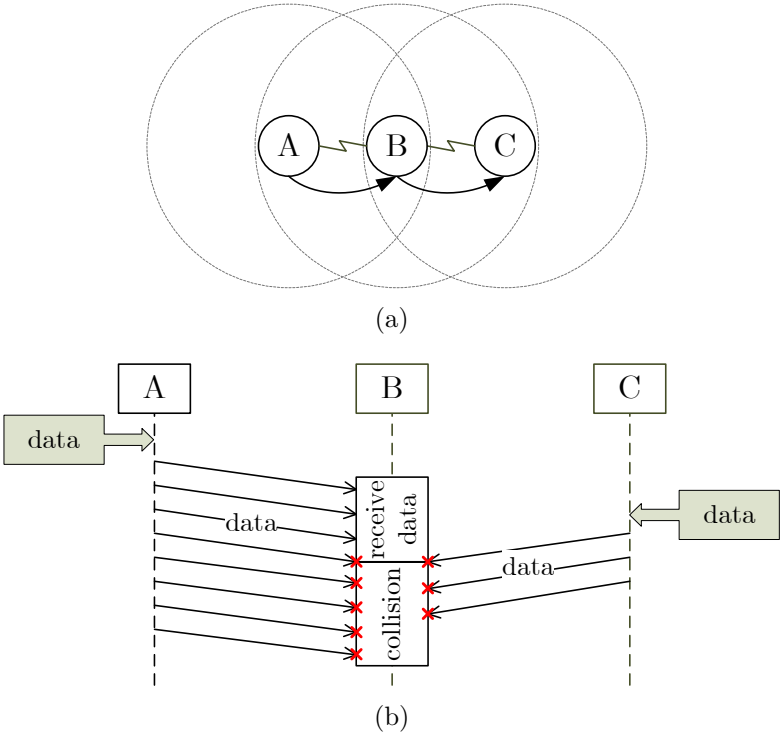

Figure 2.1: The hidden terminal problem. (a) Topology consisting of tree nodes. (b) The time sequence leading to a collision.

Allocation Vector (NAV) variable, which records the duration of time the node must defer its transmission. When node C receives CTS from B, it sets up its NAV according to the duration specified in the CTS packet. After exchanging RTS and CTS, node A sends the data frame to node B, and B replies with ACK (Acknowledgement) packet so that node A knows the packet has been successfully received at node B.

The effectiveness of the 4-way handshake mechanism is based on the assumption that hidden nodes are within transmission range of receivers. Xu et al. in [34] prove using analytic models that in multi-hop networks, such an assumption cannot hold due to the fact that power needed for interrupting a packet reception is much lower than that of delivering a packet successfully. Thus, the "virtual carrier sensing" implemented by 4-way handshake mechanism cannot prevent all interference as we expect in theory. Physical carrier sensing can complement this in some degree. However, since interference happens at receivers, while physical carrier sensing is detecting transmitters, physical carrier sensing cannot help much,

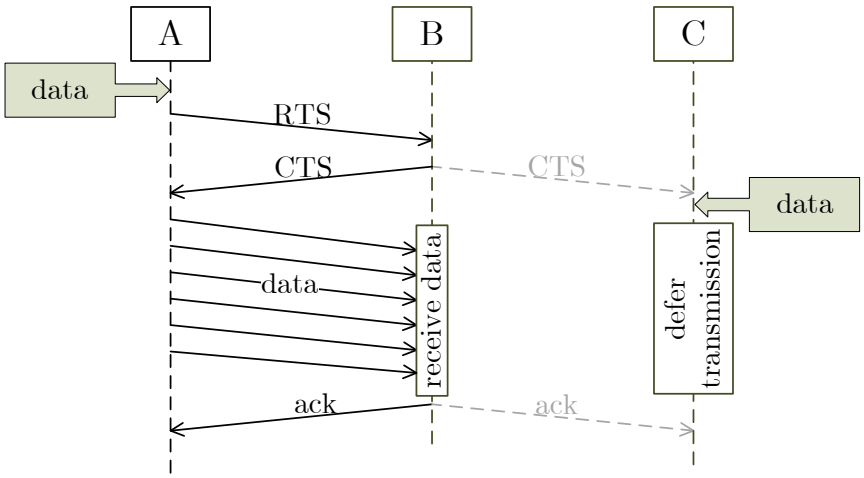

Figure 2.2: Time sequence diagram of the 4-way handshaking mechanism of DCF.

unless a very large carrier sensing range is adopted. Similar conclusions were found in [35] using simulation experiments.

2.2 Capacity of wireless networks

2.2.1 General multi-hop wireless networks

Gupta and Kumar studied the asymptotic transport capacity in general wireless multi-hop networks [13]. This analysis is based on the assumptions that communications are one-to-one within the wireless network, and sources and destinations are randomly or arbitrarily (optimally) chosen. They show that, if the nodes are randomly placed and the destinations are randomly chosen, then the achievable throughput per node is bounded by $\Theta\left(W/\sqrt{nlog(n)}\right)$, where W is the transmission capacity, n is the number of nodes in the network and Θ represents the asymptotic notation[1]. They also provide results for arbitrary (optimal) node placement and communication patterns. In this case, the achievable per node throughput become $\Theta\left(W/\sqrt{n}\right)$.

Grossglauser et al. [36] extend the work of Gupta and Kumar [13] and show that the capacity can be improved by the mobility of the nodes which can reduce the number of hops between the

[1] $f(n) \in \Theta(g(n)) : f$ is bounded both above and below by g asymptotically

source and the destination and in turn reduce the contention in the network.

Further improvements on the obtained capacity bounds can be obtained by introducing relay nodes which do not generate traffic but act as routers to deliver data to the destination as shown by Gastpar et al. [37]. In these configurations, when the number of nodes goes to infinity, a network throughput of $O(\log n)$ can be obtained, where O represents the asymptotic notation[2].

2.2.2 Stub wireless mesh networks

Different from traditional ad-hoc network, nodes in stub WMN forward their traffic to gateways, creating hot-spots at gateways. Jun and Sichitiu [38] show that available throughput increases with increase in number of network gateways while available capacity at each node is as low as $O(1/n)$. Per-node throughput of $O(1/n)$ is also achievable in WLANs but it is empirically observed that WMNs achieve a throughput which is often lesser than WLANs. The analysis in [38] is not limited to a specific MAC, but the result can be applied to IEEE 802.11. The concept of bottleneck collision domain is introduced there by defining it as the geographical area of the network that enables an upper bound on the amount of data that can be transmitted in the network.

Pathak and Dutta [39] show that WMNs achieve per-node throughput of $O(1/\delta n)$ where δ is a factor dependent on hop-radius of the network and it converges to 3 for large WMNs. It is shown that in case of multiple gateways, increasing power levels of nodes is more cost-effective because it results into increased throughput with fewer number of gateways.

For arbitrary networks where node locations and traffic patterns can be controlled, each interface capable of selecting appropriate transmission power, Kyasanur and Vaidya [11] prove that there is a loss of network capacity when the number of interfaces per node is smaller than the number of channels. In random networks where, node locations and traffic patterns are random, it is shown that

[2] $f(n) \in O(g(n))$: f is bounded above by g (up to constant factor) asymptotically

one single interface is sufficient for utilizing multiple channels as long as the number of channels is scaled to $O(\log n)$ and each channel has bandwidth of W/c. Bhandari and Vaidya of [40] extend the work in [11] to multi-channel networks with channel switching constraints. They study connectivity and capacity of a wireless network comprising n randomly deployed nodes, equipped with a single interface each, when there are $c = O(\log n)$ channels of equal bandwidth W/c are available; it considers adjacent channel assignment and the random channel assignment. In adjacent assignment, a node may switch between f adjacent channels, but the adjacent channel block is randomly assigned; in such case, per-flow capacity of $\Theta\left(W\sqrt{\frac{f}{cn\log n}}\right)$ can be achieved. In random assignment, a node can switch between fixed random subset of f channels; in such case, per-flow capacity is $O\left(W\sqrt{\frac{P_{rnd}}{n\log n}}\right)$ and $\Omega\left(W\sqrt{\frac{f}{cn\log n}}\right)$, where $P_{rnd} = 1 - \prod_{i=0}^{f-1}\left(1 - \frac{f}{c-i}\right)$, and Ω represents the asymptotic notation[3].

Scenarios where traffic is mostly generated towards gateway nodes result in many-to-one communications. The capacity of wireless networks in many-to-one scenarios for the Wireless Sensor Networks (WSN) applications was studied by Duarte-Melo et al [41]. The trivial upper bound per node is presented as W/n which can be achieved when the gateway is 100% busy in receiving, equipped with a single radio and shared by n source nodes each of which generating the same amount of data. They further show the circumstances under which this bound is achievable. For instance it is achieved when all the sources can transmit directly to the gateway node. On the other hand, if each source cannot directly communicate with the gateway, such that the communication takes place on a multi-hop network, the upper ground may or may not be achieved depending on the transmission and interference ranges of the nodes. These ranges affect the reuse possibilities of the medium and the transmitting schedules.

[3] $f(n) \in \Omega(g(n)) : f$ is bounded below by g (up to constant factor) asymptotically

2.3 Interference models

One of the major challenges of improving the capacity of wireless networks is tractable yet realistic consideration of interference. Wireless medium is a shared, broadcast medium. When simultaneous transmissions are performed on the same channel in the same spatial domain, all the unwanted transmissions can be seen as interference. If the transmissions do not interfere with each other, simultaneous transmissions can take place. A collision occurs if the received signal is too weak compared to the interfering signals. The nature and impact of interference is unpredictable and challenges the design of wireless networks. Researchers have proposed several interference models. We discuss the most important ones.

Protocol interference model [13] defines that communication between nodes a and b results in collision-free data reception at node b if no other node within a certain interference range from b is transmitting simultaneously. This model has been further extended to consider link layer reliability using acknowledgments in which interference range of node a is also considered for interference. This is often referred as disk model (or double disk model) where interference is assumed to be a binary phenomena developed in certain fixed distance from the source and the destination of any active link. The Interference range of a node is often assumed to be a constant times larger than its communication range.

The advantage of the protocol interference model is that it enables the use of simple graph-coloring based scheduling algorithms. The performance of the protocol interference model is analyzed in [42]. This study indicates that the model does not always provide a comprehensive view of reality due to the aggregate effect of interference in wireless networks. The model can also be pessimistic in the sense that two nearby communications that could take place together with a tolerable level of interference are considered to be not possible. The real behavior of complete 802.11 DCF is captured in [43] where the

4-way handshake mechanism is considered but, its application results in NP hard problems.

Physical interference model [13] defines that communication between nodes a and b results in collision-free data reception at node b if SINR (Signal to Interference plus Noise Ratio) at node b is above a certain threshold β. If P_{ba} is the signal power received at node b from a, a packet from node a is successfully received at node b if and only if $\frac{P_{ba}}{N+\sum_{i\in I} P_{bi}} \geq \beta$, where I is a set of nodes simultaneously transmitting and N is the background noise.

Physical interference model is richer than the protocol model because it can capture the interference from multiple simultaneous senders, yet it introduces more complexity on the protocol design. The impact of the physical interference model on the achievable capacity in CSMA/CA based wireless multihop networks is studied in [44]. This study shows that wireless networks designed with the physical interference model can surpass theoretically achievable performance of solutions using the protocol interference model.

k-hop interference model [45] defines that no two links within k hops can successfully transmit at the same time. IEEE 802.11 DCF corresponds to a 2-hop interference model. For a given k, a throughput-optimal scheduler needs to solve a maximum weighted matching problem subject to the k-hop interference constraints. The authors [45] show that for $k > 1$, the resulting problems are NP-Hard and cannot be approximated within a factor that grows polynomially with the number of nodes

The above mentioned interference models can be further generalized by representing the interference relationship of links using a conflict graph. In a conflict graph, every link in the network is represented as a vertex and two vertex share an edge if and only if the corresponding edges interfere with each other. Depending on interference model, the resultant conflict graph can be undirected (protocol model or k-hop interference model) or directed (physical interference model).

2.4 Multi-channel WMNs

We consider to use multiple channels to reduce the effects of interference on the capacity of WMNs. The use of multi-channel communication in multi-hop networks is a research topic for over 30 years, particularly in PRNet [46, 47], in WMN [15, 48, 49, 50, 51] and in WSN [14, 52]. Kyasanur et al. [11] and Kodialam et al. [12], study the capacity of multi-channel WMNs by extending the analysis of Gupta and Kumar [13], that we discussed in Section 2.2. They investigate the impact of the number of channels and the number of radio interfaces on the network capacity by studying the relationship between them. They show that, even if the number of interfaces is smaller than the number of available channels, multi-channel communication can enhance the network's capacity.

The objective of most of the assignment strategies for WMNs studied in the past few years ([14, 15]) was to minimize the overall network interference which is calculated based on topology and traffic information. Most of the approaches address the scenario of WMNs with multi-radio nodes ([53, 16, 17, 18]) which are not suitable for the single-radio scenario we aim to address. In the next sub-sections, we survey the existing protocols on channel assignment and multi-channel MAC protocols for WMN focusing on the case of single-radio WMNs. We classify the protocols according to the channel assignment methods: static assignment and dynamic assignment. In dynamic approaches, nodes can dynamically switch their interfaces from one channel to another between successive data transmissions. Considering the operation principle of the coordination mechanisms, dynamic approaches for single-radio networks can be classified into Receiver-fixed [46, 20], Dedicated Control Channel [54, 55], Frequency Hopping [56, 57, 21, 58], and Split Phase [20, 19, 59, 60]. In static assignment approaches, channels are assigned to radios for permanent use on a per-flow [22, 23] or per-component basis [24].

2.4.1 Dynamic channel assignment

Considering the operation principle of the coordination mechanisms, dynamic approaches for single-radio networks can be classified into Receiver-fixed, Dedicated Control Channel, Frequency Hopping, and Split Phase. This classification is based on the classifications proposed in [14, 15, 61].

In the receiver-fixed protocols, a fixed quiescent channel is assigned to each node. When a node needs to send data, the sender changes its frequency and sends data on the quiescent channel of the destination node. If the receiver is idle, it is tuned on its quiescent channel and then the data is received. When all data is sent, the sender node changes back to its quiescent channel, being free to receive data from other nodes. [46, 20] are examples of this class of protocols. The main advantage of this approach is that it is very easy to implement as, before data exchange, this kind of protocol only needs to perform a very simple decision: which channel to change to. It is also compatible with 802.11. On the other hand, with semi-dynamic channel assignment approaches a detailed coordination of channel switching is required between the senders and receivers in order to be on the same channel at the same time. The problems that arise due to the channel switching are listed as follows:

Multi-channel hidden terminal problem: This problem [19] is associated with the CSMA/CA based protocols where RTS and CTS messages is used. It occurs when the control packets (RTS and CTS) sent on a given channel cannot be received by the nodes communicating on different channels. The nodes that miss the control packets, start transmission of control packets on the destination's channel which causes a collision.

Deafness problem: The deafness problem [20] is also associated with the RTS/CTS based protocols. The problem occurs when a transmitter sends a control packet to initiate a transmission and the destination is tuned to another channel. After sending multiple requests, if the transmitter does not get any response it may conclude that the receiver is not reachable.

Broadcast support: When the nodes are switching between channels dynamically, there might be problems to support broadcasts.

In a dedicated control channel protocol, one channel is reserved for transmitting control packets, isolating them from data packets which are transmitted in other channels. This approach has the advantage of being easy to implement. However, multi-channel hidden terminal problem is a problem. Besides that, a node must sense carriers on all channels, what leads to extra processing and complex decisions on the best channel to use. Another disadvantage is that it does not scale well. With the increase in number of nodes, the control channel can be saturated. Besides, the number of channels is limited. In 802.11b/g only three orthogonal channels can be used, which means that 33% of the total bandwidth is used in the control channel. [54, 55] are examples of this class of protocols.

In frequency hopping protocols, nodes hop between multiple narrow-band frequencies. The hopping patterns can be the same for all nodes or different. In this kind of protocol, if the hopping pattern is common, all nodes listen in the same frequency at the same time. If a node wants to transmit, it remains on that channel, while other nodes that want also to transmit use another available channel. When the transmission is finished, they change back to the initial frequency. If the hopping pattern is independent, time is divided in slots, having a different individual hopping sequence. This approach has the advantage of not having a dedicated channel for control frames. Besides, it does not introduce overhead to the RTS and CTS mechanism or channel negotiations before data transmission. The main disadvantage is that they require synchronization mechanisms. Switching delay may also be a problem and may be a reason for performance decrease. Besides, the presence of the multi-channel hidden terminal problem and the incompatibility with 802.11 standard are also disadvantages of this approach. [56, 57, 21, 58] are examples of this class of protocols.

Split phase protocols consider the division of time into cycles composed of two phases: the control phase and data phases. In the control phase, all nodes listen to a common channel and negotiate

a channel to use for data exchange. When the control phase ends, data phase begins and nodes exchange data in the channel negotiated. Split protocols can be subdivided into carrier-sense-based protocols and TDMA-based protocols. [20, 19, 59, 60] are examples of this class of protocols. The multi-channel hidden terminal problem is less severe in split phase protocols. Another advantage is that the channel bottleneck problem is eliminated, with all channels being used for data transfer. Despite these advantages, fine synchronization between nodes is needed. The proper duration of both phases, which is hard to compute, and the performance decrease due to channel switching are the main disadvantages of this protocol. Moreover, carrier sense must be done on all channels simultaneously, which may also be a problem.

2.4.2 Static channel assignment

Although the assignment of the channels can be renewed, for instance due to the change of interference or topological conditions, radios do not change the operating frequency during communication. When compared with dynamic approaches, static assignment solutions present some advantages such as (i) simplicity of implementation, (ii) no changes to the off-the-shelf radio hardware or MAC algorithms, (iii) no synchronization requirements, (iv) no channel scheduling overheads, (v) and no switching between channels to serve data flows. The static approaches fit the scenarios addressed in our work, therefore we detail them below.

2.4.2.1 Load Balancing Multi Channel Protocol (LB-MCP)

The LB-MCP presented in [22] aims to increase the network performance by reducing the load in each sub-network which is achieved by reducing the active path length. This protocol is able to balance load among channels, while maintaining connectivity. The protocol discovers multiple routes to multiple APs, possibly operating on different channels. Based on traffic load information, each node selects the best route to an AP, and synchronizes its channel with the AP

.

The authors assume that a node may have multiple routes to the AP, only one route is used at any given time, and other routes are maintained for backup so that they can be used when the primary route fails. The primary routes of nodes associated with the same AP form a route tree, rooted at the AP. They also assume that most of the traffic is downlink traffic, sent from AP to mobile hosts. The proposed protocol supports uplink traffic as well, but the load estimation is based on the downlink traffic. They assume that APs are placed dense enough that most routes are short in terms of number of hops, such as 3 or 4 hops. Finally, they assume that as in single-hop infra-structured networks, neighboring APs are typically assigned different channels. So it is unlikely that a node finds short routes to two different APs that are on the same channel.

Each AP remembers the amount of traffic it has received during past T seconds. Only packets from the wired network to nodes on the route tree rooted at that AP are counted as traffic. Since the AP knows the destination, it records the amount of traffic per destination. The load is estimated using AP-measured weighted load, which considers the distance of a node to the AP, the node's traffic and node's children traffic. The weighted load metric indicates that the load for each destination should be weighted by the number of hops from the AP to the destination node. So the weighted load of the route tree $L = \sum_{i \in V} (h_i \times l_i)$, where V is the set of nodes the route tree rooted at the AP, h_i is the number of hops, from the AP to the node i, and l_i is the amount of traffic destined for the node i. The load information is then broadcasted by the AP hop-by-hop through all nodes in its route tree. Nodes also forward this information to their neighbors that are operating in other channels.

Once the necessary load information is obtained, nodes can decide whether to switch to other route trees. To make the decision, a node should obtain load information on its own route tree, other route trees, and the amount of traffic destined for the node itself and nodes in its subtree. A node compares the current load of its route tree and the load of the other tree after the node joins. Since a node may have children in the route tree, it cannot just switch channels to join other trees, because the child nodes will lose connections with the AP. Instead, if the node decides to switch channels, it should

tell all its children to switch channels as well. Effectively, the whole subtree moves to the new route tree. So the load information on the new route tree should be computed correspondingly.

A node switches channel when its current channel utilization is higher than on another channel disregarding the reduction of interference in the new channel. We believe that the network performance may be improved when avoiding interference.

2.4.2.2 Tree-based Multi-Channel Protocol (TMCP)

TMCP [23] is a tree-based multi-channel medium access protocol designed specifically for data collection applications in WSNs. The idea of TMCP protocol is to partition the whole network into multiple vertex-disjoint subtrees all rooted at a common gateway, allocate different channels to each subtree, and then forward each flow along its corresponding subtree. The authors assume that the network has a single gateway equipped with multiple radio transceivers, each of which works on one different channel, because of the tree-based channel assignment strategy. TMCP has three components, channel detection (CD), channel assignment (CA), and data communication (DC). The CD module finds available orthogonal channels which can be used in the current environment. To do this, two nodes are used to sample the link quality of each channel by transmitting packets to each other, and then among all channels with good link qualities, non-adjacent channels are selected. Assume that k represents the number of non-adjacent channels selected. Given k orthogonal channels, the CA module partitions the whole network into k subtrees and assigns one unique channel to each subtree. This is the key part of TMCP. The goal of partitioning is to decrease potential interference as much as possible. After assigning channels, the DC component manages the data collection through each subtree. When a node wants to send information to the base station, it just uploads packets along the subtree it belongs to. The authors assume that the network has a single gateway equipped with multiple radio transceivers therefore this solution does not apply to our scenario.

2.4.2.3 Component based channel assignment

The approach used in [24] increases throughput by reducing number of contending flows on a channel, which is achieved by reducing the node density; first it determines the sets of nodes belonging to intersecting flows, and then different channels are assigned to sets of contending nodes. However, reducing contention as in [24] makes the network less connected and more susceptible to the occurrence of collisions caused by hidden nodes; this strategy is not satisfactory in Internet access scenarios because collisions occur more frequently when nodes in the neighborhood of intersecting nodes (e.g. gateways) are hidden from each other, despite facing less contention.

2.5 Topology characteristics

2.5.1 Hop count

The MAC carrier sensing mechanism prevents simultaneous transmissions of neighbor nodes that can sense each other. In order to avoid collisions, the neighbors of both the receiver and the transmitter of a frame should be silent when the communication takes place. Consider the chain network on Figure 2.3(a). A single flow is transmitted along a 6 node chain network. The small solid lines around nodes B and C represent the receiving range and the carrier sensing range when the latter equals the former. The large dotted circles represent the carrier sensing range when it is the double of the receiving range. Data frames are being transmitted from left to right; when Node B is transmitting a data frame to Node C, Node A and Node D should be silent, while Node E and Node F are allowed to transmit.

Nodes with network interfaces working in half duplex are either receiving or transmitting traffic. When data transverses 2 hops to reach the destination, the network throughput is reduced to 1/2 of the capacity because each frame has to be transmitted twice though the same medium. Refer to Figure 2.3(a), considering that the Node A is the source and Node C is the flow destination. In this case, Node B can be either receiving from A or transmitting to C.

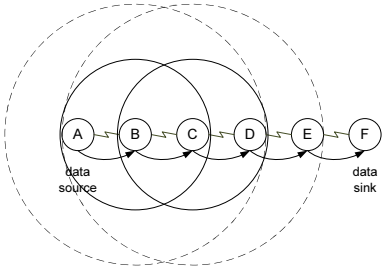

(a) Chain network topology with a single flow

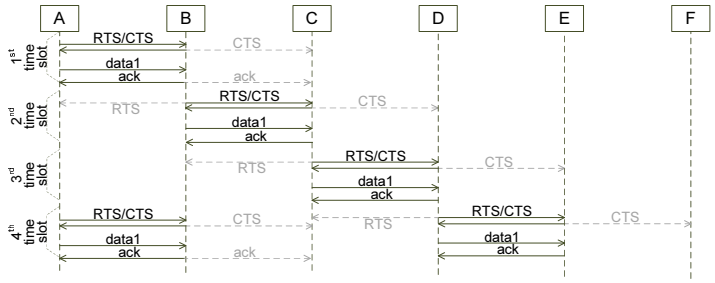

(b) Frame transmission when carrier sense range is equal to the receiving range.

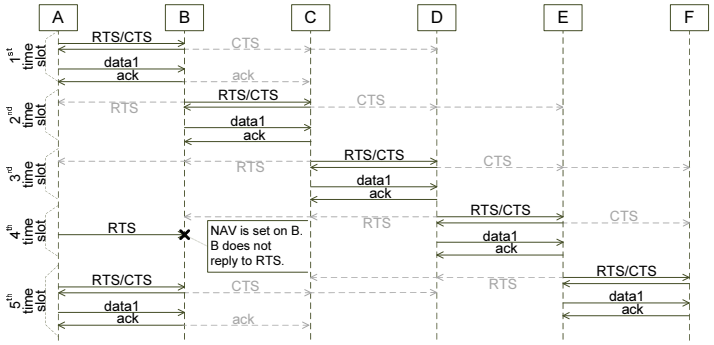

(c) Frame transmission when carrier sense range is the double of receiving range

Figure 2.3: Scenario and message sequence charts used to derive the maximum achievable data rate for a single flow on a chain topology.

If 3 hops are involved, the final data rate of the network is not expected to be more than 1/3 of the channel capacity. This capacity upper bound can be derived from the message sequence chart shown in Figure 2.3, considering an ideal scheduling.

Figure 2.3(b) shows a message sequence chart of a multi-hop communication when the carrier sense range is equal to the receiving range. On the first time slot the first frame is transmitted from Node A to Node B. On the second time slot, while Node B forwards

the frame to Node C, Node A senses the medium as being busy and defers the transmission of the second frame. On the third time slot, Node C transmits the frame to Node D. At the same slot Node A senses the medium as free and sends a RTS, but Node B senses the medium as busy and does not respond with CTS. On the fourth time slot two simultaneous communications are possible, Node D transmits the first frame to Node E and Node A transmits the second frame to Node B. This example shows that each hop can only transmit every 3 other time slot, leading the network throughput to 1/3 of the channel capacity, independently of the chain length.

Figure 2.3(c) shows the same scenario when the carrier sense range that is the double of the receiving range. In this case, the second packet is transmitted on the fifth time slot as, until then, Node B senses the medium occupied and does not respond to the RTS message. This leads to a network throughput that is 1/4 of the channel capacity. For a non ideal scheduling, a throughput of 1/5 of channel data rate has been reported in [62] when the carrier sense range doubles the receiving range. In [63], simulation results shown that the chain network throughput is 1/7 of the single-hop throughput for this network topology.

For chain networks such as those represented in Figure 2.3(a) it is possible to demonstrate that the length of the chain does not affect the maximum achievable throughput when a single flow is using the network; however, when several sources are used, the length of the chain influences the maximum achievable throughput.

The concept of bottleneck collision domain is introduced by [38] (see Section 2.2) enables the derivation of the impact the mean number of hops H has in a given network, when all nodes are sources of flows with the same packet rate of $\lambda packet/s$ destined to a common sink. The mean number of hops H traversed by a packet in the network of Figure 2.4(a) is given by Eq. 2.1, where N indicates the number of nodes in the network.

$$H = \frac{1}{N} \sum_{n=1}^{N} n = (N+1)/2 \tag{2.1}$$

The bottleneck collision domain of the network of Figure 2.4(a) is

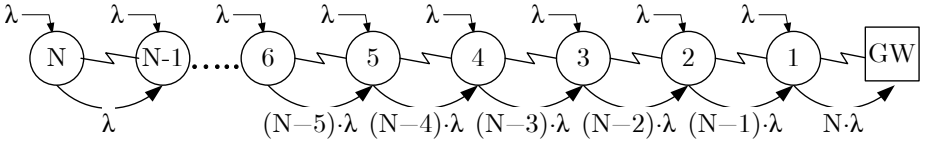

(a) Chain Topology with N flows

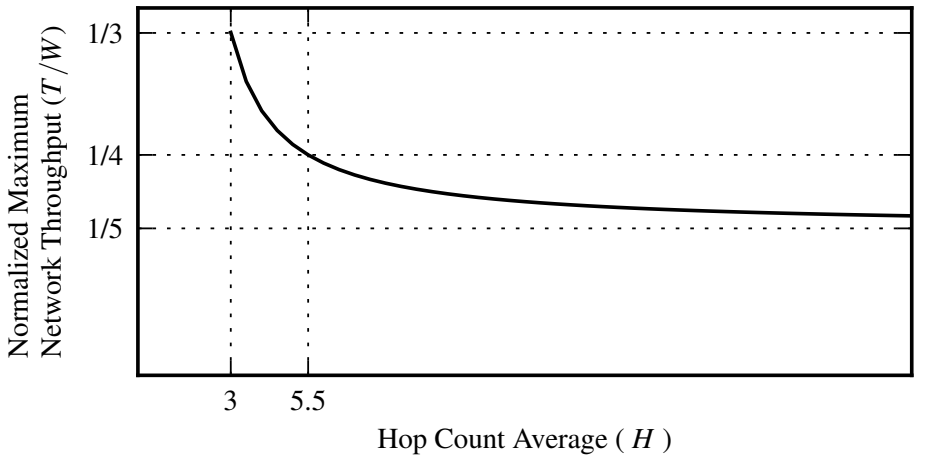

(b) Maximum network throughput T as a function of mean hop count H for a given channel data rate W

Figure 2.4: Chain topology with N hops and the throughput upper bound for this topology.

the collision domain of link 2-3 composed by links {GW-1, 1-2, 2-3, 3-4, 4-5} [38]. Each collision domain has to forward the sum of the traffic of its links. In this case, the collision domain of link 2-3 has to forward $\lambda \cdot [(N-4)+(N-3)+(N-2)+(N-1)+N] = \lambda \cdot (5N-10)$. The collision domain cannot forward more traffic than the channel data rate W, what means that $W \geq \lambda \cdot (5N-10)$. Therefore, the maximum throughput available for each node is $\lambda_{max} = W/(5N-10)$ and the maximum network throughput T is given by Eq. 2.2, where $N = 2H-1$ comes from Eq. 2.1.

$$\begin{aligned} T &\leq N\lambda_{max} \\ &\leq \frac{N \cdot W}{5N-10} = \frac{W\,(2H-1)}{5(2H-1)-10} = \frac{W\,(2H-1)}{10H-15} \end{aligned} \tag{2.2}$$

Figure 2.4(b) represents a plot of Eq. 2.2. The global throughput T decreases with the mean number of hops on a chain but it is lower bounded by $W/5$.

Let us consider now topology of Figure 2.5(a), that combine a chain of N_c nodes and a star of $N - N_c$ nodes. When $N_c = 0$ the network has star topology (Figure 2.5(f)); when $N_c = N - 1$ the network is a chain topology (Figure 2.5(b)). All the topologies present the same number of nodes $N = 8$ but different mean hop count H. In this case, the mean hop Count H is given by Eq. 2.3, where the first addend refers to the N_c nodes on the chain part of the network, and the second addend refers to the $N - N_c$ nodes on the star part of the network.

$$\begin{aligned} H &= \frac{\sum_{n=1}^{N_c} n + [(N - N_c) \cdot (N_c + 1)]}{N} \\ &= \frac{(N_c + 1)(N - N_c/2)}{N} \end{aligned} \tag{2.3}$$

When $N_c \leq 4$, all links are on the same collision domain [38]; the traffic on this collision domain is the traffic on links on the star part of the network given by $\lambda(N - N_c)$ and the traffic on the chain part of the network given by $\lambda \sum_{n=0}^{N_c-1} (N - n)$. The collision domain cannot transport more traffic than the channel data rate W, as presented by Eq. 2.4

$$\begin{aligned} W &\geq \lambda(N - N_c) + \lambda \sum_{n=0}^{N_c-1} (N - n) \\ &\geq \lambda N \frac{(N_c + 1)(N - N_c/2)}{N}), N_c \leq 4 \end{aligned} \tag{2.4}$$

By using H from Eq. 2.3 in Eq. 2.4 it is possible to obtain $W \geq \lambda N H$ for $N_c \leq 4$. Therefore, the maximum throughput available for each node is $\lambda_{max} = W/(NH)$ and the upper bound of network throughput $T = N\lambda_{max}$ is given by Eq. 2.5.

$$T \leq \frac{W}{H}, N_c \leq 4 \tag{2.5}$$

When $N_c > 4$, the bottleneck collision domain on star-chain networks of Figure 2.5 is the collision domain of link 2-3 composed by links {GW-1, 1-2, 2-3, 3-4, 4-5} [38]. Each collision domain has to forward the sum of the traffic of its links. In this case, the collision domain of link 2-3 has to forward $\lambda \cdot [(N-4) + (N-3) + (N-2) + (N-1) + N] = \lambda \cdot (5N - 10)$. The collision domain cannot for-

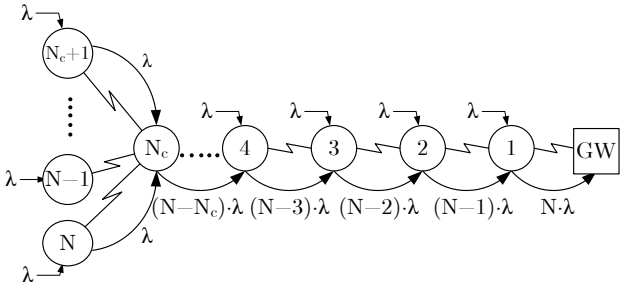

(a) Star chain topology with N flows

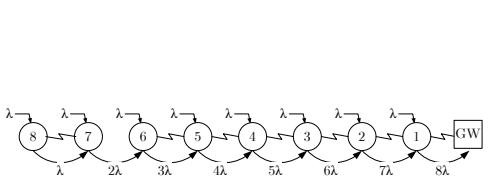

(b) $N_c = 7$, $H = 4.5$

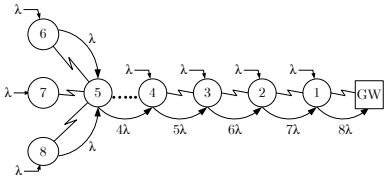

(c) $N_c = 5$, $H = 4.125$

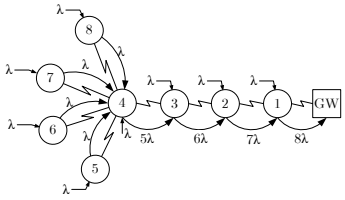

(d) $N_c = 4$, $H = 3.75$

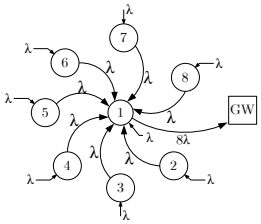

(e) $N_c = 1$, $H = 1.875$

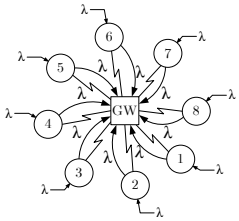

(f) $N_c = 0$, $H = 1$

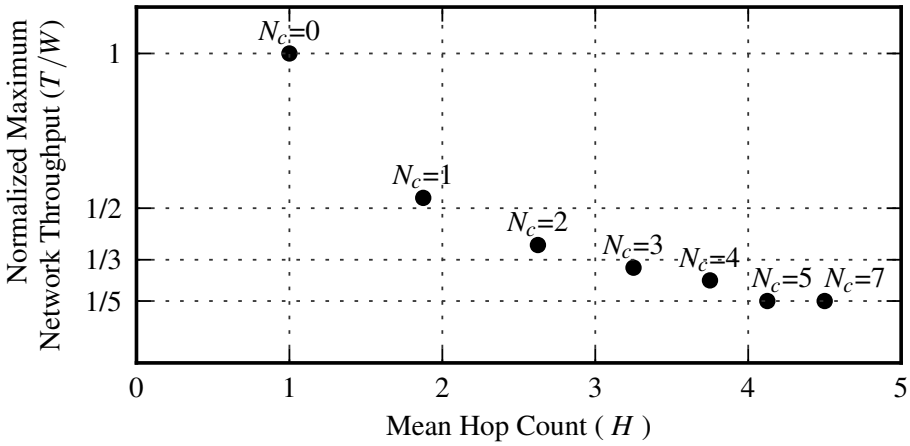

(g) Maximum network throughput T as a function of mean hop count H for a given channel data rate W

Figure 2.5: Topologies combining a chain of N_c nodes and a star of $N - N_c$ nodes and the upper bound of the throughput this topology as a function of the mean hop count.

ward more traffic than the channel data rate W, what means that $W \geq \lambda \cdot (5N - 10)$. Therefore, the maximum throughput available for each node is $\lambda_{max} = W/(5N - 10)$ and the upper bound of network throughput $T = N \cdot \lambda_{max}$ is given by Eq. 2.6.

$$T \leq \frac{WN}{5N - 10}, N_c > 4 \tag{2.6}$$

The maximum achievable throughput given by Eq. 2.5 and Eq. 2.6 is represented in the lower part of Figure 2.5 as a function of H for $N = \infty$; this graph shows that, for these topologies, the maximum achievable throughput T tends to the inverse of H. However, T does not always vary with H; for $H \geq 5$, which corresponds to $N_c \geq 4$, T is fixed to $W/5$. Therefore, the inference of the maximum achievable throughput is not possible for a generic network by just knowing H.

2.5.1.1 Discussion

Two simple topologies were studied relating the mean hop count and an upper bound of the network throughput calculated as in [38]. In both examples, it was shown that when the mean hop count is not too small, i.e. $H > 6$, the influence of the mean hop count on network throughput is negligible.

In [13] the authors proved that the amount of traffic λ generated by each node that can be transmitted through the network is inversely proportional to the mean number of hops H of the network. The number of MAC transmissions generated by each flow is given by $H\lambda$. With a total number of N nodes, the total offered traffic becomes $T_n = H\lambda N$. In ideal conditions, the offered traffic has to be served by N nodes each capable of transmitting W, thus $H\lambda N \leq NW$. An upper bound of the throughput per node is $\lambda_{max} = W/H$. However, a closer upper bound can be found if constraints such as spacial concurrency were introduced.

2.5.2 Neighbor node density

Neighbor node density is defined as the mean number of nodes in the carrier sensing range of each node in the network. Assuming a CSMA/CA MAC, the higher the number of active nodes is

in a region the less will be the throughput per node due to contention. Consider the network topology on Figure 2.6 containing $N = 6$ nodes. The lines represent links between nodes; if a line is not represented between two nodes, these nodes cannot sense each other's transmissions. Each node generates a data flow destined to Node F which is the gateway of this network. Data is transmitted through the paths defined by the links represented by lines with arrows. The neighbor node density d is calculated as the mean number of neighbors a node has. In this case we have nodes A, B, E and F with 2 neighbors, and nodes C and D with 3 neighbors, thus the neighbor node density for Figure 2.6 is $d = [(4 \times 2) + (2 \times 3)]/6\,\text{nodes} = 2.33$.

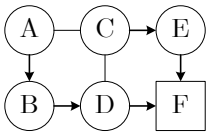

Figure 2.6: Sample topology used to discuss the topology metrics of a network.

Assuming the protocol interference model, the throughput λ obtainable by a node is shown [13] to decrease with the increase of the neighbor node density and given by $\lambda = \Theta\left(W/(\sqrt{n \log n})\right)$ [13] where W is the channel capacity and n is the number of nodes in the network.

Consider now the topologies of Figure 2.7, all of them containing $N = 12$ nodes. The lines represent wireless links between nodes; if a line is not represented between two nodes, these nodes cannot sense each other's transmissions. Each node generates a data flow of $\lambda\, packet/s$ destined to the gateway. Data is transmitted through the paths defined by the links represented by lines with arrows. Paths are the same on all topologies, therefore the mean hop count is $H = 2.5$ for the 9 topologies presented. The label of a link indicates the amount of traffic transported by that link. Stronger lines indicates the bottleneck collision domains calculated as in [38].

The neighbor node density d is calculated as the mean number of neighbors a node has in the network. Each topology presents a different neighbor set for each node by adding new links to the base

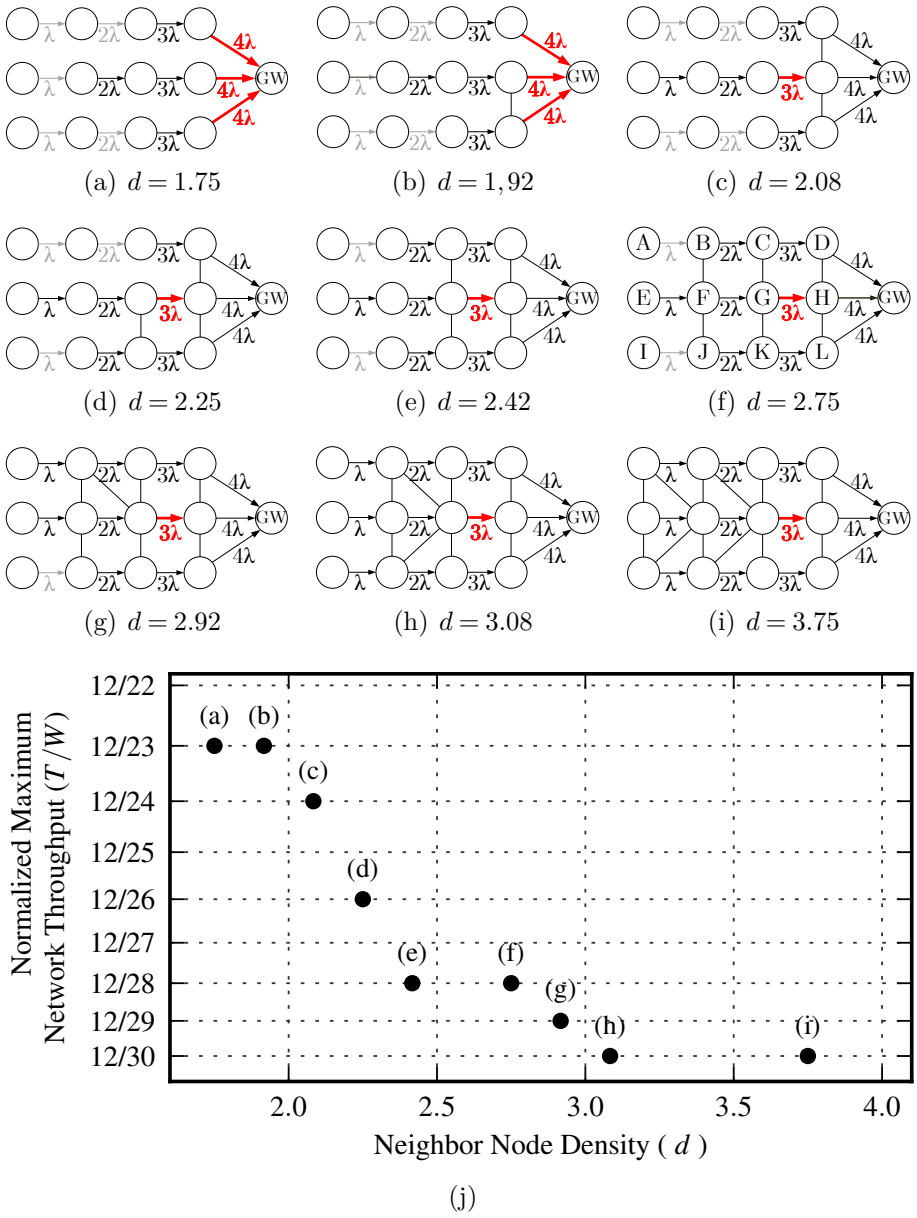

Figure 2.7: Throughput upper bound of a set of scenarios plotted as a function of the neighbour node density of those scenarios.

network topology of Figure 2.7(a), thus originating different node densities.

The maximum achievable throughput for these scenarios is calculated according to the model presented in [38] described earlier. The link found as the bottleneck collision domain of each topology is represented by a red strong line and the links not belonging to that collision domain are represented in gray. For instance, the bottleneck collision domain of the network on Figure 2.7(f) is the col-

lision domain of the link G-H composed by links {D-GW, H-GW, L-GW, C-D, G-H, K-L, B-C, F-G, J-K, E-F} [38]. This collision domain has to forward the sum of the traffic of its links which is $(4+4+4+3+3+3+2+2+2+1)\lambda = 28\lambda$. The collision domain cannot forward more traffic than the channel data rate W what implies that $28\lambda \leq W$. Therefore, the maximum throughput available to each node is $\lambda_{max} = W/28$ and the maximum network throughput is $T = N\lambda_{max} = 12W/28$, considering that $N = 12$.

The maximum achievable throughputs of topologies represented in Figure 2.7(a) to Figure 2.7(i) are plotted in Figure 2.7(j) as a function of the calculated neighbor node density d. This graph shows that, for these topologies, the maximum achievable throughput T tends to be the inverse of d. However, T does not always vary with d. As shown by these topologies, in general it is difficult to infer maximum achievable throughput by just knowing the neighbor node density d.

In [64], Kuo et al. prove that the throughput of a node λ is asymptotically defined as a function $f(d)$ of node density d given by Eq. 2.7, where c is a constant, and represented in Figure 2.8.

$$\lambda = \Theta\left(f(d)\right), \quad f(d) = \frac{1-(d^{-1}e^{-d/c})}{d} \tag{2.7}$$

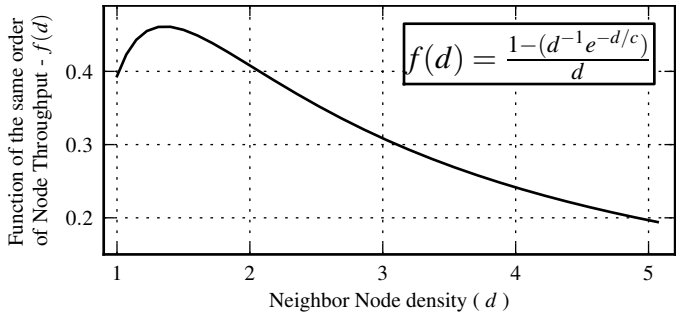

Figure 2.8: Asymptotic boundary function of per node throughput vs neighbor node density as presented by Kuo et al.

Kuo et al. in [64] argue that $f(d)$ is a trade-off between hop progress on the numerator and contention on the denominator. The numerator $1-(d^{-1}e^{-d/c})$ shows that the throughput increases with the neighbor node density; when a node has a large number of neighbors, the probability that the next node on the multi-hop path is

closer to the destination increases, and so does the hop progress. As a result, a large neighbor node density d leads to a smaller path hop count for each flow, which in turn reduces the traffic to be relayed by the network. The denominator shows that a large neighbor node density also introduces more contentions in the access to the wireless channel by the nodes in the receiving range. When d is small, the hop progress is more important than the contention effect; when d grows, the contention dominates. The study in [64] does not consider collisions caused by hidden nodes nor simultaneous transmissions both highly related with neighbor node density. The works reported in [65, 66, 67] address these problems. Packet collisions due to simultaneous transmissions are expected to increase with the increase of neighbor node density since it is more likely that two or more nodes of a neighborhood transmit at the same time slot. However, collisions due to hidden nodes can decrease when the neighbor node density increases since the number of hidden nodes can also decrease, what implies that for some topologies the throughput can increase when neighbor node density is high.

2.5.3 Hidden nodes

The hidden node problem is partially solved by the RTS/CTS mechanism of IEEE 802.11 on wireless local area networks. However in multi-hop networks it is proved [68] that hidden mesh nodes cause severe problems on network performance even when the RTS/CTS mechanism is used, since it does not solve the mesh hidden node problem and it increases the network overhead, leading to performance degradation.

For a given topology, the mean number of hidden nodes can be measured by averaging the number of hidden nodes of each active link in the network. The number of hidden nodes of a link is the number of neighbors of the link's receiver that are not neighbors of the link's transmitter. For instance, on Figure 2.6 there are 5 active links, which are the links used to transmit data, represented by arrows. Node D is hidden from link A-B, C and F are hidden from B-D, F is hidden from C-E, E is hidden from D-F, and D is

hidden from E-F. The mean number of hidden nodes of the topology of Figure 2.6 is $(1+2+1+1+1)/5 = 1.2$ nodes.

Attempts to analytically characterize the impact of hidden nodes on multi-hop networks are described in [69, 70, 65, 66]. In [69], authors derive the number of hidden nodes of a link considering the length of the link, but the relationship between the number of hidden nodes and throughput is not analyzed. The work in [70] studies the effect of hidden nodes on the network performance; the performance metrics studied there include throughput and delay but fairness is not addressed.

In [65], the authors introduce the miss ratio metric which is a global measure of the severity of the hidden nodes in a network. To describe the miss ratio metric, the authors first define a set of graphs that capture the physical interferences and the carrier sensing constraints between links in a network: if-graph, tc-graph, and rc-graph. In these graphs a vertex represents a wireless link. The if-graph can be used to capture the physical interference constraints graphically; an if-graph edge between vertex 1 and vertex 2 indicates that, in order to prevent future collisions, link 1 (node T_1 to node R_1) must be capable of forewarning link 2 (node T_2 to node R_2) not to transmit after link 1 initiates a transmission. The tc-graph models the transmitter-side carrier sensing; an tc-graph edge between vertex 1 and vertex 2 means that link 1 can and will forewarn link 2 not to transmit when link 1 is transmitting. The rc-graph models the receiver-side carrier-sensing constraints; an rc-graph edge between vertex 1 and vertex 2 indicates that R_2 will ignore T_2 transmission when the R_2 already senses a transmission on link 1. For the network of Figure 2.6, if-graph, tc-graph and rc-graph are presented in Figure 2.9(a), Figure 2.9(b), and Figure 2.9(c)

Using the graphs described above it is possible to obtain the hidden links on the network by $\overline{TC} \cap (IF \cup RC)$ where IF, TC, and RC are respectively the set of edges on if-graph, tc-graph, and rc-graph, and $\overline{TC}$ represents the set of edges that are not on the tc-graph. The number of hidden links is given by $N_{HN} = \left|\overline{TC} \cap (IF \cup RC)\right|$. If a tc-edge does not exist from link 1 to link 2, the transmission of link 1 will not be sensed by T_2. But if a rc-edge or a if-edge exists between link 1 and link 2, it indicates that either R_2 will ignore T_2

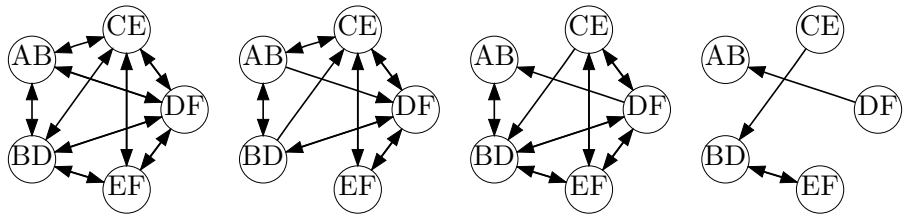

(a) if-graph (b) tc-graph (c) rc-graph (d) hidden links

Figure 2.9: In the topology of Figure 2.6, (a) is the if-graph, (b) is the tc-graph, (c) is the rc-graph, and (d) represents the hidden links.

when R_2 senses a transmission on link 1 (rc-edge), or that there is physical interference from link 1 to link 2 (if-edge). In both cases, T_2 will interpret it as a collision and we can say that link 1 is hidden from link 2. The hidden links of Figure 2.6 are represented in Figure 2.9(d). The miss ratio metric is then the ratio between the number of hidden links N_{HN} and the number of edges belonging to rc-graph or if-graph, as given by Eq. 2.8.

$$miss\,ratio = \frac{N_{HN}}{|IF \cup RC|} \tag{2.8}$$

When $TC = \{IF \cup RC\}$ there are no hidden links N_{HN} and miss ratio=0, which is the ideal value to avoid collisions on a network. For the network on Figure 2.6, $\{IF \cup RC\} = \{IF\}$ and $|IF| = 18$, thus miss ratio$= 4/18 = 0.22$. In [65], the authors do not relate miss ratio with the network throughput.

In [66], the authors model the per-hop throughput T_h as a function of network parameters such as the communication sense range R, the number of nodes D per m^2, the expected duration of frames transmission, the propagation delay, the duration of an idle slot, the minimum MAC backoff window size, and the MAC retry limit. They also show that the number of collisions caused by hidden nodes is higher than the number of collisions caused by simultaneous transmissions; this analysis is shown by graphs that plot the probability of collision caused by simultaneous transmission p_{cx}, the probability of collisions caused by hidden nodes p_{ch} and the probability of total collisions p as a function of R for a fixed number of D nodes per m^2.

R and D enable to derive the neighbor node density as $d = \pi R^2 D$ and it is possible do plot the probability of collisions as a function of d, as shown in the left hand graph of Figure 2.10. These plots show that the probability of collisions increase with the increase of the neighbor node density d. However the probability of collisions caused by hidden nodes p_{ch} does not increase continuously with d; when there are more neighbors around a node, the neighbors of the node's neighbors are all inside the communication range of each other reducing the occurrence of hidden nodes. On the other hand, the probability of collision caused by simultaneous transmission always increase with the increase of node density; when the number of nodes in the neighborhood of a node increases it is more likely that two or more nodes start transmitting simultaneously. In [66] is also provided a graph representing the per-hop throughput T_h as a function of the communication range R. Using this graph and that relating the probabilities of collision and R, it is possible to plot the per-hop throughput Th as a function of the probabilities of collision p, p_{ch} and p_{cx} shown in the right hand side of Figure 2.10. This graph shows that the per-hop throughput is very influenced by the probability of collisions, as expected. In particular, the probability of collisions caused by hidden nodes p_{ch} has a high correlation with the throughput Th.

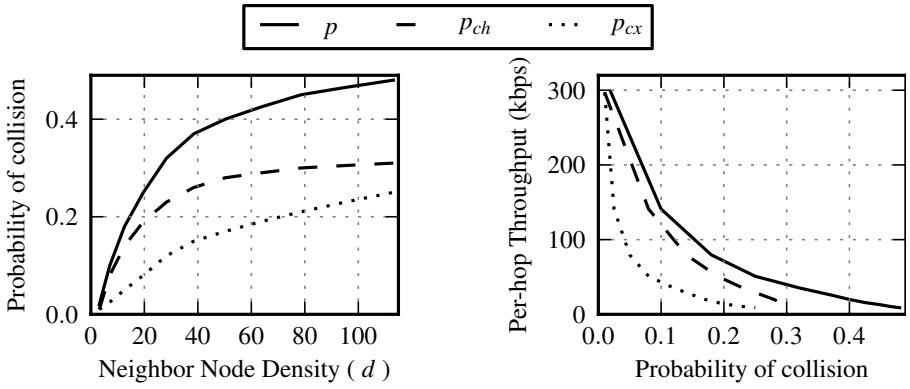

Figure 2.10: Relation between neighbor node density and per-hop-throughput based on the results presented by Abdullah et al.

2.6 Summary

In this chapter we presented the state-of-the art relevant for the work addressed in this thesis.

We described the operation of the CSMA/CA MAC protocol used in IEEE 802.11 standard and presented the hidden terminal problem that is highly responsible for decreasing the capacity of WMNs.

Studies that establish boundaries on the wireless networks in general and the WMNs in particular were surveyed. Gupta and Kumar [13] present a boundary for wireless networks in general and Jangeun and Sichitiu [38] introduce the concept of bottleneck collision domain by defining it as the geographical area of the network that enables an upper bound on the amount of data that can be transmitted in the network. This concept is used in the last part of the chapter. The state of the art interference models were also surveyed. The protocol interference model enables the use of simple graph-coloring solutions to avoid interference on WMNs which eventually turns out into NP-hard problems. The physical interference model is more complex but more realistic. The k-hop interference model defines that only one link can be active at one time within a k-hop distance which results NP-Hard problems when $k > 1$.

We presented a survey and a classification of channel assignment methods in single-radio WMNs. The objective of most of the assignment strategies for WMNs studied in the past few years ([14, 15]) was to minimize the overall network interference which is calculated based on topology and traffic information. Most of the approaches address the scenario of WMNs with multi-radio nodes ([16, 17, 18]) which are not suitable for the single-radio scenario we aim to address. The single-radio approaches found can be classified as dynamic or static. Dynamic approaches are mostly MAC layer protocols that stand on channel switching ([19], [20], [21]) which are difficult to implement with currently deployed 802.11 hardware and present problems such as the multi-channel hidden node problem. The static approaches found are three: (1) a distributed routing protocol [22] that uses traffic information to balance the load between channels disregarding the reduction of interference, (2) a

centralized tree-based multi-channel scheme [23] designed for data collection applications in dense WSN that assumes the existence of a single gateway, and (3) a couple of algorithms [24] designed to realize a component based channel assignment strategy that do not address stub networks.

A survey of studies that relate topology characteristics of WMNs with the network performance was also made and metrics for these characteristics were provided. In what concerns mean hop count and neighbor node density, we conclude that it is not possible to predict the maximum network throughput by just using these metrics; nevertheless, there exists an inverse relationship between network throughput and mean hop count, as well as between throughput and neighbor node density. We presented two metrics to measure the hidden nodes on a network: the mean number of hidden nodes, and the miss ratio.

Chapter 3

Identification of relevant topology metrics

In a single-radio WMNs the goal of a quasi-static channel assignment algorithm is to determine in which channel each node should be working on. We recall that we assume that a single radio WMN node is a node that can use a single network interface and a single channel at time for communicating with the other mesh nodes. Everytime a mesh node is assigned to a new channel, the topology of the network changes.

We argue that the network performance can be improved by controlling the network topology characteristics. As seen in Section 2.5, state-of-the art works related the network performance with topology metrics such as the mean hop count, the neighbor node density, the mean number of hidden nodes and the miss ratio. In this chapter we introduce a set of metrics related with the gateway neighborhood (1^{st} ring): the size of the 1^{st} ring, the mean number of hidden nodes on the 1^{st} ring, and the miss ratio on the 1^{st} ring. These metrics change when a node is assigned to another channel. In this chapter, we aim to investigate if these metrics have a relevant impact on the network throughput.

The rest of the chapter is organized as follows. Section 3.1 describes the methodology used in our study. Section 3.2 presents a detailed study of the two scenarios that were used. Section 3.3

discusses the impact of the mean hop count metric on the network throughput. Section 3.4 describes the impact that the neighbor node density and the gateways position have on the network throughput using a single channel scenario. Section 3.5 investigates the impact that topology metrics related to the gateway neighborhood have on throughput. Section 3.6 presents a summary of this study.

3.1 Methodology

We investigate the impact of the topology of a network on its performance, by means of extensive simulation analysis. We defined a lattice topology and simulated 18 dual-channel arbitrary deployments.

The 18 arbitrary channel assignment scenarios were applied to a 36 node network displaced in a 6x6 lattice topology disposed in an area of 1000 m×1000 m, as represented on Figure 3.1. The number inside a circle identifies the node. The lines represent wireless link layer connectivity; horizontal and vertical links (e.g. 1-2 or 1-7) measure 176 m and diagonal links (e.g. 1-8) measure 249 m. On figures of next sections (Figure 3.2 to Figure 3.13), the squares represent the gateways that have a wired connection to the Internet. Dark circles in these figures represent nodes configured on a channel, and light circles represent nodes on an orthogonal channel; these two networks are interconnected through their gateways.

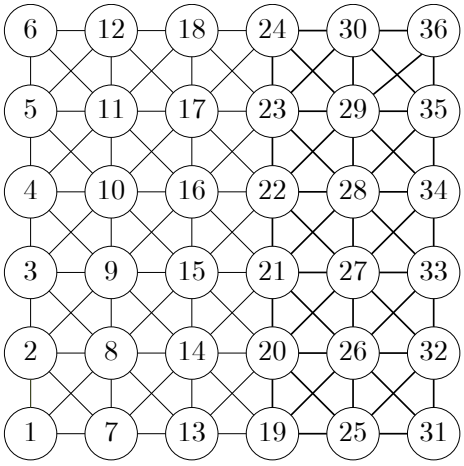

Figure 3.1: 6x6 lattice used to study the impact of topology characteristics on the network throughput.

The two channel assignment schemes A1 and A2 represented in Figure 3.2, along with a single channel scenario (A-SCh), were used as the base scenarios to study the impact of the topology characteristics on network throughput. Scenarios B1 and B2 of Figure 3.8, based on A1 and A2 but with fewer nodes, were simulated to study the effect of hop count. Scenarios C1, C2 and C-SCh of Figure 3.9, based on A1 and A2 with larger carrier sensing range, were used to study the neighbor node density. Scenarios D1, D2 and D-SCh of Figure 3.10, based on A1, A2 and A-SCh with gateways positioned on the center of the network, were used to understand the impact of the gateways position. Scenarios E1, E2, E3 and E4 of Figure 3.12 and scenarios A3, A4 and A5 of Figure 3.13 were used to study the impact of the gateway neighborhood in terms of neighbor node density and hidden nodes.

3.1.1 Simulator parameters

The parameters used in simulation are presented on the Table 5.3. The simulation tool ns-2 was used with two-ray propagation model in the physical layer, and MAC DCF 802.11 in the link layer. The Hybrid Wireless Mesh Protocol (HWMP) [1, 71] was used to establish routes since it is defined in the IEEE standard to WMNs [72]. RTS/CTS handshake was also used and the Carrier Sense Threshold (CSThresh) was configured to guarantee a carrier sensing range of 350 m.

3.1.2 Traffic flows

Each node generates a User Datagram Protocol (UDP) flow towards the gateway, so 17 flows were simulated on each channel on all scenarios except the single channel scenario with 34 flows on a single channel, and scenarios B1 and B2 which have 13 flows on each channel. A set of simulations was carried out. In each simulation all flows generated the same bit rate. Flow's bit rates from $10\,kbit/s$ to $7.5\,Mbit/s$ were used. Flow packets are generated by a Poisson process without bursts, characterized by exponentially distributed

Parameter	Value
Propagation Model	Two ray ground
Channel data rate	11 Mbit/s
Receiving Threshold	-70.2 dBm, 350 m
Node distance	176 m
Main flow packet size	1500 bytes
RTS/CTS	ON
Max. retransmission retries	7
Routing protocol	HWMP
Flow source type	Poisson (UDP)
WarmUp flow packet size	256 byte
WarmUp flow data rate	10 packet/s
Simulation runs	10

Table 3.1: Parameter values used in ns-2.29 simulations of networks with lattice topology.

inter-arrival times. Poisson process was selected to avoid simultaneity problems caused by other simpler approaches such as Constant Bit Rate (CBR). All flows are configured with similar parameters, which are fixed for each simulation; each simulation was run with 10 different seeds.

Simulations run for 60 seconds, what may imply the generation of 37500 packets. During the first 3 seconds there are no data flows; this period is used to allow the HWMP routing protocol to execute the proactive tree building functionality; in this phase a route to one of the gateways is added to each node as described in the proactive Path Request (PREQ) mechanism [1]. The expiration period of routes and routing messages are set to be larger than the simulation run. This option avoids the exchange of routing messages during the main flows simulation which cause avoidable overhead and also avoids the hop count shift problem described in [73].

Between second 3 and second 4 the warm up flow takes place between each node and the gateway; this flow enables the Address Resolution Protocol (ARP) tables of each node to be filled. On second 5, the main flows start and go on until second 50. The last 10 seconds of each simulation are used to enable packets to be

dequeued.

3.1.3 Queuing model

Preliminary experiences with the topologies of Figure 3.2 showed that the simulated scenarios exhibited serious fairness problems; for medium to high loads, only the nodes directly connected to the gateway could transmit their packets to the destination. This problem occurred because the queue of each node started to be filled by packets originated by the node's flow, and the packets received by downstream neighbors were dropped because there were no available buffers on the queue. This is an well identified and solved problem in the literature, as described in [74] and then in [75]. In our study a solution based on [75] was used where each node shares evenly the available queue among all the flows that are being forwarded by a node, including the node's flow. In practice, a different queue was created for each flow and these queues were served by a single server using a round robin strategy. Using this approach we could guarantee that all flows have the same chance to transmit their packets at each hop of the path and we could focus on the main objective of the study which consists in analyzing the impact of topology characteristics on the network throughput.

The queue size used in this study was 50 packets. So a node forwarding $N-1$ flows plus its own generated flow, is able to accommodate $N \times 50$ packets. The N queues are, as said, served in round robin. In order to guarantee that these values do not affect the simulation results, we carried out simulations with smaller queue size (3 packets) and with infinite queues (200000 packets); results obtained showed that the queue size does not affect the network throughput.

3.1.4 Measuring network metrics

To calculate the network topology and performance metrics, the two sub-networks resultant from the channel assignment are treated as a single network. The metrics aggregate the performance and the topology characteristics of all nodes in the network, independently

of the channel each node is configured in. Metrics are calculated by analyzing the trace files generated by ns-2 using python scripts and the graphs presented were created using matplotlib python library.

The performance metrics considered are the per-hop throughput and the end-to-end throughput. The per-hop throughput is defined as the mean bit rate of each data link in the network and is calculated as the total number of MAC frames successfully transmitted on the links of the network divided by the number of active links on the network which is 34 in these scenarios; non acknowledged frames are not considered. The end-to-end throughput of the network is defined as the sum of the bit rate received by the two gateways, divided by the number of sources of the network which is 34, except for scenarios B1 and B2.

3.2 Basic scenarios

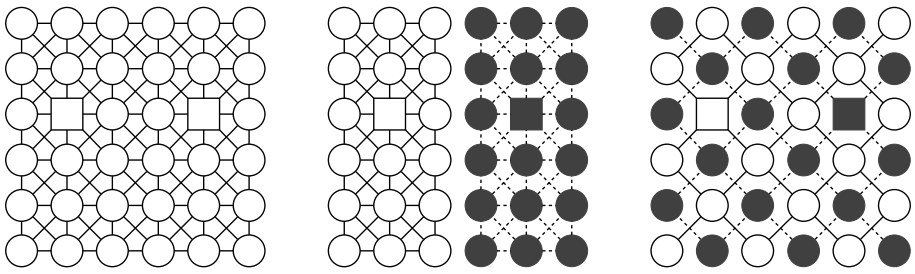

Figure 3.2: The channel assignment scheme used in A1 minimizes the number of hops to the gateway. The scheme used in A2 aims to reduce the number of contending neighbors. In the single channel scheme, A-SCh, the two gateways and the rest of the nodes are on the same channel.

Figure 3.3 shows the throughput and topology characteristics of the two scenarios represented in Figure 3.2, and compares it with a third scenario (Scenario A-SCh) where all nodes and gateways of Figure 3.1 work in a common channel. Figure 3.3(a) presents the per-hop throughput. For each source node debit, Figure 3.3(b) presents the mean of end-to-end throughput and the 90% confidence interval calculated using the results of the 10 simulations runs. Topology characteristics of these scenarios are presented on

Figure 3.3(c), and they were calculated as explained on Chapter 2; the 90% confidence intervals of the topology metrics are also shown and indicate that the values shown are very accurate. The results on Figure 3.3 are compared with results from simulations with variants of scenarios A1 and A2 and discussed in the following subsections.

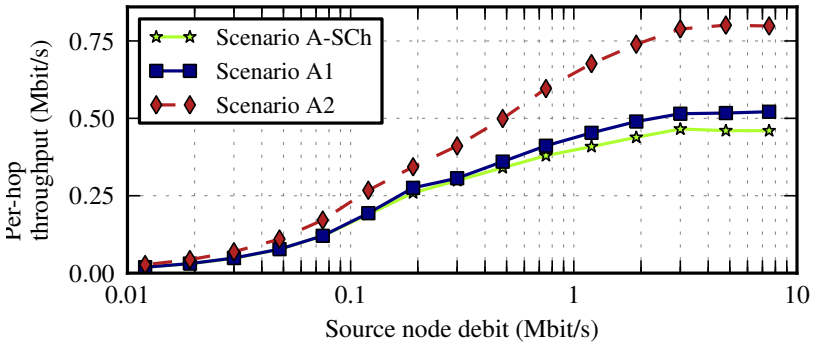

(a)

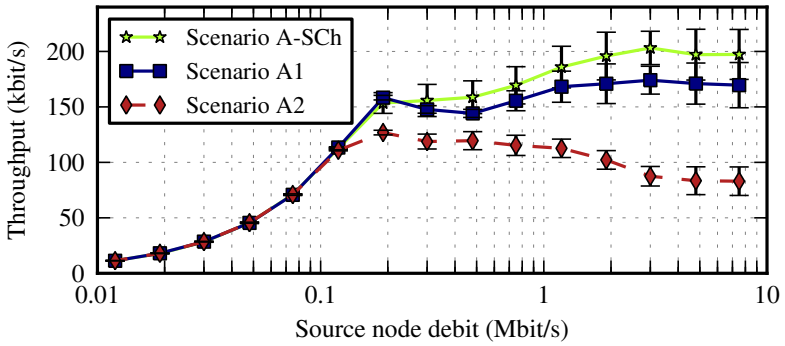

(b)

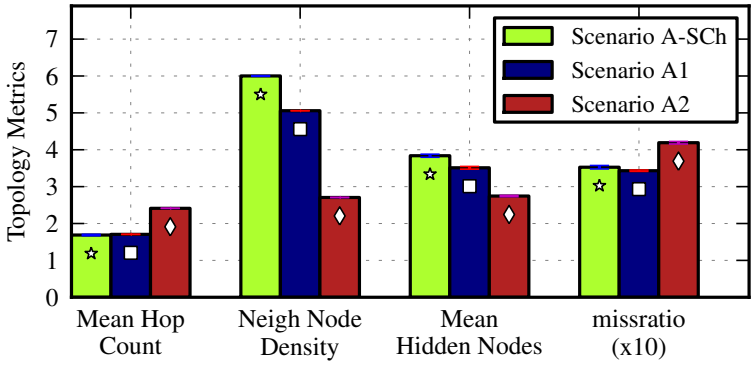

(c)

Figure 3.3: (a) per-hop throughput (b) end-to-end throughput and (c) topology metrics of two dual-channel and one single channel assignment schemes presented on Figure 3.2. The 90% confidence intervals of the throughputs and topology metrics are also shown.

3.2.1 Impact of traffic conditions

Estimate network capacity IEEE 802.11's theoretical data rate for each gateway is $11\,Mbit/s$, but more than 50% [76] of it is used in overhead, leaving $5.5\,Mbit/s$ per gateway available to transmit packets from 34 flows. The maximum mean data rate for each flow is $5.5\,Mbit/s \times 2\,gateways/\ 34\,nodes = 323\,kbit/s$. Considering that each frame is forwarded through multiple hops until it reaches the gateway, the maximum achievable end-to-end throughput is even lower. Therefore, it is expectable that a considerable amount of frames are lost when the sources debit is above $0.3\,Mbit/s$.

Low load traffic conditions Low load traffic conditions are assumed when each source generates less than $120\,kbit/s$. In these conditions every channel assignment scheme, including the single channel, presents the same end-to-end throughput results. In low load traffic conditions, all the packets are delivered to the destination without noticeable losses, independently of the scenario used; Figure 3.3(b) proves this by showing that for debits below $120\,kbit/s$, the end-to-end throughput is equal to the source debits. The per-hop throughput graph of Figure 3.3(a) shows that the number of MAC transmissions in these conditions correspond to the number of packets received by the gateways multiplied by the number of hops of the paths followed by packets whose values are shown in Figure 3.3(c). The mean path length in Scenario A1 and in single channel scenario is 1.7, while Scenario A2 has a mean path length of 2.41. When the throughput is 120 kbit/s, which occurs when the individual source debit is 120 kbit/s, the amount of data generated by each flow along its path is $1.7 \times 120\,kbit/s = 200\,kbit/s$ in the case of Scenario A1, and $2.41 \times 120\,kbit/s = 290\,kbit/s$ for Scenario A2.

High traffic load conditions When the traffic load is higher than $120\,kbit/s$, the end-to-end throughput starts growing slowly, in opposition to the linear growing for low loads. The networks start to lose packets and the differences of performance between the

topologies start to be evident. When each individual source generates more than $3\,Mbit/s$, the end-to-end throughput stops growing indicating that the network is near its saturation point.

3.2.2 End-to-end and per-hop throughputs

Figure 3.3(b) shows that the maximum end-to-end throughput of Scenario A2 is $127\,kbit/s$ for the offered load of $190\,kbit/s$, what suggests the existence of an optimum offered load; the existence of an optimum offered load was also reported in [62] and [63]. For Scenario A1, the end-to-end throughput increases even when it starts to lose significant amounts of data (when each node source debit is higher than $300\,kbit/s$), and it continues to grow with increasing amounts of offered load until it reaches a saturation value of $170\,kbit/s$. The inefficiency of Scenario A2 for high loads is caused by hidden nodes which cause collisions. Despite the mean number of hidden nodes in Scenario A2 being lower than in the other scenarios, as shown by Figure 3.3(c), the neighbor node density is also lower indicating that most of the neighbors are hidden from each other, as revealed by the miss ratio of Scenario A2, which is higher than in Scenario A1.

The per-hop throughput shown in Figure 3.3(a) increases with the offered load until reaches the saturation. The saturation values are 520 kbit/s, 800 kbit/s and 460 kbit/s respectively for scenarios A1, A2 and A-SCh. Scenario A2 presents the highest per-hop throughput. There are two reasons for that: 1) the large value of the mean hop count of Scenario A2 observed on Figure 3.3(c); 2) the low neighbor node density on the topology of Scenario A2.

3.2.3 Node density impact on per-hop throughput

The per-hop throughput can be easily correlated with the neighbor node density for scenarios A1 and A2 on Figure 3.2. High node density results on low number of frames successfully delivered to the MAC receivers as also shown in Figure 2.7. However, Scenario A2 has high per-hop throughput but low end-to-end throughput which

represents the amount of packets actually delivered to the final destination. This apparent contradiction indicates that a substantial part of the frames are lost before reaching the final destination. It is expectable that frames are lost when debits are higher than 0.3 Mbit/s since all flows are destined to the gateway which is the network bottleneck.

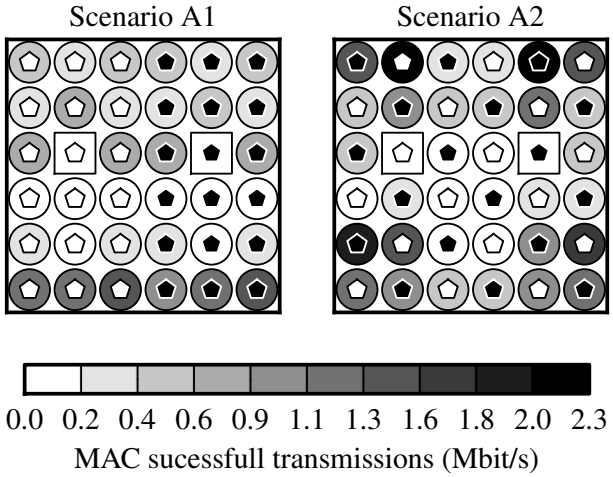

Figure 3.4: Amount of data transmissions on the networks of scenarios of Figure 3.2 when each node is generating a flow of 3 Mbit/s to a destination on the Internet. The white and black centers of each node represent the gateway used to forward the packets to the Internet. The face color of a node represents the amount of data frames that were successfully sent by that node.

Figure 3.4 shows the number of successful MAC transmissions when each node generates a traffic flow of 3 Mbit/s. This load corresponds to the saturation point of Figure 3.3(a). Nodes on the boundary of the network tend to acquire the channel and transmit much more packets than the other nodes on the path towards the gateway. The boundary nodes on both scenarios have few contending neighbors and the CSMA nature of IEEE 802.11 MAC protocol allows them to get the opportunity to transmit more often than subsequent nodes on the path to the gateways which have more contending neighbors. Border nodes transmit more MAC frames then interior nodes despite interior nodes have more frames to transmit, because they have to transmit their own frames and forward the frames coming from downstream neighbors. This effect makes the network inefficient because the packets that were transmitted

in the first hops are then dropped near the gateway. Border nodes transmit more MAC frames on Scenario A2 than in Scenario A1 because Scenario A2 has an higher difference between the number of neighbors on border and interior nodes. This is why Scenario A2 is more inefficient than Scenario A1, what confirms the results on Figure 3.3(b).

3.2.4 Analysis of generated packets

In our scenarios, the sources generate more packets than those that can be transported by the network. There are four possible destinies for a generated packet: 1) the packet is dropped by the source node because its queue is full; 2) the packet is dropped in an intermediate node because that queue is full if the medium around is congested; 3) the packet is dropped because the maximum number of retries defined by the IEEE 802.11 MAC is exceeded; 4) the packet succeeds if it reaches the gateway. Figure 3.5 quantifies these destinies for Scenario A1 and Scenario A2 of Figure 3.2.

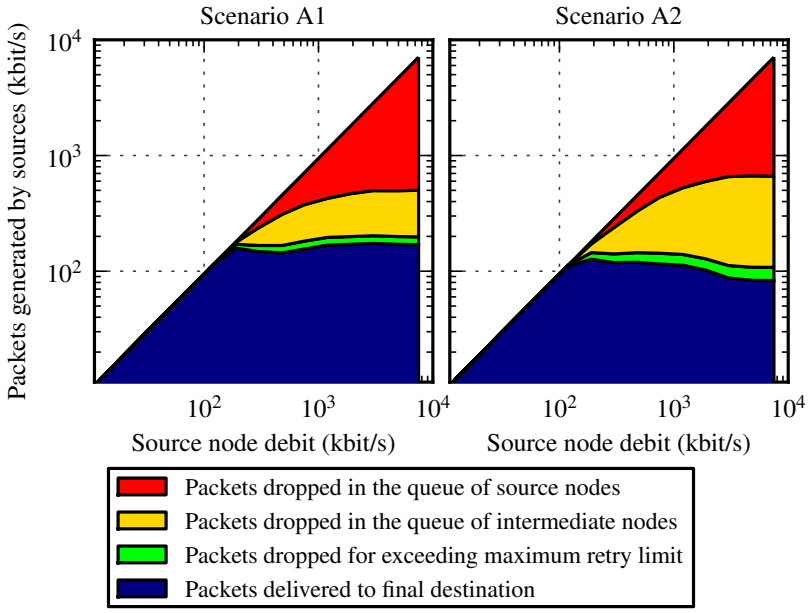

Figure 3.5: Packets generated by sources (1) dropped in the queue by source nodes, (2) dropped in the queue by intermediate nodes, (3) dropped after exceeding the maximum retransmission retries limit, or (4) delivered to the final destination.

The graphs on Figure 3.5 confirm the results in Figure 3.3(b) showing that Scenario A1 has a higher end-to-end throughput than Scenario A2, represented in Figure 3.5 by the bottom layer of the curve in dark blue. The number of drops caused by exceeding the maximum retransmission retries, represented by the second layer in light green of graphs of Figure 3.5, shows that the amount of collisions in Scenario A1 is lower than in Scenario A2. The number of packets dropped due to an excessive number of retries is a little fraction of the number of retransmissions.

While the nodes are retransmitting a packet multiple times due to collisions, the other packets are buffered in the queues waiting for their opportunity to be transmitted. This will cause the queue to increase and causes the drop of new packet arriving. These losses are represented in Figure 3.5 by the third and fourth layers in light yellow and dark red; the combined value of drops in the queues are higher in Scenario A2 due to the amount of time that nodes in this scenario spend on retransmissions, due to collisions.

Despite the total number of drops in the queues of Scenario A2 is higher than in Scenario A1, the number of these drops that occurred in the source nodes is higher on Scenario A1. This confirms the results in Figure 3.4, which show that nodes on border nodes transmit more MAC frames on Scenario A2 than in Scenario A1.

Scenario A2 shows more drops in the queues of intermediate nodes than Scenario A1, what is explained by the large number of successful transmissions by border nodes of Scenario A2. These packets are delivered to intermediate nodes which have neighbor node density higher than border nodes so the contention in the later causes packets to be buffered for more time and leads to packet drops in these queues. The asymmetry between the number of neighbors of border and interior nodes is higher in Scenario A2 than in Scenario A1.

3.2.5 Analysis of collisions

The packet losses caused by exceeding the MAC retransmission retries in Scenario A2, observed in Figure 3.5, indicates that this scenario has a larger amount of collisions than scenario A1. In order to

better understand the causes and impact of collisions on the network performance, the number tentatives for transmitting data frames were studied for both scenarios; result are presented in Figure 3.6. For that purpose we characterize the number of RTS messages sent by nodes. After an RTS message is sent, the following may happen: (1) RTS is not received; (2) RTS is successfully received but the receiver does not answer with CTS because it senses that some other node is using the medium; (3) RTS is followed by a CTS and then a data frame is sent which is not received; or (4) the RTS/CTS and the DATA/ACK pairs are successfully exchanged.

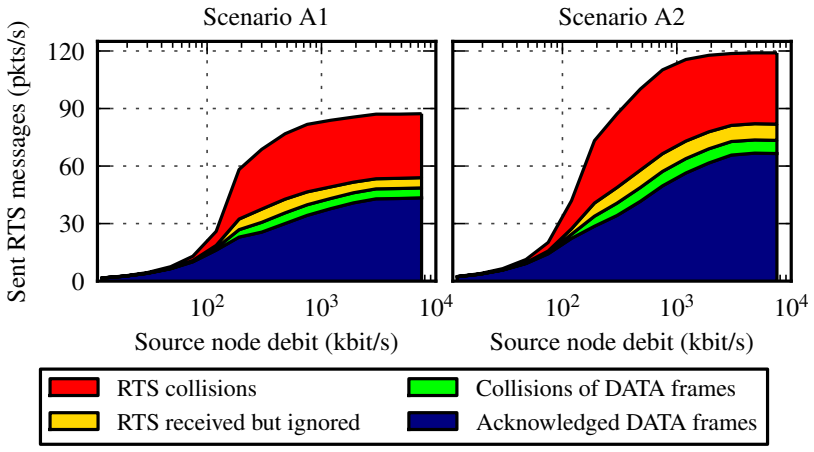

Figure 3.6: After a RTS message is sent, the following may happen (1) RTS is not received, (2) RTS is successfully received but the receiver does not answer with CTS, (3) RTS is followed by a CTS and then a data frame is sent which is not received, or (4) the RTS/CTS and the DATA/ACK pairs are successfully exchanged.

The number of tentatives for transmitting frames, shown in Figure 3.6 by the total number of RTS messages sent, is higher for Scenario A2 than for Scenario A1; this is explained, as discussed above, by the higher mean hop count and lower average number of neighbors of Scenario A2 when compared with Scenario A1. The number of RTS collisions represented by the first (top) layer in dark red of Figure 3.6 is higher on Scenario A2; this can be explained by the higher miss ratio of Scenario A2.

When a RTS message is received, the receiver may not respond to it if it senses the medium busy. In this case the CTS is not sent and the sender of the RTS will interpret this as a collision. From the

efficiency point of view this is less prejudicial than a real collision, since a single retransmission is required of the ignored RTS. Real collisions, causes the retransmission of both the RTS and the large data frame that was already being transmitted or received by the receiver. The amount of RTS messages ignored by the receiver is represented by the second layer of Figure 3.6 in light yellow, and it is higher for Scenario A2.

If the RTS is not ignored and the medium is free, a CTS message is sent. In our experiences, CTS packets were always successfully delivered. The sender, then transmits the data frame. The number of data frame collisions, represented by the third layer of Figure 3.6 in light green, is very low in both scenarios because the RTS/CTS mechanism avoids most of this type of collisions.

The dark blue bottom layer of Figure 3.6 represent the per-hop throughput and it confirms the results also presented in Figure 3.3(a) showing that Scenario A2 has a higher per-hop throughput than Scenario A1.

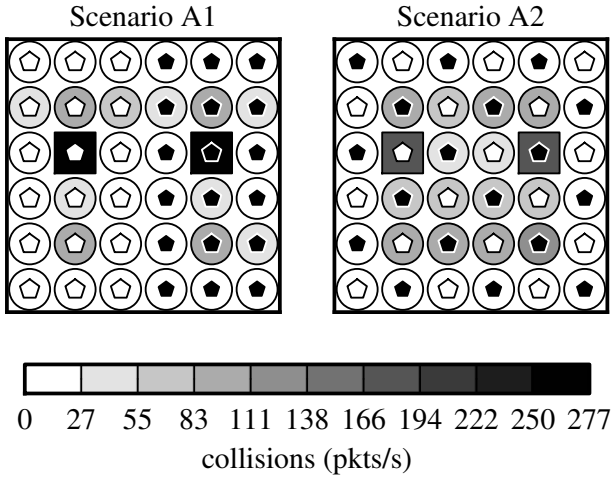

Figure 3.7: Amount of collisions on the networks of scenarios of Figure 3.2 when each node is generating a flow of 3 Mbit/s to a destination on the Internet. The white and black centers of each node represent the gateway used to forward the packets to the Internet. The face color of a node represents the amount of collisions perceived by that node.

Figure 3.7 shows the amount of collisions for each scenario when each node generates a traffic flow of 3 Mbit/s, that corresponds to

the saturation point referred earlier. Data collisions and RTS collisions are now considered on the receiver of each link. This graph shows that despite the gateway nodes of Scenario A1 have experienced more collisions than gateways of Scenario A2, the total number of collisions of Scenario A2 is higher because all the interior nodes of Scenario A2 suffer collisions, while in Scenario A1 only the a third of all nodes suffer collisions.

3.3 Mean hop count

An experiment was performed to understand the impact of the mean hop count on the end-to-end throughput of the networks of Scenario A1 and Scenario A2. Nodes on positions 2, 4, 6, 9, 11, 27, 29, 32, 34 and 36 (refer to Figure 3.1) were removed from networks on both scenarios in order to get similar mean hop count; the resulting networks are Scenario B1 and Scenario B2, shown in Figure 3.8(a).

The networks of Scenarios B were subjected to the same tests and loads described before. The achieved end-to-end throughputs with the correspondent 90% confidence intervals and the topology metrics are also shown in Figure 3.8. The shape of these graphs are similar to those presented in Figure 3.3 showing that the mean hop count of these networks does not have a great impact on the network performance. An increase of about 30% on the maximum end-to-end throughput was observed for scenarios B1 and B2, when compared with scenarios A1 and A2. This increase was expected since fewer nodes are sharing the gateways and the channel. However, the maximum total end-to-end throughput of the network $T = N\lambda_{max}$ is higher on scenarios A1 and A2 as shown in Table 3.2.

T_{A1}	T_{A2}	T_{B1}	T_{B2}
$34 \times 170 =$ $5.78 Mbit/s$	$34 \times 130 =$ $4.42 Mbit/s$	$24 \times 220 =$ $5.28 Mbit/s$	$24 \times 180 =$ $4.32 Mbit/s$

Table 3.2: Total end-to-end throughput of the network is higher on scenarios A1 and A2 than in with B1 and B2.

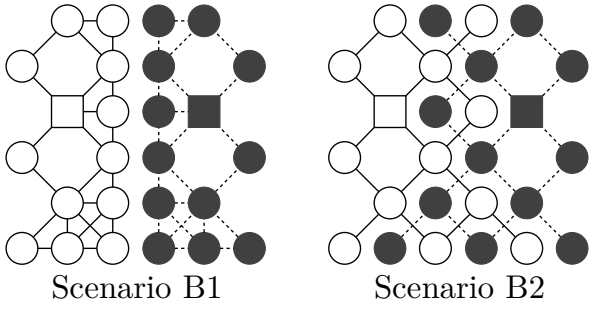

(a)

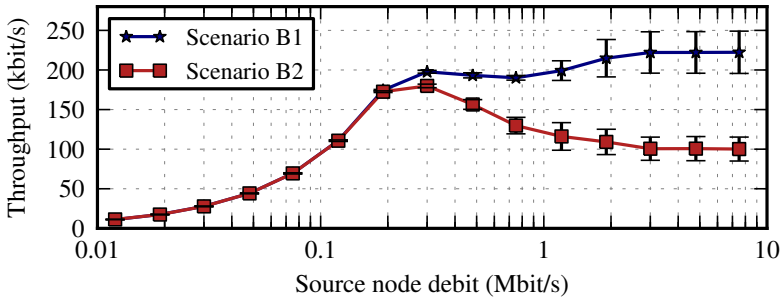

(b)

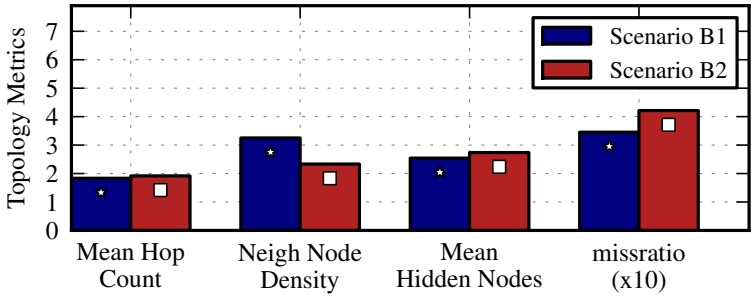

(c)

Figure 3.8: The network topology, end-to-end throughput with 90% confidence intervals and topology metrics of a reduced version of scenarios on Figure 3.2, where nodes on positions 2, 4, 6, 9, 11, 27, 29, 32, 34 and 36 (refer to Figure 3.1) were removed.

3.4 Single channel scenario

3.4.1 Neighbor node density

Figure 3.3(b) shows that the single channel scenario presents an end-to-end throughput higher than the scenarios using two channels. This result is true when the two gateways are deployed beyond the carrier sensing range of each other. The following experiment was performed to understand the impact of increasing the carrier sensing

distance on the network end-to-end throughput. The networks of Figure 3.2 were configured with a carrier sensing threshold that guarantees a carrier sensing range of 550 m, which enables gateways to sense each other's transmissions. The resultant networks and their wireless connections are presented in Figure 3.9; these networks were subjected to the same tests and loads described before. The achieved end-to-end throughputs and the topology metrics are also shown in Figure 3.9; the correspondent confidence intervals were omitted in order to simplify the figure, but they are of the same order of those represented in Figure 3.3.

In the Scenario A-Sch (Single Channel) with carrier sensing range configured to 350 m (Figure 3.3), the two gateways are on the same channel but not on the communication range of each other, therefore they can receive traffic from neighboring nodes simultaneously. When the carrier sensing range enables the gateways to sense each other's transmissions, as in Scenario C-Sch of Figure 3.9, the gateways share the channel and are on the communication range of each other; it implies that gateways cannot receive packets simultaneously and there is a decrease of network end-to-end throughput as shown by Figure 3.9, when comparing Scenario C-Sch and Scenario A-Sch.

Another interesting result is that end-to-end throughput of Scenario C1 is higher than Scenario A1 while Scenario C2 presents lower end-to-end throughputs than Scenario A2, as shown by the end-to-end throughput graph of Figure 3.9. This can be explained by the miss ratio, the mean number of hidden nodes and the neighbor node density. As shown in the topology metrics graph of Figure 3.9, all channel assignment schemes with wider carrier sensing range - scenarios C1, C2 and C-SCh - have neighbor node densities higher than schemes of scenarios A1, A2 and A-SCh. However, the number of hidden nodes and the miss ratio have different behaviors for the different channel assignment schemes when the neighbor node density increases. When it comes to scenarios A1 and C1, the mean number of hidden nodes and miss ratio decreases when the neighbor node density rises; for scenarios A2 and C2 as well as single channel scenarios A-SCh and C-SCh, the mean number of hidden nodes and miss ratio increases with the neighbor node density.

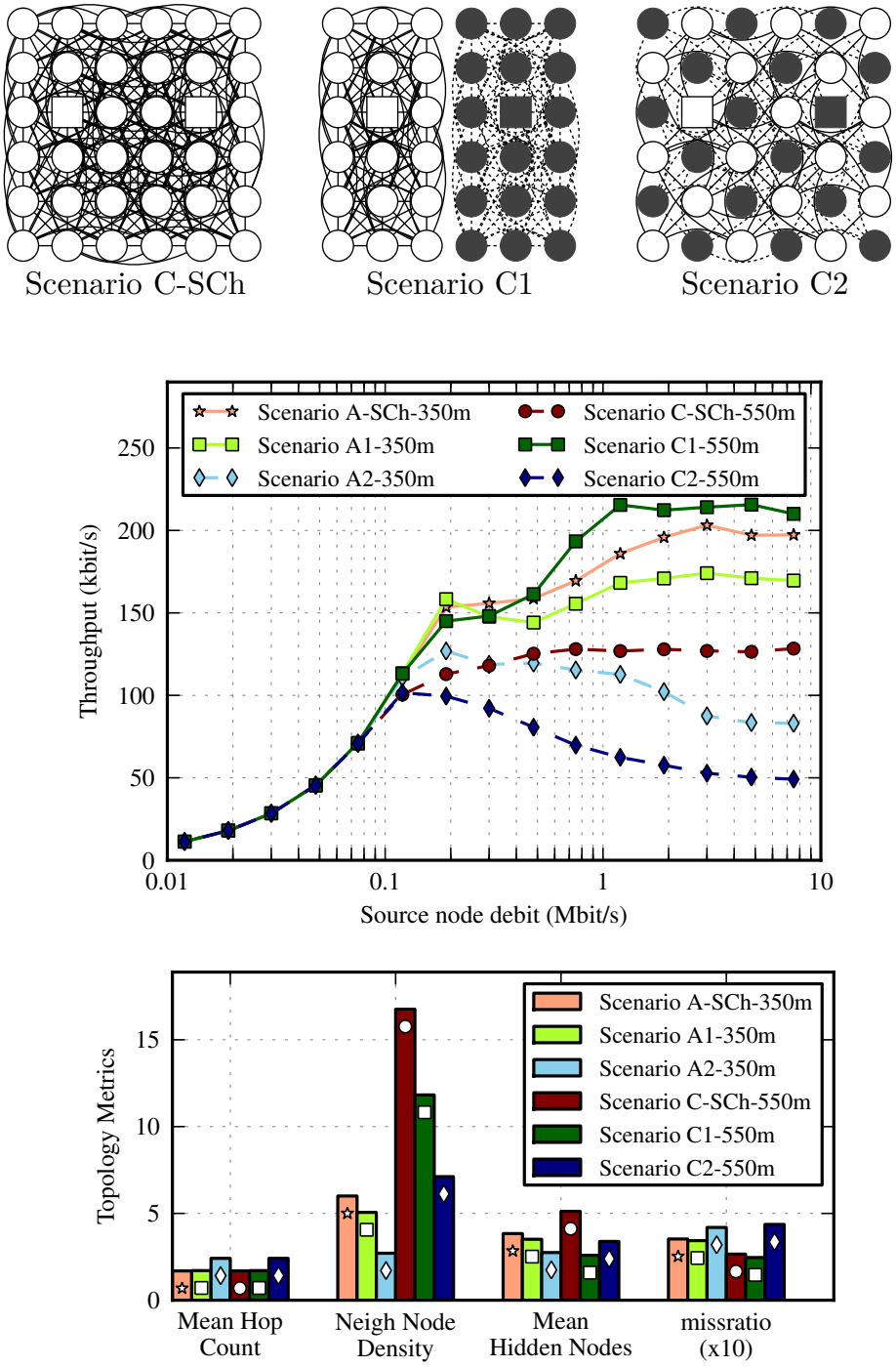

Figure 3.9: Network topology when carrier sense range is 550 m using the same channel schemes of Figure 3.2. When the carrier sense range enables the gateways to sense each other's transmissions, the single channel scenario (Scenario C-Sch) performance is lower than the Scenario A-Sch. The decrease and increase respectively of hidden nodes from Scenario A1 to Scenario C1 and A2 to C2 justifies the increase and decrease on the end-to-end throughput.

3.4.2 Gateways position

In order to confirm that single channel scenarios, where gateways are placed on the communication range of each other, present worst results than when two channels are used, a new experiment was carried out. The gateways were deployed in positions 15 and 21 (refer to Figure 3.1), as shown in Figure 3.10. The networks of Scenarios D were subjected to the same tests and loads described before. The achieved end-to-end throughputs with the correspondent 90% confidence intervals and the topology metrics are also shown in Figure 3.10. The end-to-end throughput for single channel scenario with centered gateways, Scenario D-Sch on Figure 3.10, is less than half of the end-to-end throughput obtained when the gateways are out of the communication range of each other (Scenario A-Sch on Figure 3.3(b)).

In Scenario D-Sch it is possible to have different routing paths on each simulation run. Different routing paths turns out in different miss ratios as shown by the wider confidence interval of miss ratios on Scenario D-Sch presented in the topology metrics graph on Figure 3.10. These variations on miss ratio leads to variations on the end-to-end throughput as shown by the wider confidence intervals of end-to-end throughputs of Scenario D-Sch when compared with Scenario D1 and Scenario D2.

3.5 Gateway neighborhood

In a scenario where a WMN is used to extend Internet access, we foresee that gateway position has a great impact on performance of the wireless network. A gateway at a central position leads to short paths; a gateway deployed at the edge of the WMN may lead to a small number of contending nodes around it.

In order to characterize the position of the gateway we introduce the concept of ring. The n^{th} ring is the set of nodes located n hops away from the gateway as defined in [77]. The 1^{st} ring seems to be of particular interest, since its nodes share the bottleneck of the network, which is the wireless channel around the gateway. The neighbor node density around the gateway can be measured by

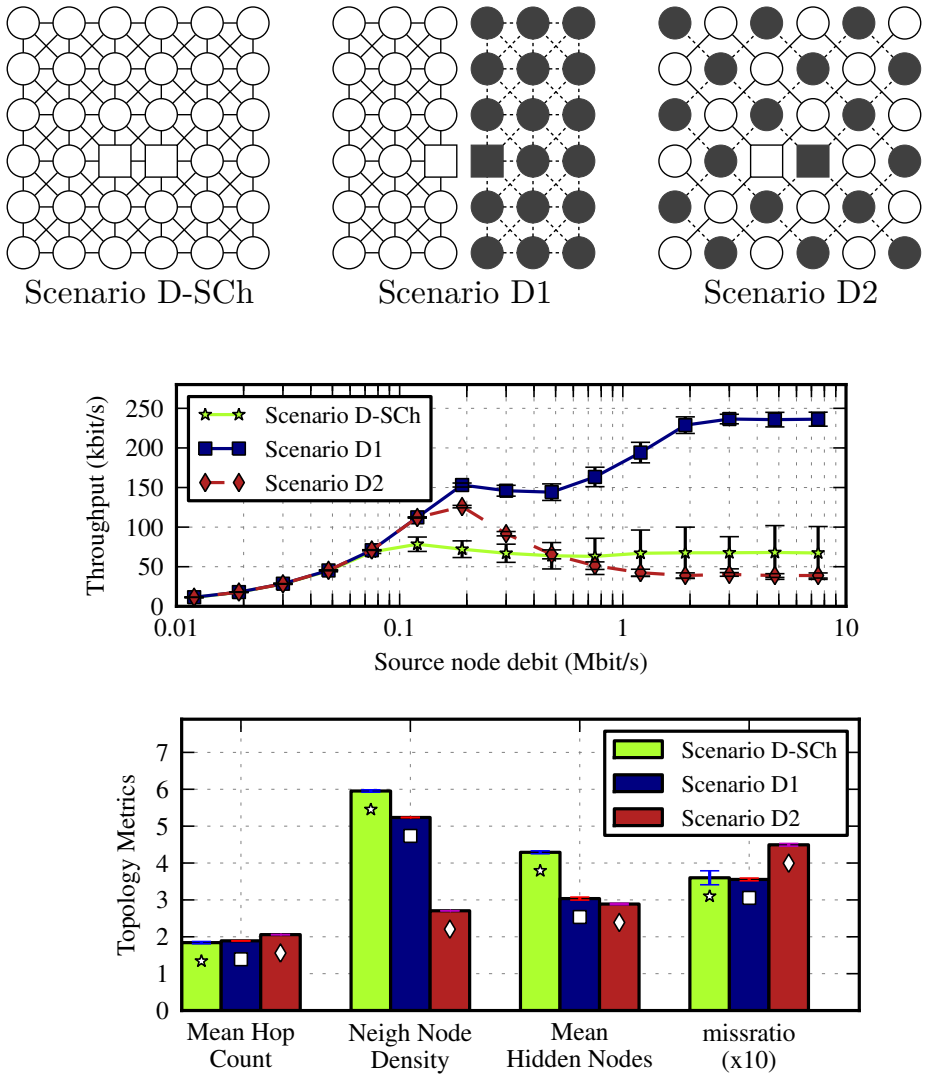

Figure 3.10: Network topology, end-to-end throughputs with 90% confidence intervals and topology metrics when gateways are deployed in positions 15 and 21 on the center of the network.

simply checking the size of the 1st ring, which is the number of nodes at one hop distance to and from the gateway. The hidden nodes of the 1st ring can either be measured by calculating the mean number of hidden nodes of 1st ring links or by calculating the miss ratio of the 1st ring. The 1st ring links are the links between the 1st ring nodes and the gateway.

Recall the set of graphs that capture the physical interferences and the carrier sensing constraints between links in a network: if-graph, tc-graph, and rc-graph described in Section 2.5.3. The 1st ring miss ratio is calculated using IF_{R1}, TC_{R1} and RC_{R1} which

are respectively the set of edges on if-graph, tc-graph and rc-graph which affect the gateway, as given by Eq. 3.1

$$missratio_{R1} = \frac{N_{HN_{R1}}}{|IF_{R1} \cup RC_{R1}|} \tag{3.1}$$

where $N_{HN_{R1}} = \left|\overline{TC_{R1}} \cap (IF_{R1} \cup RC_{R1})\right|$ is the number of links hidden from 1st ring links. For the network on Figure 3.11(a), the IF_{R1}, TC_{R1}, RC_{R1}, and HN_{R1} are the bold red edges in the graphs of Figure 3.11, $|IF_{R1} \cup RC_{R1}| = 7$ and $|HN_{R1}| = 1$ thus miss ratio$_{R1}$ = $1/7 = 0.14$.

(a) Network graph

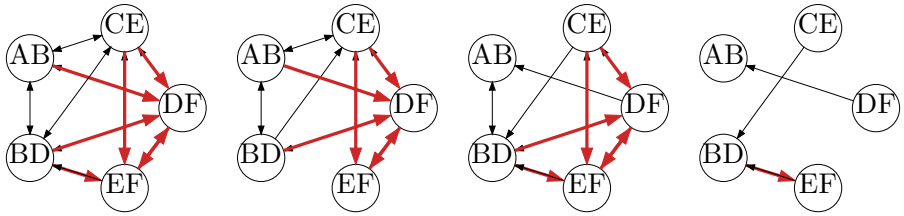

(b) if-graph (c) tc-graph (d) rc-graph (e) hidden links

Figure 3.11: In the topology of(a), (b) is the if-graph, (c) is the tc-graph, (d) is the rc-graph, and (e) represents the hidden links. The 1st ring edges on these graphs represented as red strong lines.

3.5.1 Size of the gateway neighborhood

In order to understand the impact of the characteristics of a gateway neighborhood, scenarios E1, E2, E3 and E4 were simulated. These scenarios, on Figure 3.12, show channel assignment schemes with 1, 2 and 3 nodes around the gateway. Scenarios E1 and E4 are, respectively, based on Scenarios A2 and A1 presented in Figure 3.2, moving the gateways to the corners of the lattice. Scenarios E2 and E3 are variants of Scenario E1 where the gateway neighborhood was modified to get respectively 2 and 3 nodes around the gateway.

The networks of Figure 3.12 were offered the same traffic and tests described earlier. The networks end-to-end throughputs with

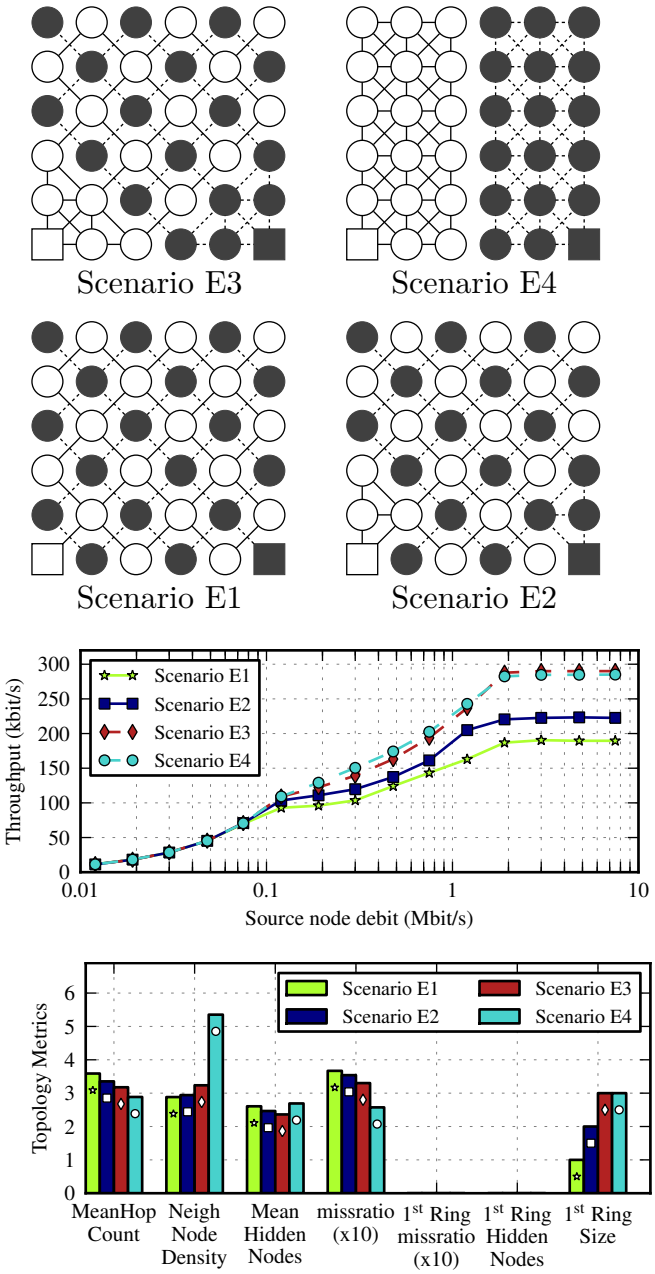

Figure 3.12: Channel assignment schemes with few full connected nodes on the neighborhood of the gateway. End-to-end throughputs with 90% confidence intervals and topology metrics are also presented.

90% confidence intervals and the topology metrics are also presented in Figure 3.12.

Results in Figure 3.12 show that end-to-end throughput depends on the 1st ring size which is the neighbor node density around the gateway. The higher is the 1st ring size, the higher is the end-to-end

throughput obtained. Also, the mean hop count and the miss ratio shown in the topology metrics graph of Figure 3.12 present an inverse relationship with the observed end-to-end throughputs shown in the end-to-end throughputs graph; in this case the higher is the hop count and miss ratio the lower are the end-to-end throughputs obtained.

The end-to-end throughput obtained in Scenario E3 and Scenario E4 are similar. Curiously, most of these two topologies metrics are different, except the size of the 1st ring. This observation enable us to conclude that the size of the 1st ring may have a great importance on the performance of the network.

From the 4 channel assignment schemes tested, Scenario E3 and Scenario E4 present the highest end-to-end throughput. In fact, the $290\,kbit/s$ achieved is near the maximal theoretical end-to-end throughput for a 34 flows destined to 2 gateways when the channel data rate is $11\,Mbit/s$, which is $323\,kbit/s$ as explained above. All the scenarios reaching near the maximum end-to-end throughput, have similar 1st ring topology characteristics: three full connected nodes around the gateway.

3.5.2 Hidden nodes on the gateway neighborhood

In order to verify the impact of 1st ring hidden nodes and 1st ring miss ratio on the network performance, the scenarios of Figure 3.13 were also tested. Scenarios A3, A4 and A5 are variants of Scenario A2, previously presented in Figure 3.2, where size of 1st ring becomes respectively 3, 2 and 1. On these scenarios, all 1st ring nodes are hidden from each other in order to verify the importance of 1st ring size in the presence of hidden nodes around the gateway.

The networks on Figure 3.13 were offered to the same traffic and tests described earlier. The networks end-to-end throughputs and the topology metrics are also presented in Figure 3.13; the correspondent confidence intervals were omitted in order to simplify the figure, but are of the same order as those represented in Figure 3.12.

In opposition to what was observed in Figure 3.12, for Scenarios A2, A3, A4 and A5 the end-to-end throughput decreases with the

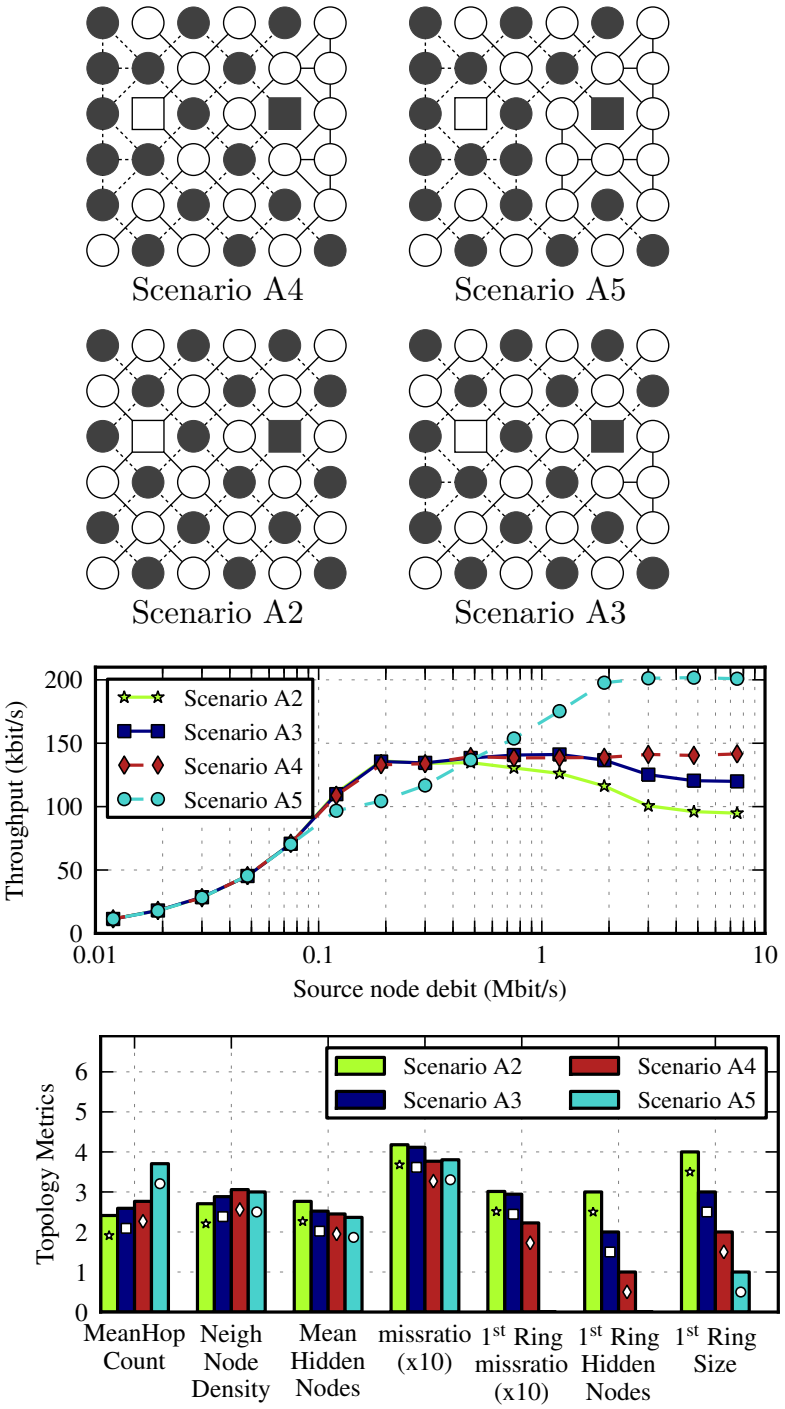

Figure 3.13: Channel assignment schemes with few nodes on the neighborhood of the gateway, all hidden from each other. End-to-end throughputs with 90% confidence intervals and topology metrics are also presented.

increase of the size of the 1st ring size, as shown in Figure 3.13. However, on scenarios of Figure 3.13, the number of hidden nodes around

the gateway increases with the increase of 1st ring size. Based on that, we conclude that the number of hidden nodes on the 1st ring influences more the network performance than the size of the 1st ring.

The miss ratio$_{R1}$ is the miss ratio calculated considering only the links hidden from 1st ring links, as defined in Section 2.5. The miss ratio$_{R1}$ shown in the topology metrics graph of Figure 3.13 are clearly related with the end-to-end throughput also shown in that figure. The miss ratio$_{R1}$ of Scenarios A2, A3 and A4 have small differences between them, while the miss ratio$_{R1}$ of Scenario A5 is much smaller. Notably, this relationships are also present between the end-to-end throughputs of Scenarios A2, A3, A4 and A5 on Figure 3.13.

Scenario A5 has the best performance presented in Figure 3.13 because it has a single node on the 1st ring and therefore does not have nodes hidden from this single link to the gateway. However, the end-to-end throughput of Scenario A5 does not reach the maximum achievable end-to-end throughput observed at Scenarios E3 and E4 on Figure 3.12 because a single link of Scenario A2 is not able to make hay of channel capacity as the three 1st ring links of Scenarios E3 and E4.

Having three nodes on the 1st ring that cannot hear each other, as on Scenario A3, causes a great amount of collisions between them causing inefficiency on the network bottleneck which is the gateway neighborhood. On the contrary, when there are three nodes on the 1st ring that can hear each other, the medium around the gateway is used more efficiently, leading to better network end-to-end throughputs as shown by Figure 3.14.

The amount of collisions on Scenarios E4, E3 and A3 are shown on Figure 3.15. Scenarios E4 and E3 present less collisions around the gateway than Scenario A3. The amount of collisions and consequent network inefficiency is related to the number of hidden nodes on the 1st ring. The inefficiency around the gateway has high impact in the network end-to-end throughput, since it is the network bottleneck.

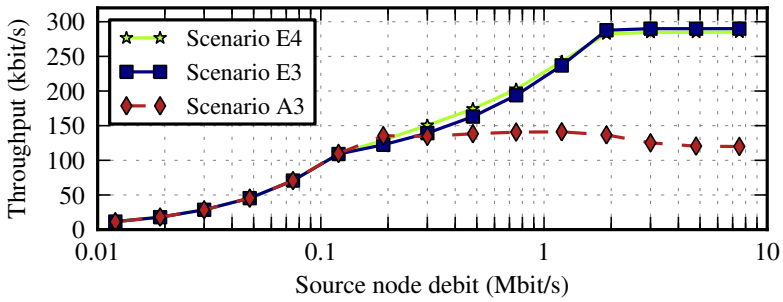

Figure 3.14: Comparison of the end-to-end throughputs of networks of Scenarios E4, E3 of Figure 3.12 and Scenario A3 of Figure 3.13.

3.6 Summary

In this chapter we clarify which network topology characteristics are relevant to improve network performance and which metrics can be used quantify these characteristics.

We consider this characterization fundamental for designing a quasi-static channel assignment algorithm for single-radio WMNs and, to the best of our knowledge, it is new.

The impact of the topology of a network on its performance was estimated by means of extensive simulation analysis. We defined a set of experiments with 18 arbitrary channel assignment scenarios in a 6x6 lattice topology network. At each experiment each node generates a UDP flow towards the gateway, all flows have the same bit rate. Flow's bit rates from $10\,kbit/s$ to $7.5\,Mbit/s$ were used. The performance metrics considered are the per-hop throughput and the end-to-end throughput. To calculate the network topology and performance metrics, the two sub-networks resultant from the channel assignment are treated as a single network. Metrics are calculated by analyzing the trace files generated by ns-2 using python scripts.

Two channel assignment schemes were applied to the 36 node lattice network and were used as the basis for this study together with a single channel scenario, where the 36 nodes share the same channel. While the channel assignment scheme used in Scenario A1 minimizes the mean hop count, the scheme used in Scenario A2 aims to reduce the neighbor node density. Scenario A-Sch is the single channel scenario. Scenario A2 was found to have a higher per-hop throughput but a lower end-to-end throughput when compared to

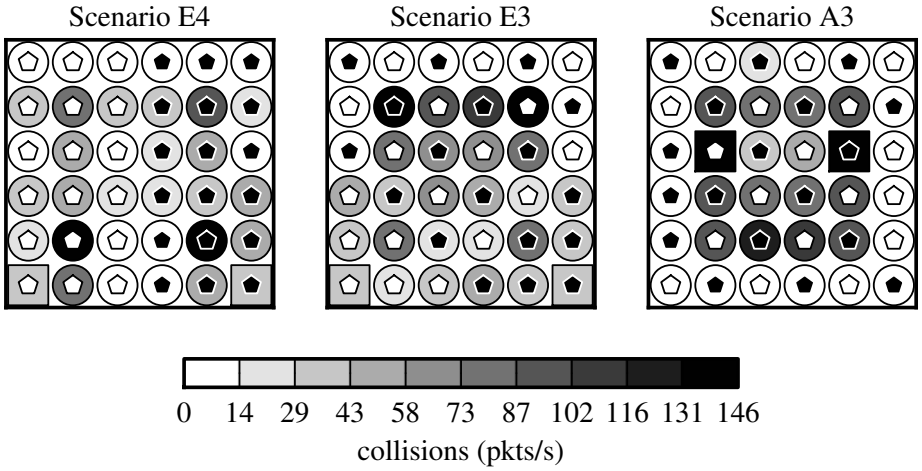

Figure 3.15: Amount of collisions on the networks of scenarios E4, E3 and A3 when each node is generating a flow of 3 Mbit/s to a destination on the Internet. The white and black centers of each node represent the gateway used to forward the packets to the Internet. The face color of a node represents the amount of collisions perceived by that node.

Scenario A1. The inefficiency of Scenario A2 is caused by the hidden nodes which cause collisions. The per-hop throughput can be easily correlated with the neighbor node density of a network; higher node density results on lower number of frames successfully delivered.

We simulated two new scenarios, Scenario B1 and Scenario B2, which are variants of Scenario A1 and Scenario A2 where a set of nodes were removed from both basic scenarios in order to get similar mean hop count but maintain the rest of the topology metrics. The simulation results on this new scenarios show that, in these cases, the mean hop count has low impact on the end-to-end throughput.

The three new scenarios Scenario C1, C2, and C-Sch, are variants of the basic scenarios in which we increased the carrier sense range. The three new scenarios Scenario D1, D2, and D-Sch, are variants of the basic scenarios in which we repositioned the gateways to central positions. The simulation results of these scenarios show that neighbor node density does not have impact on the end-to-end-throughput.

In order to understand the impact of the characteristics of a gateway neighborhood we simulated a set of scenarios E1, E2 and E3 which differ from each other by the number of nodes around the

gateway. The results show that the size of the gateway neighborhood has a great impact on the end-to-end-throughput. In order to verify the impact of 1^{st} ring miss ratio on the network performance we tested a set of scenarios with different values of 1^{st} ring miss ratio and sizes of 1^{st} ring. The simulation results showed that the number of hidden nodes on the 1^{st} ring influences more the network performance than the size of the 1^{st} ring.

The findings discovered by this study on the arbitrary lattice topologies can be summarized as follows:

- the miss ratio on the gateway neighborhood and the number of nodes around the gateway have a huge impact on the network performance, since the gateway neighborhood is the network bottleneck and it is important to use it efficiently;
- mean hop count, neighbor node density and the overall miss ratio have low impact on the network performance for the topologies studied in this chapter.

Chapter 4

Ranking of topology metrics

The work presented in this Chapter aims to quantify and rank the impact that the topology metrics identified in Chapter 3 have on the WMN performance. The network performance is characterized by three metrics: throughput, fairness and delay. Selecting the channel each node is operating, we control the network topology. This control is achieved because the set nodes operating on different channels form sub-networks with different topologies. The topology of each network is summarized by a set of metrics identified in Chapter 3 that includes mean hop count, neighbor node density, number of nodes in the gateway neighborhood, the miss ratio of the overall network, and the miss ratio on the gateway neighborhood. The number of nodes using each radio channel is also an important characteristic when the channel assignment is applied to random networks; this metric was not considered in Chapter 3 because the topologies studied there were regular and the channel assignment resulted in symmetric sub-network topologies.

The analysis made in Chapter 3 gave important hints about the relative importance of network topology characteristics in network performance. However, the scenarios studied were few and arbitrarily selected. In this chapter we study an extended set of random network topologies, with the purpose of ranking the impact of the

network topology on the WMN performance. Using a data mining technique to extract information from the results of simulations of a large number of random networks, we aim to quantify the impact that each network topology metric has on the network performance.

The rest of the chapter is organized as follows: Section 4.1 describes the data mining techniques used in this chapter, their applications and concurrent techniques; Section 4.2 describes the research methodology used in this work; Section 4.3 characterizes the performance of the simulated networks; Section 4.4 characterizes their network topology metrics; Section 4.5 presents and analyses the data mining results; Section 4.6 summarizes the results of this study.

4.1 Data mining

Data mining aims to extract useful knowledge from raw data and it includes techniques from different disciplines such as artificial intelligence, statistics and databases. One important data mining goal is to build predictive models, under a supervised learning paradigm that learns an unknown underlying function that maps a set of inputs into a target variable [78]. Such learning is performed over a training dataset and once a data-driven predictive model is built, it is possible to issue predictions for unseen (test) data. There are different types of learning problems and these are binary classification, multi-class classification and regression. Binary classification is a problem with binary outputs (e.g. classify the type of credit, "good" or "bad", that is assigned to a client given the status of her/his bank account). Multi-class classification is a problem with a finite number of outputs (e.g. person recognition based on photographs). The regression consists in estimating a real (numeric) value (e.g. predict house prices based on their number of rooms, age and other characteristics). This work is seen as a regression problem since we aim to quantify the impact that each topology metric has on the network performance.

4.1.1 Regression techniques

There are several machine learning algorithm to perform regression from which we highlight two: Artificial Neural Networks (ANN) and Support Vector Machines (SVM). Despite the complexity of these two models, it is still possible to extract knowledge in terms of input variable importance [79] with high accuracy. SVM and ANN have been successful used to solve a wide range of problems in statistics [80], science [81], pattern recognition [82], structural civil engineering [83] and in telecommunications engineering [84].

ANN models for complex systems. ANN mimics some basic aspects of brain functions, which processes information by means of interaction between neurons. They can be used both for classification and regression problems. ANN consist of three layers, namely, the input layer, the hidden layer and the output layer. The input layer represents the model inputs and the output layer represents the model outputs. The hidden layer consists of nodes that, during optimization, attempt to functionally map the model inputs to the model outputs. There are numerous ANN architectures such as the multilayer perception and the radial basis function.

SVM is a classifier derived from statistical learning theory and was initially proposed by Cortes and Vapnik in 1995 for classification tasks [85]. Like ANN, SVM can be used both for classification and regression problems [86]. In regression problems, a non-linear function is learned by a linear learning machine in a kernel induced feature space, while the capacity of the system is controlled by a parameter that does not depend on the dimensionality of the space. The basic idea when using SVM to regression problems is to map the input space to the high dimensional feature space in a non-linear manner.

The popularity of SVM in data mining is due to several advantages that SVM present over other supervised learning techniques. Similarly to neural networks, SVM is a flexible model (i.e. no *a priori* restriction is imposed) that is robust to noise and capable of complex nonlinear mappings. Hence, SVM often provides a good predictive performance, in particular if compared with simpler models, such as multiple regression. Moreover, during the training phase,

the SVM learning model always converges to the optimal solution, which is not the case of other random initialization learning techniques, such as ANN.

4.1.2 Applications in telecommunications

Given the increasing interest in data mining and the development of data-driven models, several supervised learning algorithms have been applied to the computer networks field. For instance, in [84] neural networks were successfully used to predict TCP/IP traffic from two large Internet service providers (regression task), outperforming classical forecasting methods (i.e ARIMA and Holt-Winters). In [87], several data mining models were explored to perform intrusion detection in wireless mesh networks (classification approach). The best results were achieved using a SVM (e.g. 99.9% detection rate for probe flooding attack), outperforming both a decision tree and a bayesian method. More recently, a SVM regression modeling was performed in [88], with the intention of modeling the relation between probe packets inter-arrival times and the user's throughput, achieving a predictive error of 0.37 (mean squared error) and 0.89 (R^2).

4.1.3 Concurrent techniques

Several studies exist on the effect of network topology characteristics on the network performance [89, 90, 64, 66, 70, 91]. Most of these studies address a single network topology characteristic an a single network performance metric but [91] present boarder studies including topology metrics.

The study in [89] compares the triangular, square and hexagonal topologies with different number of nodes per network; they study the effect of the topology on the capacity using the maximum hop count to the gateway as a topology metric. The work in [90] studies the effects of different distributions used to create random network topologies on the network throughput. The studies in [64, 66, 70] are surveyed in Chapter 2.

Robinson and Knightly [91] explore topology and deployment factors in mesh network design and study their impact on the performance of a general wireless mesh network. The performance metrics considered are access-tier coverage area, backhaul tier connectivity, and fair mesh capacity. They compare random, triangular, square and hexagonal topologies with different values of node density. The objective of the methodology of the study in [91] is to design and analyze a set of fractional factorial Monte Carlo experiments in order to isolate and study each factor's influence. In our work we use a data mining approach, where the network performance is modeled as a regression function, as given by the SVM algorithm, that is dependent of several topology metrics. Given that the obtained data-driven models present high predictive capabilities, we then measure the influence of each topology metric in the SVM model, under a sensitivity analysis, thus showing the relationships between the topology metrics and the network performance metrics. To the best of our knowledge, there are no studies on the effect of topology on the WMN performance using such data mining approach.

4.2 Methodology

In this chapter we study an extended set of network topologies, with the purpose of better understanding the impact of the network topology on the wireless network performance. The methodology adopted in this work, shown in Figure 4.1, has five stages. In the first stage, 7000 dual-channel random WMN topologies are generated. In the second stage these networks are simulated in ns-2 with UDP traffic. In the third stage the simulation results are measured to obtain the corresponding network topology metrics and the performance metrics. In the fourth stage a set of SVM models are generated; the topology metrics are the inputs and the performance metrics are the output of each model. In the last stage, these data mining models are used to quantify the importance of each topology metric on each performance metric through a 1-D sensitivity analysis [92].

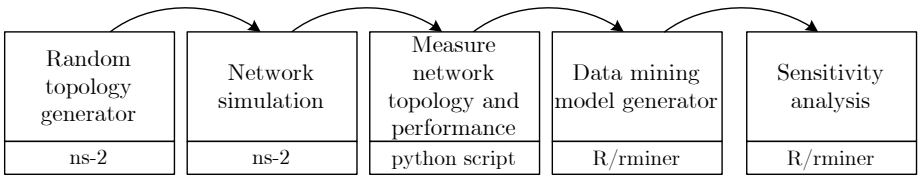

Figure 4.1: Methodology adopted in this study. The five stages are the random network topology generation, the network simulation, the measurement of simulation results, the generation of the data mining model and the sensitivity analysis.

4.2.1 Random network generation

A tcl script was included in ns-2 [93] to generate 3500 network topologies. Each network has 36 nodes, including the gateways, spread in a area of 1000 m×1000 m. The position of each node, defined by its (x,y) coordinates, was generated using two independent uniform distributions. Random positions locating two nodes at a distance smaller than 50 m are rejected and another position is generated. After generating the 36 positions, the connectivity of the network is verified. If a node does not have at least one neighbor located at a distance less than $RXThreshold = 350\,m$, meaning that the node is isolated, the network is rejected and a new network is generated. The first two generated positions are selected to be the gateways.

Different radio channels are assigned to each gateway. Two channel assignment strategies were applied to nodes on each topology. In the first assignment strategy, the channel assigned to each node is generated using a random variable using a uniform distribution. If in the generated scheme there are at least one isolated node, the network is rejected and a new network is generated. In the second assignment strategy, the channel whose gateway is closer was assigned to each node. For doing that, first all nodes are configured in the same channel, and the gateways broadcast advertisement messages through the network using the Proactive PREQ mechanism defined by IEEE 802.11s [1]. Using the advertisement messages received, nodes select the closer gateway or the gateway that sent the first advertisement received by the node if both are at the same distance. Then, different channels are assigned to each gateway and the channel assigned to each node is the same as the chosen gateway.

Fig. 4.2 represents two instances of the generated networks; the lines between nodes represent wireless connectivity between them.

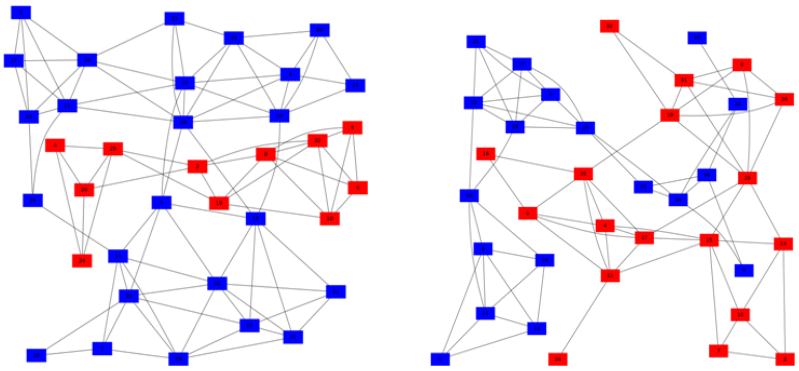

Figure 4.2: Examples of generated random network topologies.The lines between nodes represent wireless connectivity between them. Nodes in different colors are in a different channel.

4.2.2 Network simulation

Each WMN node, except the gateways, generates a traffic flow whose packets are generated by a Poisson process; these packets are UDP and are destined to a node in the Internet through the serving gateway. Simultaneously, a node outside the mesh network generates a similar flow destined to each node in the network, except the gateways. All flows are configured with similar parameters, which are fixed for each simulation.

The IEEE 802.11 data rate used in this study is 54 Mbit/s, but the overhead of lower layers of the communication stack is about 50% [94], leaving $27\,Mbit/s$ per gateway available to transmit packets from 34 nodes. The maximum data rate per flow is $794\,kbit/s = (27\,Mbit/s \times 2\,gateways)/34\,nodes/2\,flows$. Considering that each frame is forwarded through multiple hops until it reaches the gateway, the maximum achievable end-to-end throughput is even lower. Therefore, it is expectable that a considerable amount of frames are lost when the sources debit is above $700\,kbit/s$. We used flows with a data rate of 480 kbit/s to test the networks with low loads and flows with a data rate of 4.8 Mbit/s to test the

networks with high loads which is a saturation situation. Each generated network was simulated four times using ns-2.29; with the two data rates and with 2 different seeds.

The parameters used in simulation are presented on Table 5.3. The simulation tool ns-2 was used with two-ray propagation model in the physical layer, MAC DCF 802.11 in the link layer, and the HWMP [1] was used to establish routes.

Parameter	Value
Propagation Model	two ray ground
Channel data rate	54 Mbit/s
RX Threshold	-70.2 dBm, 350 m
Node distance	176 m
Packet size	1500 bytes
sources debit	4.8 Mbit/s or 480 kbit/s
RTS/CTS	ON
Routing	HWMP
Source type	Poisson (UDP)
WarmUp	10 packet/s × 256 byte
Simulation runs	2

Table 4.1: Parameters used in ns-2.29 simulations of the random network topologies.

The duration of each simulation was configured to give time to generate 10^4 packets on each flow; the exact duration depends on the flow data rate. During the first 3 seconds there are no data flows; this period is used to allow the HWMP routing protocol to execute the proactive tree building functionality; in this phase a route to one of the gateways is added to each node as described in the the Proactive PREQ mechanism [1]; the reverse path is also created. Between second 3 and second 10 the warm up flow takes place between each node and the gateway; this flow enables the ARP tables of each node to be filled. Warm up flows are not considered to calculate the network performance metrics.

4.2.3 Measurement of network topology and network performance

In order to calculate the metrics of network topology and network performance, the two sub-networks resultant from the channel assignment are are either treated separately or as a single network. The metrics are calculated per sub-network when resume the performance of topology of nodes sharing a channel; in this case the two sub-networks are treated separately. The metrics are calculated on the global network when they aggregate the performance and the topology information of all nodes in the network. The metrics are calculated using python scripts that process the simulation trace files provided by ns-2. The performance and topology metrics considered to this study are detailed in Section 4.3 and Section 4.4.

4.2.4 Data mining model

In our work we use a data mining approach, where each network performance metric is modeled as a regression function, as given by the SVM algorithm, that is dependent of the several topology metrics.

The main idea of the SVM is to transform the input data into a high-dimensional feature space by using a nonlinear mapping ϕ. For regression, the ε-insensitive cost function is commonly used [86], which sets a tube around the residuals, being the tiny errors within this tube discarded (Figure 4.3). Then, the SVM finds the best hyperplane within the feature space:

$$\hat{y} = w_0 + \sum_{i=1}^{m} w_i \phi_i(\mathbf{x}) \tag{4.1}$$

where $\hat{y}$ is the predicted value, w_i are the weights (set by the SVM training algorithm), m is the number of support vectors (set by the ε-insensitive tube) and $\mathbf{x}$ is a vector with the input variables.

The ϕ transformation (which is not explicitly known), depends on the adopted kernel function. The Gaussian kernel is the most popular one, presenting less parameters than other kernels, and thus

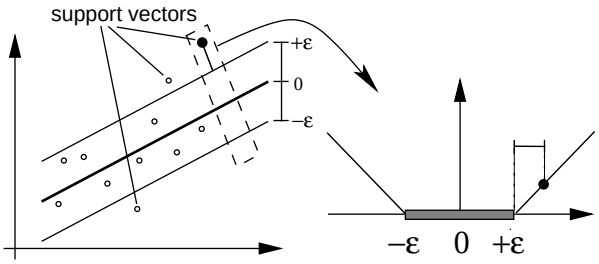

Figure 4.3: Example of a SVM and regression using the ϵ-insensitive tube.

it is adopted in this work:

$$k(x, x') = e^{-\gamma \times \left\| x - x' \right\|^2}, \gamma > 0 \tag{4.2}$$

Under this setup, performance of the regression is affected by three parameters: γ is the parameter of the kernel, C is a complexity penalty parameter, and ε is the width of a ε-insensitive zone. To reduce the search space, the last two values will be set using the heuristics proposed in [95]: $C = 3$ (for a standardized output) and $\varepsilon = \hat{\sigma}/\sqrt{N}$, where $\hat{\sigma} = 1.5/N \times \sum_{i=1}^{N}(y_i - \hat{y}_l)^2$ and $\hat{y}_l$ is the value predicted by a 3-nearest neighbor algorithm. To optimize the most relevant SVM hyper-parameter (γ), we adopted a grid search under the range $\{2^{-15}, 2^{-13}, ..., 2^3\}$, and an internal (i.e. over the training data) 3-fold cross validation was used to select the best γ value (i.e. that produces the lowest absolute deviation error on the validation data produced by the 3-fold scheme) [78]. After setting γ, the SVM was retrained with all training data.

In order to evaluate the performance of the SVM predictions, we considered two popular regression metrics: Mean Absolute Error (MAD), and Coefficient of determination (R^2). Let y denote the target value, $\hat{y}$ the predicted value, $\overline{y}$ and $\overline{\hat{y}}$ the mean of these variables. Then:

$$\begin{aligned} MAD = &\ \textstyle\sum_{i=1}^{N} |y_i - \hat{y}_i| / N \\ R^2 = &\ 1 - \left(\textstyle\sum_{i=1}^{N} (y_i - \hat{y}_i)^2 / \sum_{i=1}^{N} (y_i - \overline{y})^2 \right) \end{aligned} \tag{4.3}$$

Lower values of MAD and R^2 values close to the unit value correspond to a higher predictive capacity. To get robust estimates of the predictive performances of the SVM model, we applied 5 runs of an external (i.e. over all data) 5-fold cross validation, in a total of 25 SVM trainings for each tested configuration. The predictive errors (i.e. MAD and R^2) shown in this work are reported in terms for the mean values of these runs and computed over the test (i.e. unseen) data defined by the 5-fold procedure. All experiments reported were implemented using the rminer library of the R tool [96].

4.2.5 Sensitivity analysis

Another important data mining goal is related with descriptive knowledge, i.e. if it is possible to extract useful understandable knowledge from the data-driven models. In this application domain, this issue is handled by using the fitted SVM data mining models to estimate the impact of topology metrics on the wireless network performance. Despite the high complexity the SVM models (due to the nonlinear kernel transformation), it is still possible to extract knowledge in terms of input variable importance and Variable Effect Characteristic (VEC) curves by using a 1-D sensitivity analysis [92]. This sensitivity analysis works by successively holding all inputs to their average values except one input, which is varied through its range of values in order to observe its effect on the target responses. The higher the variance observed in the responses, the higher is the importance of the input variable. Thus, the set of input variables can be ranked according to the variance measure of the sensitivity responses. In addition, during this 1-D sensitivity analysis, the average effect of an all probed individual input levels on the model predictions can be stored. By using such data, it is possible to plot the respective VEC curve, which gives a visual and easy to read information about the average impact of a given input variable in the fitted model.

4.3 Network performance metrics

Network performance can be characterized using measures such as throughput, delay and packet loss. In our study we focus on node throughput and delay. First we want to maximize the average node throughput. Second, we want to maximize fairness among node's throughput, to be sure that each mesh node offers an effective connection of its stations to the infra-structured network. Third, we want to minimize the end-to-end delay experienced by packets transmitted to and from the mesh nodes and the infra-structured network. These metrics are defined below.

The present section defines the performance metrics considered to this study and characterizes the metrics obtained on the simulations carried out. The set of 28000 experiments (7000 topologies $\times$ 2 seeds $\times$ 2 data rates) was studied statistically considering that each of the metrics is a random variable and the measures taken from the simulation are samples of those variables. The probability density function (PDF) of each network performance metric is shown in Fig. 4.4 for simulations with low and high loads calculated per sub-network or over the global network. The mean value and standard deviation of the performance metrics of the samples are represented in graphics as μ and σ respectively.

4.3.1 Throughput

The throughput is defined as the sum of the bit rate received by destinations. Formally, the throughput T_A measured on channel A is given in bits per second by Eq. 4.4 where T_i^{RX} is the number of packets received by node i, T_i^{TX} is the number of packets received by the gateway sent by node i, and L is the packet length given in bits.

$$T_A = \frac{\sum (T_i^{RX} + T_i^{TX}) L}{duration\ of\ simulation} \tag{4.4}$$

The histogram of the throughput is presented in Figure 4.4(a), 4.4(d), 4.4(g), and 4.4(j) for simulations with low and high loads calculated per sub-network or over the global network. When the network is low loaded, the achieved network throughput is also low;

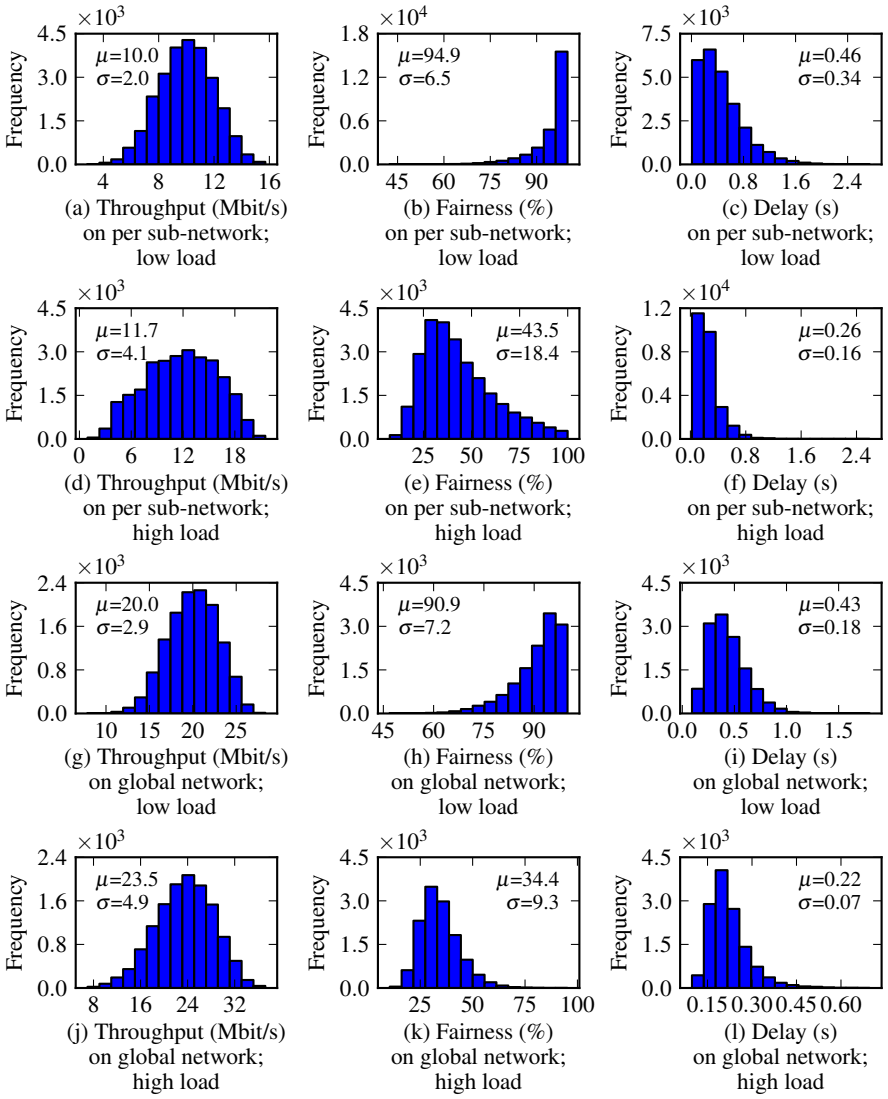

Figure 4.4: Histograms of performance metrics.

this is shown by comparing Figure 4.4(a) with Figure 4.4(d), and Figure 4.4(g) with Figure 4.4(j).

Experiments with high source load data rates show a wider histogram and larger standard deviation (4.1 Mbit/s for per sub-network and 4.9 Mbit/s for global network) when compared with low source load data rates (2.0 Mbit/s for per sub-network and 2.9 Mbit/s for global network) meaning more uncertainty in the throughput results when the network is saturated.

Throughput results for the global network are about the double of those calculated per sub-networks since the number of flows considered is also the double. This is the reason why the mean values

of throughput global network measures (20.0 Mbit/s for low source load data rates and 23.5 Mbit/s for high source load data rates) are the double of the mean values of throughput sub-network measures (10.0 Mbit/s for low source load data rates and 11.7 Mbit/s for high source load data rates). Despite the standard deviation of the throughput in global network measures (2.9 Mbit/s for low source load data rates and 4.9 Mbit/s for high source load data rates) is higher than the standard deviation of throughput sub-network (2.0 Mbit/s for low source load data rates and 4.1 Mbit/s for high source load data rates), it is not the double. This is why global network throughput present a narrowest histogram when compared with per sub-network.

4.3.2 Fairness

The measure of the fairness of the achieved throughput among flows in the network or in the sub-network is estimated using the Jain Index [97]. Eq. 4.5 shows how fairness is calculated, where T_i is the sum of T_i^{RX} and T_i^{TX}. The fairness J is independent of scale, applies to any number of nodes and is bounded between 0 and 1, where $J = 1$ indicate a totally fair network.

$$J = \frac{(\sum T_i)^2}{n \sum T_i^2} \tag{4.5}$$

The histogram of the fairness is presented in Figure 4.4(b), 4.4(e), 4.4(h), and 4.4(k) for simulations with low and high loads calculated per sub-network or over the both sub-networks. Figure 4.4(e) and 4.4(k) show that when 34×2 flows (download plus upload flow per node) of 4.8 Mbit/s are inserted in the network, it gets saturated because fairness is low. Nodes that are not in the neighborhood of the gateways have more difficulty to transmit their packets through long multi-hop routes and low values of fairness are achieved by most of the experiments.

Figure 4.4(b) shows that when the flow data rate is low, the fairness is high (around 100%) in most experiences, showing that all nodes in each sub-network have similar chances of transmitting their

packets because the network is not saturated. With these load conditions, the fairness measured using the throughput achieved by all nodes in the network is lower when compared with per sub-network fairness, as shown by Figure 4.4(h); the two sub-networks of each scenario typically have different topological characteristics, mostly the number of nodes per sub-network, and even if the bandwidth is evenly distributed among the nodes in a sub-network, the achieved per node throughput on each sub-network is different, resulting in lower fairness.

4.3.3 Delay

The delay is calculated as the mean time elapsed between the creation of a packet and its reception by the final destination. Lost packets are not considered. The histogram of the delay is presented in Figure 4.4(c), 4.4(f), 4.4(i), and 4.4(l) for simulations with low and high loads calculated per sub-network or over the both sub-networks. When the flow data rate is high (Figure 4.4(f) and 4.4(l)), most packets to and from nodes that are not in the gateway neighborhood are lost. Therefore most of the packets considered to calculate the delay, which are those successfully delivered to their destinations, have to be forwarded through less hops when compared with the low data rate scenarios leading to lower delays when compared with low traffic load conditions.

Overall network delay is the weighted mean of delays of packets delivered in both sub-networks, therefore the overall network and per sub-network delays have a similar mean; the standard deviation is lower.

4.4 Network topology metrics

The topology of each network is summarized by a set of metrics identified in Chapter 3 that includes mean hop count, neighbor node density, number of nodes in the gateway neighborhood, the miss ratio of the overall network, and the miss ratio on the gateway neighborhood. The number of nodes using each radio channel is an important characteristic when the channel assignment is applied

to random networks. This metric is being considered in this study because the topologies that were studied were regular and the channel assignment resulted in symmetric sub-network topologies. The topology metrics are detailed in the next sub-sections.

The present section defines the performance metrics considered to this study and characterizes the metrics obtained on the simulations carried out. The set of 28000 experiments (7000 topologies $\times$ 2 seeds $\times$ 2 data rates) was studied statistically considering that each of the metrics is a random variable and the measures taken from the simulation are samples of those variables. The probability density function (PDF) of each network topology metric is shown in Fig. 4.4 for the simulated networks calculated per sub-network or over the global network. The mean value and standard deviation of the performance metrics of the samples are represented in graphics as μ and σ respectively.

4.4.1 Number of nodes

The number of nodes using each radio channel is an important characteristic when the channel assignment is applied to random networks. In Chapter 3 this metric was not considered because the topologies that were studied were regular and the channel assignment resulted in symmetric sub-network topologies.

The total number of nodes in all simulated random network scenarios is 36. When the channel assignment scheme is applied to these networks, the resultant sub-networks may have different number of channels. When each sub-network is analyzed alone, i.e. the metrics are calculated per sub-network, the number of nodes metric counts the nodes using a common channel. The histogram of the number of nodes found over all the simulations carried out is presented in Figure 4.5(a). Since the channel was randomly assigned to nodes on the topology, the mean number of nodes on each channel is 18 which is half the total number of nodes on the networks (36).

When the global network is considered the metric is the number of nodes difference which is the difference between the number of nodes n in sub-networks of a same network. Nodes in a sub-network share a common radio channel and their packets are

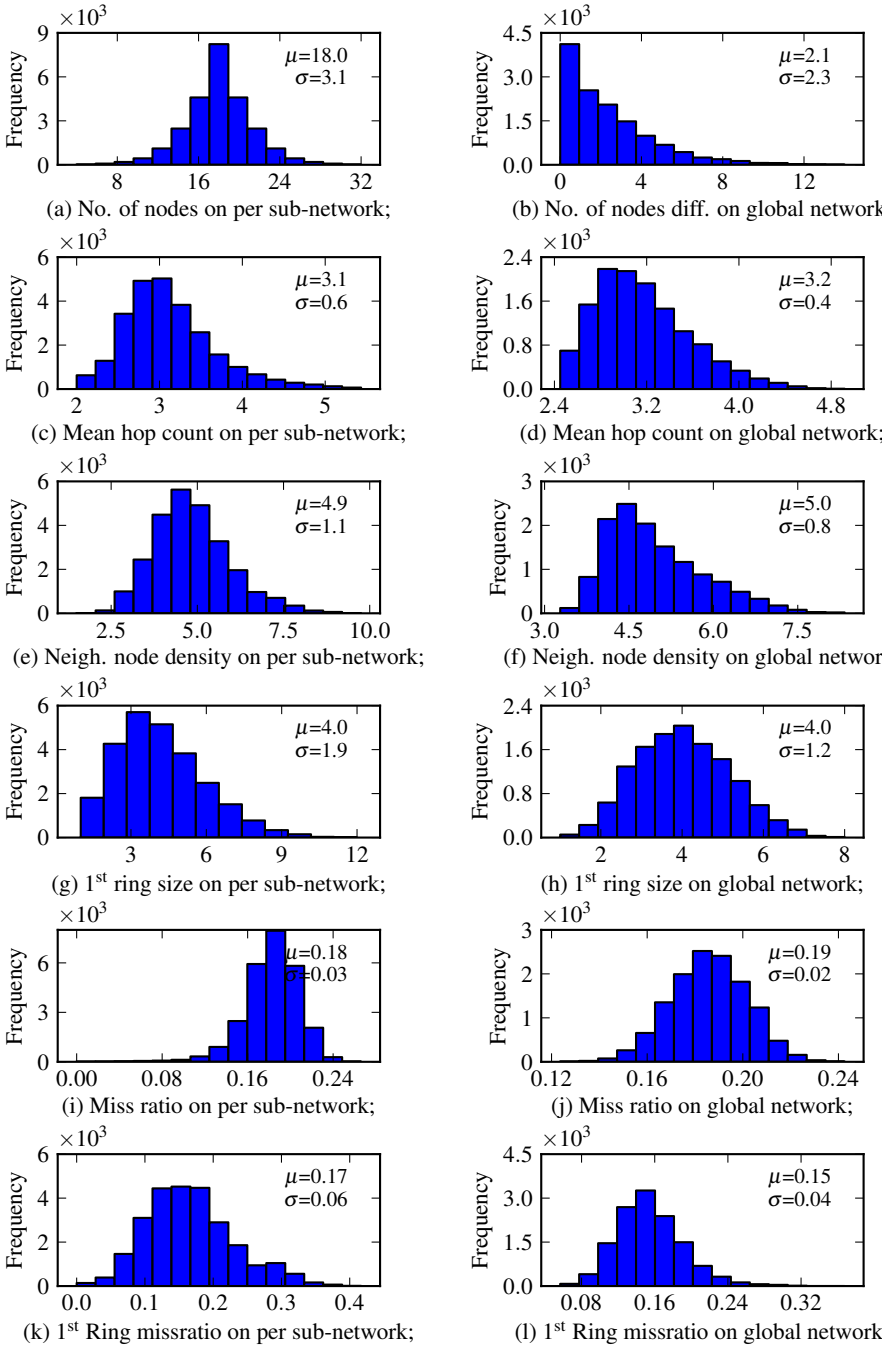

Figure 4.5: Histograms of topology metrics.

forwarded through a common gateway. For instance, if the sub-network using channel A has 20 nodes and the sub-network using channel B has 16 nodes, then the number of nodes difference is 4. The histogram of the number of nodes difference found over all the simulations carried out is presented in Figure 4.5(b).

4.4.2 Mean hop count

The mean hop count is the mean number of hops that a packet has to be forwarded to reach the gateway when it is sent by a node in the wireless mesh network. For packets sent to wireless mesh nodes from the infra-structured network, the hop count is number of times a packet has to be forward inside the mesh network until it reaches its wireless mesh node. The gateways and nodes on the 1st ring are not considered in this calculation since the size of 1st ring metric already includes this topological characteristic. For reasons related with minimizing the data mining model errors, it is preferable to use independent metrics when possible. For instance, considering the sample network in Figure 4.6 the hop count of each node that is not on the 1st ring is $H_A = 3$, $H_B = 2$, $H_C = 2$ and the mean hop count of the network is $H = (3+2+2)/3 = 2.33$.

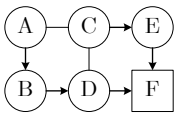

Figure 4.6: Sample topology used to show the calculation of topology metrics of a network; the square node F is the network sink.

The histogram of the mean hop count found over all the simulations carried out is presented in Figure 4.5(c), and 4.5(db) respectively for per sub-network and the global network. The minimum mean hop count measured in the simulated sub-networks is 2, which means that all networks have at least 1 node on the 2nd ring.

4.4.3 Neighbor node density

Neighbor node density is defined as the mean number of nodes in the carrier sensing range of each node in the network. Regarding the graph theory, the neighbor node density is the mean degree of the network graph. For the network on Figure 4.6 we have nodes A, B, E and F with 2 neighbors, and nodes C and D with 3 neighbors, thus the neighbor node density for Figure 4.6 is $d = [(4 \times 2) + (2 \times 3)]/6\, nodes = 2.33$. The histogram of the neighbor node density found over all the simulations carried out is presented

in Figure 4.5(e), and 4.5(f) respectively for per sub-network and the global network.

4.4.4 1st ring size

The 1st ring size is the number of nodes at one hop distance of the gateway, which is also the neighbor node density of the gateway. In graph theory, this metric is the degree of the gateway vertex. The histogram of the size of 1st ring found over all the simulations carried out is presented in Figure 4.5(g), and 4.5(h) respectively for per sub-network and the global network. Most of simulated sub-networks have 3, 4 or 5 nodes around the gateway (Figure 4.5(g)), but there are sub-networks with just 1 or up to 12 nodes directly connected to the gateway resulting a mean value of 4 nodes. The metric calculated for the global network, is the mean of number of nodes on the neighborhood of gateways on each sub-network. This measure presents the same mean as the one measured per sub-network, however the variance is smaller.

4.4.5 Miss ratio

The miss ratio, defined in Chapter 2 (Eq. 2.8 on page 39), is a measure of the severity of the hidden nodes in the network. The histogram of the miss ratio found over all the simulations carried out is presented in Figure 4.5(i), and 4.5(j) respectively for per sub-network and the global network. These graphs show that the severity of the hidden nodes in the network is low since this metric varies between 0 and 1 and the higher value observed is 0.26 in the case of the metric calculated per sub-network.

4.4.6 1st ring miss ratio

The 1st ring miss ratio, defined in Chapter 3 (Eq. 3.1 on page 63), is a measure of the severity of the hidden nodes in the neighborhood of the gateway. The histogram of the 1st ring $missratio$ found over all the simulations carried out is presented in Figure 4.5(k), and 4.5(l) respectively for per sub-network and the global network. These graphs show that the severity of the hidden nodes in the

neighborhood of the gateway is not high since this metric varies between 0 and 1 and the higher value observed is 0.4 in the case of the metric calculated per sub-network.

4.4.7 Correlation with performance metrics

The linear correlation ρ between the performance metrics and each of the topology metrics, presented in Table 4.2, is given by Eq. 4.6, where $\overline{x}$ and σ_x are respectively the mean value and standard deviation of each of the topology metrics samples, $\overline{y}$ and σ_y are respectively the mean value and standard deviation of the performance metrics of the samples, and n_e is the number of considered experiments; ρ can take values in the interval $[-1,1]$, where $\rho = 0$ means that the throughput and the topology metric are uncorrelated and $|\rho| = 1$ means that the throughput and the topology metric have a linear relation positive ($\rho = 1$) or negative ($\rho = -1$).

$$\rho = \frac{\sum_{i=1}^{ns}(x_i - \overline{x})(y_i - \overline{y})}{(n_e - 1)\sigma_x \sigma_y} \tag{4.6}$$

4.5 Data mining models results

The results obtained after the data mining process are presented in Figure 4.7, Figure 4.8 and Figure 4.9. The models obtained for low loaded scenarios have less errors (lower MAD values and higher R^2) than the models obtained with high loads, showing that non saturated networks have a more predictable behavior, as expected. On the top of each figure are represented the importance graphs which show the relative importance for each topology metric on each model. For each model the sum of importances of all topology metrics is 1. The rest of the graphs on the figures show the joint probability function graphs of each pair (topology metric, performance metric) under the VEC curves of each topology metric for each model. The simple histograms shown in Figure 4.4 and Figure 4.5 are represented on the top and on the right of each figure for ease the reading of the joint probability function graphs. On the joint probability function graphs, a dark spot represents more

			Number of nodes	Mean hop count	Neigh. node density	Size of 1st ring	Miss ratio	1st ring miss ratio
Throughput	per sub network	480k	-0.01	-0.68	0.17	0.82	-0.11	-0.45
		4800k	-0.27	-0.37	-0.03	0.80	-0.36	-0.76
	overall network	480k	-0.32	-0.77	0.13	0.84	-0.20	-0.37
		4800k	-0.03	-0.39	0.16	0.75	-0.19	-0.59
Fairness	per sub network	480k	-0.37	-0.69	0.04	0.36	-0.18	-0.15
		4800k	-0.25	-0.37	0.10	0.06	-0.25	0.10
	overall network	480k	-0.69	-0.45	-0.3	0.34	0.00	0.02
		4800k	-0.09	-0.40	0.18	0.39	-0.09	-0.05
Delay	per sub network	480k	0.63	0.66	0.23	-0.59	0.35	0.54
		4800k	0.46	0.28	0.25	-0.59	0.27	0.72
	overall network	480k	0.31	0.76	-0.13	-0.76	0.23	0.36
		4800k	0.02	0.39	-0.16	-0.69	0.20	0.64

Table 4.2: Values of correlation between network topology metric and network performance metrics obtained on simulation results.

occurrences of networks showing that topological and performance metric simultaneously.

4.5.1 Model for throughput

Figures 4.7(a), 4.7(b), 4.7(c) and 4.7(d) show the importance of graphs for the throughput models obtained for data rates of 480 kbit/s and 4.8 Mbit/s calculated per sub-network and over the global network. These graphs show that the size of 1st ring is the most important parameter for throughput models, with a relative importance of respectively 0.41 and 0.39 for low and high traffic loads when measures are taken per sub-network, and respectively 0.52 and 0.73 for low and high traffic loads when measures are taken on the global network.

Figure 4.7(a) shows that for the measures taken per sub-network, when the network has low traffic loads, the mean hop count and the number of nodes difference metrics are also important to the throughput model with importances of 0.24 and 0.22 respectively.

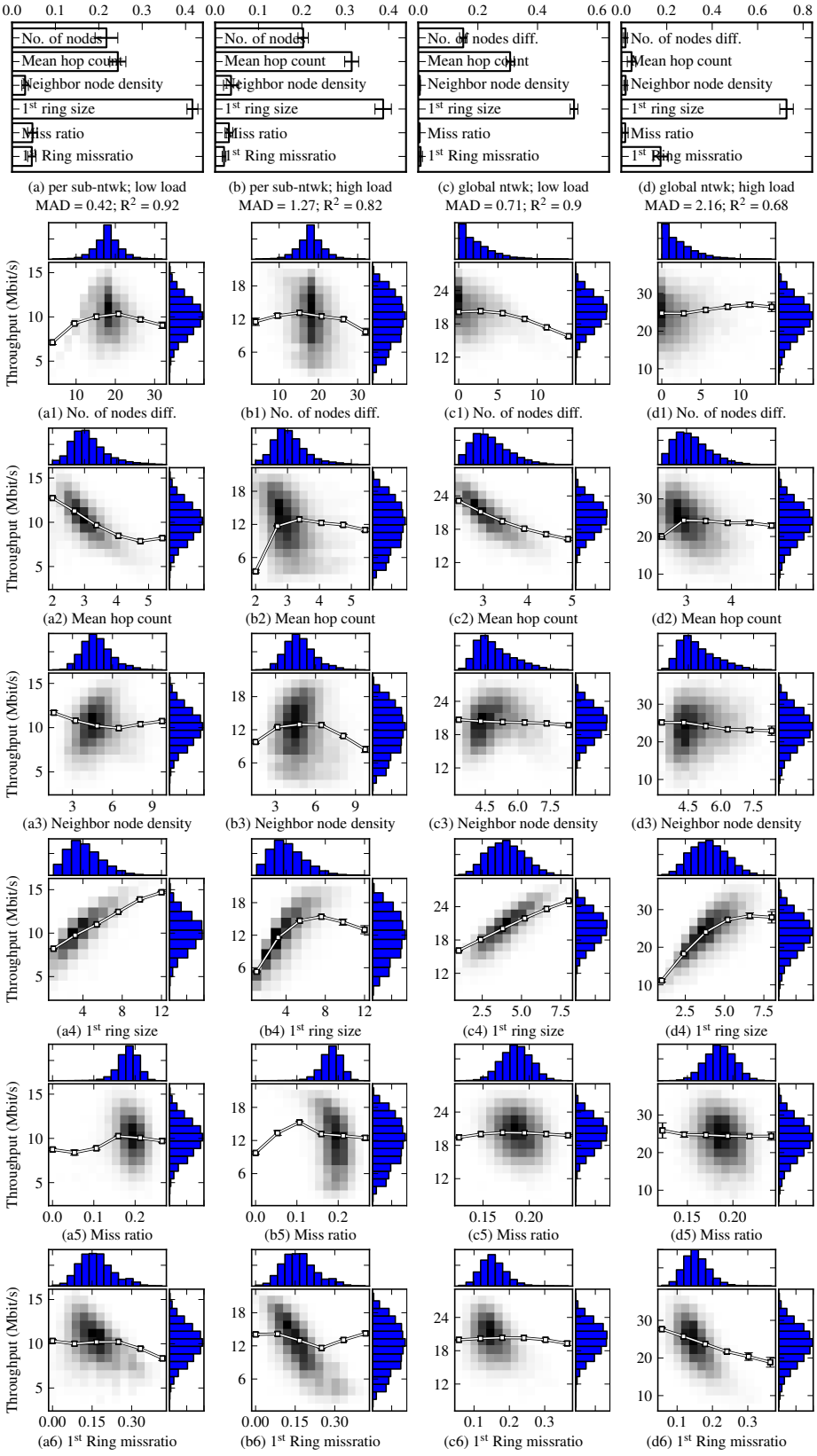

Figure 4.7: Throughput models.

The miss ratio on the overall network, 1st ring miss ratio metric and neighbor node density have importances below 0.1 and are considered to have no impact on this model output.

Figure 4.7(b) shows that for the measures taken per sub-network, when the network has high traffic loads, the mean hop count and number of nodes difference metrics are also important to the throughput model with importances of 0.31 and 0.20. The miss ratio on the overall network, 1st ring miss ratio metric and neighbor node density have importances below 0.1 and are considered to have no impact on this model output.

Figure 4.7(c) shows that for the measures taken over the global network, when the network has low traffic loads, the mean hop count and the number of nodes difference metrics are also important to the throughput model with importances of 0.31 and 0.15 respectively. The miss ratio on the overall network, 1st ring miss ratio and neighbor node density have importances below 0.1 and are considered to have no impact on this model output.

Figure 4.7(d) shows that for the measures taken over the global network, when the network has high traffic loads, the 1st ring miss ratio metrics are also important to the throughput model with importance of 0.17. The mean hop count, neighbor node density, miss ratio on the overall network, and number of nodes difference metrics have importances below 0.1 and are considered to have no impact on this model output.

4.5.1.1 Number of nodes

Figures 4.7(a1), 4.7(b1), 4.7(c1) and 4.7(d1) represent the joint probability density function graphs and the VEC curves of the number of nodes in the network and the throughput obtained for data rates of 480 kbit/s and 4.8 Mbit/s calculated per sub-network and over the global network. The joint probability density function graph on these figures show that highest throughputs were obtained by scenarios with equal number of nodes in each channel.

The VEC curve in Figure 4.7(a1) shows that, when the network is low loaded and the metrics are taken per sub-network, a low number of nodes results in low throughput. If the network is not

saturated, all traffic generated is delivered; if the sub-network has a low number of nodes, less traffic is generated and the throughput is low. However, the VEC curve in Figure 4.7(c1) shows that, when the network is low loaded and the metrics are taken over the global network, the highest throughputs were obtained by scenarios with equal number of nodes in each channel. When the two sub-networks on a same network have an unbalanced number of nodes, one of the sub-networks may obtain a high throughput, but the throughput of the global network is low.

The VEC curve in Figure 4.7(b1) shows that, when the network is high loaded and the metrics are taken per sub-network, a low number of nodes results in high throughput. The network is more saturated if there is more traffic in the network; if the sub-network has a low number of nodes, less traffic is generated, the sub-network is less saturated (less collisions) and the throughput is high.

The VEC curve in Figure 4.7(d1) shows that, when the network is high loaded and the metrics are taken over the global network, the number of nodes has a low impact on the obtainable network throughput because the slight gain in having a sub-network with less nodes and therefore with high throughput, is canceled by the high saturated sub-network that has more nodes.

4.5.1.2 Mean hop count

Figures 4.7(a2), 4.7(b2), 4.7(c2) and 4.7(d2) represent the joint probability density function graphs and the VEC curves of the mean hop count in the network and the throughput obtained for data rates of 480 kbit/s and 4.8 Mbit/s calculated per sub-network and over the global network.

The joint probability density function graph on figures 4.7(a2) and 4.7(c2) show that, when the network is low loaded, the throughput and the mean hop count of the network have an almost linear inverse relationship meaning that networks with higher mean hop count obtain lower throughputs. VEC curves on these figures show the same result. Higher throughputs are obtained when nodes in the network are closer to the gateway (low mean hop count). That

result was expectable because data packets have to be forwarded less times in the mesh network until they reach the final destination.

The joint probability density function graph on figures 4.7(b2) and 4.7(d2) show that, when the network is high loaded, the throughput and the mean hop count of the network continue to be inversely related despite having a less clear relation. With this traffic conditions, only nodes on the gateway neighborhood can transmit and receive packets as shown in [28] and by the low values of fairness shown in Figure 4.4(h), therefore the hop count of nodes that are not directly connected to the gateway is less important.

For high loaded networks the impact of the mean hop count on the throughput when metrics are taken per sub-network is much higher than when metrics are taken over the global network as shown by figures 4.7(b) and 4.7(d) and by the VEC curves on figures 4.7(b2) and 4.7(d2).

4.5.1.3 Neighbor node density

Figures 4.7(a3), 4.7(b3), 4.7(c3) and 4.7(d3) represent the joint probability density function graphs and the VEC curves of the neighbor node density in the network and the performance metrics obtained for data rates of 480 kbit/s and 4.8 Mbit/s calculated per sub-network and over the global network. The flat VEC curves, the joint probability density function graphs, and the low correlation between throughput and neighbor node density shown in Table 4.2 show that neighbor node density has a low impact on the network throughput.

4.5.1.4 Size of 1st ring

Figure 4.7(a4), 4.7(b4), 4.7(c4) and 4.7(d4) represent the joint probability density function graphs and the VEC curves of the size of 1st ring in the network and the throughput obtained for data rates of 480 kbit/s and 4.8 Mbit/s calculated per sub-network and over the global network. The joint probability density function graphs and the high values of correlation between the size of first ring and the throughput in Table 4.2 shows that the throughput and the size of 1st ring of networks have an almost linear relationship.

The VEC curves for throughput models are presented as a white line in Figure 4.7(a4), 4.7(b4), 4.7(c4) and 4.7(d4). VEC curves show that high values of throughput are obtained when more nodes are in the neighborhood of the gateways (size of 1st ring), but the relationship between the two metrics is not linear when the network is high loaded.

When a large number of nodes are directly connected to the gateway, there are two effects that contribute to increase the throughput: (1) data packets have to be forwarded only once in the mesh network until they reach the final destination, what means that less radio resources are used, leaving more opportunities to other packets to be transmitted; (2) the gateway can manage well the radio resources using the carrier sense and RTS/CTS, thus reducing the number of collisions.

4.5.1.5 Miss ratio

Figures 4.7(a5), 4.7(b5), 4.7(c5) and 4.7(d5) represent the joint probability density function graphs and the VEC curves of the miss ratio of the network and the throughput obtained for data rates of 480 kbit/s and 4.8 Mbit/s calculated per sub-network and over the global network. The flat VEC curves, the joint probability density function graphs, and the low correlation between throughput and miss ratio shown in Table 4.2 show that miss ratio has a low impact on the network throughput.

4.5.1.6 1st ring miss ratio

Figures 4.7(a6), 4.7(b6), 4.7(c6) and 4.7(d6) represent the joint probability density function graphs and the VEC curves of the 1st ring miss ratio of the network and the throughput obtained for data rates of 480 kbit/s and 4.8 Mbit/s calculated per sub-network and over the global network. The joint probability density function graphs in these figures show that low 1st ring miss ratio topologies results in high network throughputs.

The flat VEC curves on figures 4.7(a6), 4.7(b6) and 4.7(c6) show that for low loaded situations, the 1st ring miss ratio has a low impact on the network throughput. The joint probability density

function graphs on the same figures show that an inverse relation exists between the 1st ring miss ratio and the throughput; however, the other topology metrics were considered to have more impact on the throughput model resulting in flat VEC curves.

The VEC curve in Figure 4.7(d6) shows that, when the network is high loaded and global network metrics are considered, low 1st ring miss ratio have a high impact on the network throughput. When the network is high loaded, there are more collisions [28], in those situations the existence of more hidden nodes around the gateway, which are given by the 1st ring miss ratio, increase the occurrence of collisions on the bottleneck of the network reducing the throughput.

4.5.2 Model for fairness

Figures 4.8(a), 4.8(b), 4.8(c) and 4.8(d) show the importance graphs for the fairness models obtained for data rates of 480 kbit/s and 4.8 Mbit/s calculated per sub-network and over the global network.

Figure 4.8(a) shows that for measures taken per sub-network, when the network has low traffic loads, the number of nodes and the mean hop count are the most important metrics in the fairness model with importances of 0.45 and 0.36 respectively. The miss ratio on the overall network, 1st ring miss ratio, the neighbor node density, and the 1st ring size have importances below 0.1 and are considered to have no impact on this model output.

Figure 4.8(b) shows that for the measures taken per sub-network, when the network has high traffic loads, the number of nodes is the most important metric with an importance of 0.37. The 1st ring size and the mean hop count metrics are also important to the fairness model both with importance of 0.20. The miss ratio on the overall network has an importance of 0.12. The 1st ring miss ratio and neighbor node density have importances below 0.1 and are considered to have no impact on this model output.

Figure 4.8(c) shows that for measures taken over the global network, when the network has low traffic loads, the mean hop count and the number of nodes difference are the most important metrics to fairness model with importances of 0.43 and 0.42 respectively. The miss ratio on the overall network, 1st ring miss ratio metric,

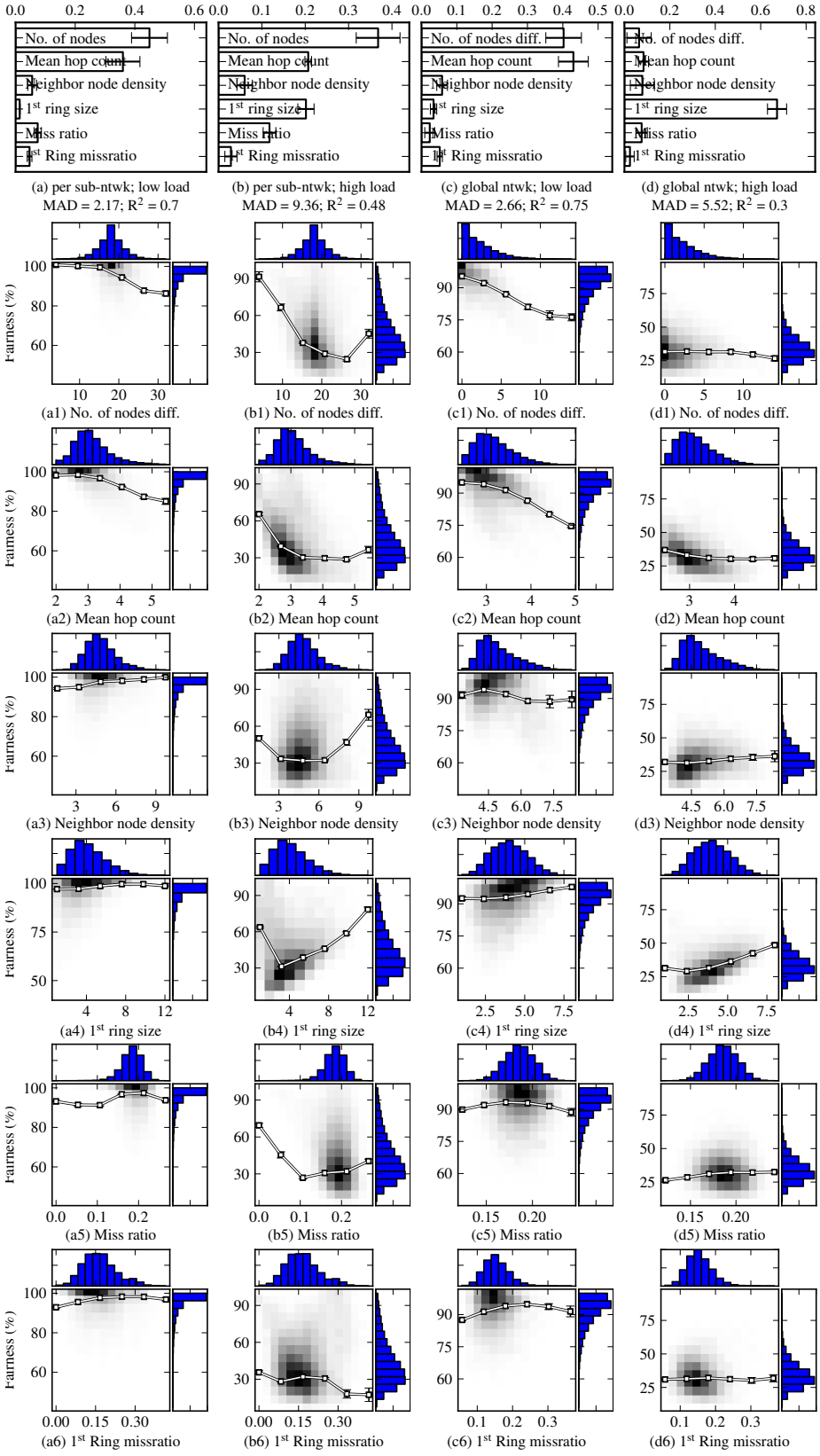

Figure 4.8: Fairness models.

the 1st ring size, and the neighbor node density have importances below 0.1 and are considered to have no impact on this model output.

Figure 4.8(d) shows that for the measures taken over the global network, when the network has high traffic loads, the 1st ring size is the most important metric for the fairness model with an importance of 0.67. All the other metrics have importances below 0.1 and are considered to have no impact on this model output. Under these traffic load conditions, the network becomes saturated and only nodes on the neighborhood of the gateway are able to transmit and receive their packets. When more nodes are around the gateway, the network becomes more fair, as shown in Figure 4.8(d1).

On unsaturated mesh networks, all nodes are able to transmit and receive their packets, therefore fairness is close to 100% in most of the cases. However, if an unbalanced number of nodes exist in sub-networks using different channels, the overall network becomes unfair as shown in figures 4.8(a1) and 4.8(c1). The same applies when several nodes are more than 4 hops away from the gateway as shown in figures 4.8(a2) and 4.8(c2).

Fairness models have high errors when compared with the throughput and delay models. This is because the considered topology metrics do not have a great impact on the network fairness as can be seen by the flat shape of VEC curves. These curves show that even the topology metrics with more importance imply a small variability on the output of the model. This shows that fairness is a very unpredictable performance metric in wireless mesh networks mostly when high traffic loads are involved.

4.5.3 Model for delay

Figure 4.9(a), Figure 4.9(b), Figure 4.9(c) and Figure 4.9(d) show the importance graphs for the delay models obtained for data rates of 480 kbit/s and 4.8 Mbit/s calculated per sub-network and over the global network.

Figure 4.9(a) shows that for the measures taken per sub-network, when the network has low traffic loads, the number of nodes is most important metric in the delay model with an importance of 0.59.

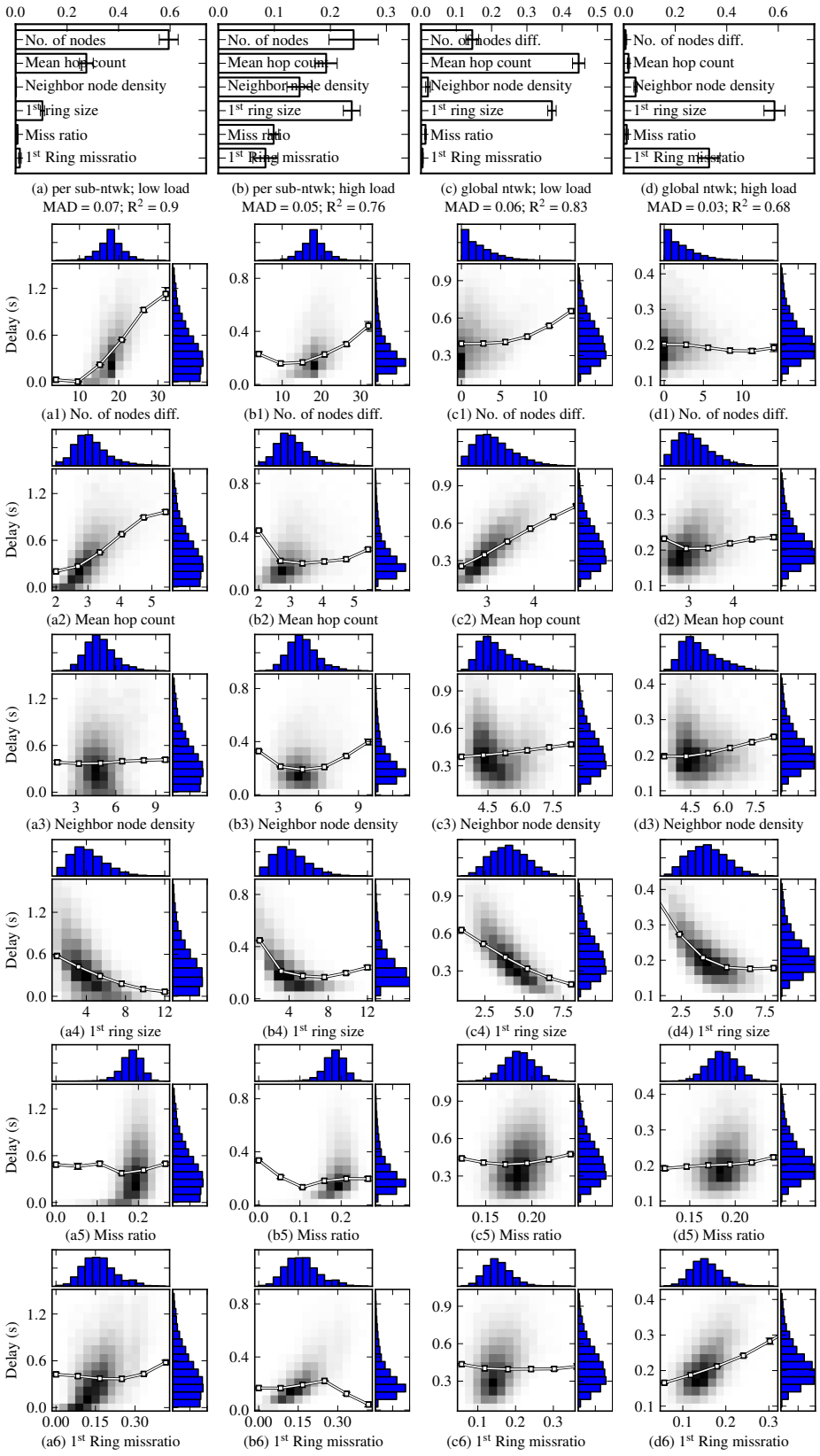

Figure 4.9: Delay models.

The mean hop count and the 1st ring size are also important metrics to the delay model with importances of 0.27 and 0.11 respectively. The miss ratio on the overall network, 1st ring miss ratio, and the neighbor node density have importances below 0.1 and are considered to have no impact on this model output.

Figure 4.9(b) shows that for the measures taken per sub-network, when the network has high traffic loads, the number of nodes and the 1st ring size are the most important metrics both with importances of 0.24. The mean hop count is also important to the delay model both with an importance of 0.19. The 1st ring miss ratio and neighbor node density have importances below 0.1 and are considered to have no impact on this model output.

Figure 4.9(c) shows that for measures taken over the global network, when the network has low traffic loads, the mean hop count and the 1st ring size are the most important metrics to delay model with importances of 0.45 and 0.37 respectively. The number of nodes is also important to the delay model with an importance of 0.15. The miss ratio on the overall network, 1st ring miss ratio, and the neighbor node density have importances below 0.1 and are considered to have no impact on this model output.

Figure 4.9(d) shows that for the measures taken over the global network, when the network has high traffic loads, the 1st ring size is the most important metric for the delay model with an importance of 0.59. The 1st ring miss ratio is also important to the delay model with an importance of 0.33. The other topology metrics have importances below 0.1 and are considered to have no impact on this model output. Under these traffic load conditions, the network becomes saturated and only nodes on the neighborhood of the gateway are able to transmit and receive their packets. When more nodes are around the gateway, most of the packets are transmitted over a single hop resulting in low delay, as shown in Figure 4.9(d4). If the miss ratio on the 1st ring is low then there are less collisions on the gateway neighborhood which causes less retransmissions and the delay is low, as shown in Figure 4.9(d6).

Delay and throughput are related performance metrics as shown by the join probability function plot on Fig. 4.10. Low throughputs occur when the delay is high; when packets take more time to reach

the final destination, radio resources are less time available to transmit other packets, resulting in lower throughputs. The importance values are slightly different on the two models, but they share all the important input parameters as can be observed by comparing Figures 4.7(a), 4.7(b), 4.7(c) and 4.7(d) with Figures 4.9(a), 4.9(b), 4.9(c) and 4.9(d). The VEC curves on Figure 4.9 reflect the inverse relation between delay and throughput metrics since they have the oposite behaviour of VEC curves on Figure 4.7.

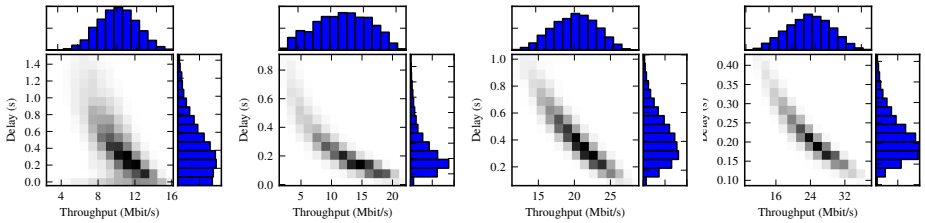

(a) Low traffic load (b) High traffic load (c) Low traffic load (d) High traffic load

Figure 4.10: Join probability function plot of delay and throughput.

4.6 Summary

In this chapter we rank the relative importance of network topology characteristics on the performance of a single-radio multi-channel IEEE 802.11 WMN. A set of 3500 topologies with 36 randomly positioned nodes was created using the network simulator ns-2 [93]. Two channel assignment strategies were then applied to each of the 3500 topologies, assigning one of two possible channels to each node. Each of the 7000 networks was simulated four times using ns-2 with two possible traffic loads and two different simulation seeds; low load and high load were simulated. The topological and performance metrics from the 28000 network simulations were used to train a data mining model. The considered topological metrics were (1) the number of nodes per sub-network, (2) the mean hop count, (3) the neighbor node density, (4) the number of nodes in the 1^{st} ring, (5) the *miss ratio*, and (6) the 1^{st} ring *miss ratio*. The input parameters of the models are six topology metrics enumerated above and the output of each model was the three performance metrics: network aggregate throughput, fairness, and delay. Using fitted data

mining models, the effect of topology metrics on performance was quantified using a sensitivity analysis procedure which revealed the relative importance of each topology metric for each model; the sum of the importance of all topology metrics is 1 for each model and are the following:

Throughput Model: When the network has low traffic loads, the size of 1^{st} ring, the mean hop count and the number of nodes difference metrics are important to the throughput model with relative importance of 0.52, 0.31 and 0.15 respectively. When the network has high traffic load, the size of 1^{st} ring and the miss ratio on the 1^{st} ring are important to the throughput model with relative importance of 0.72 and 0.17 respectively.

Fairness Model: When the network has low traffic load, the mean hop count and the number of nodes difference are important to the fairness model with relative importance values of 0.43 and 0.32 respectively. When the network has high traffic load, the size of 1^{st} ring is the most influential parameter of the fairness model with a relative importance of 0.67.

Delay Model: When the network has low traffic load, the mean hop count, the size of 1^{st} ring, and the number of nodes difference are important to the delay model with relative importance values of 0.45, 0.37 and 0.14 respectively. When the network has high traffic load, the size of 1^{st} ring and the 1^{st} ring miss ratio are important to the delay model with relative importance values of 0.59 and 0.33 respectively.

These results suggest that the topology metric that has the greatest impact on the performance of a WMN is the number of nodes that are directly connected to the gateway: a larger 1^{st} ring results in increased data throughput, increased throughput fairness, and lower delay. Hop distance of nodes to the gateway and the difference of number of nodes between sub-networks also impact network performance, but mostly in provisioning of fairness. That study also suggests that throughput and delay could be improved by avoiding

hidden nodes, in particular on links to the gateway. Other topology metrics are considered to have little influence on the models output.

SVM have been successful used to solve a wide range of problems in statistics, science and engineering. To the best of our knowledge, these techniques have not yet been applied to the study of wireless networks topologies or used to rank the impact of topology metrics on the wireless network performance, which is a complex problem.

Chapter 5

Topology Aware Channel Assignment

This chapter addresses the problem of assigning channels to nodes. Channel assignment is made based solely with topological information that can be obtainable by a network manager. The use of multiple channels when a single-radio interface per node is available leads to the problem of deciding which channel to assign to each node; in order to provide a good quality of experience to users, such channel assignment should consider three important aspects: (a) balance the load among the available channels, (b) improve the connectivity of the gateways neighborhood, and (c) minimize the number of hidden nodes.

Balance the load among the available channels. For small or medium (up to 32) nodes stub WMN, the network radius is roughly below 3 hops. Therefore, most of the links operating in the same channel will interfere with each other [62, 63]. Since in CSMA/CA the interference depends on the traffic on the network links [18], the minimization of the overall interference demands that the traffic on links of each channel are kept at minimum values. This can be achieved by minimizing the load in each of the sub-networks operating in each channel which requires the balancing of the traffic among the channels.

Improve the connectivity of the gateways neighborhood. In stub WMN the gateways are the network bottlenecks. When the network connectivity degree decreases due to channel assignment, the vulnerabilities of the gateway neighborhood become even more exposed unless a special attention given to the design of this part of the network.

Minimize the number of hidden nodes. When multiple channels are assigned to single-radio nodes, the degree of network connectivity will be sacrificed for the benefit of improving the network capacity; we may assert that channel spatial reuse [98] improves the network capacity. However, by decreasing the connectivity degree of the network, the hidden node problem becomes more notorious. This problem is even more serious on the gateway neighborhood.

These three aspects were brought by the studies presented in Chapter 3 and Chapter 4, however, it adopts a different set of topology metrics. In this chapter we introduce a new metric, the load on a channel, that is a topology metric that combines the hop distance of nodes to the gateway and the number of nodes using the channel. This combined metric was found to be more simple, and to have more impact on fairness than the two simple metrics (hop distance of nodes to the gateway and the number of nodes using the channel) used separately. We also introduced the load balance metric that is basically the difference between the load on different channels. The neighbor node density is not considered in this chapter as it was found irrelevant to estimate the performance metrics on the scenarios we have studied in Chapter 3 and Chapter 4.

Our channel assignment problem is defined as a multi-objective optimization problem, which we prove to be NP-hard. Thus, we propose TILIA which is an efficient algorithm that runs reasonably fast and enables the WMN to have good performance. TILIA uses a breadth-first tree growing technique, but instead of growing a single tree, TILIA grows a forest. A forest is a set of trees rooted at each gateway and operating on different channels. All the trees grow simultaneously and their union spans the network. TILIA solves more than the channel assignment problem since it enables

the selection of paths between each node and the gateway that has minimum number of hops and hidden nodes. Nodes in the network are assigned to the least used channel and, within that channel, to the least used parent who forwards the traffic towards the gateway. When different channels and parents are equally loaded, the tie-break is made in two stages: first by the distance to the gateway, and then by the number of hidden nodes. The novelty of TILIA when compared to the state-of-the-art proposals [22], [23],[24] is that TILIA reduces interference caused by the hidden node problem [22], it considers the existence of multiple gateways [23], and it was designed for stub WMN [24]. TILIA presents gains of respectively 29% and 45% on packet delay and packet loss, when compared to state-of-the-art proposal [22].

This chapter introduces the joint topology metric *tmet* that considers relevant topology characteristics such as hidden nodes, the number of nodes directly connected to the gateways, and the number of hops between each node and the gateway. This metric can predict the network performance with an accuracy of 94% and can be used to rank different channel assignment schemes generated by TILIA for a given network topology. To the best of our knowledge this is the first composed metric for WMNs based on network wide topological information.

The rest of the chapter is organized as follows: Section 5.1 introduces the network model and assumptions of this work, Section 5.2 formulates the problem, Section 5.3 describes the algorithm proposed to solve the problem, Section 5.4 evaluates TILIA, and Section 5.5 summarizes the chapter.

5.1 Notation and models

In this section we present the network and interference models and the assumptions considered in our work. Our aim is to define models which can help us understanding how network topology characteristics can be used to predict the performance of single-radio stub WMN. Table 5.1 presents the notations adopted in this work, which are based on the notations used in [99].

Notation	Description
$N(V,E)$	network graph
V	set $\{u,v,a,b,...\}$ of nodes in the network
E	set of links in the network
$dist(u,v)$	is the Euclidean distance between u and v
ϱ	radio receiving and interfering range
κ	number of gateways in G
G	set of gateways $\{g_1,g_2,...,g_\kappa\}$ on the WMN
$\mathcal{V}$	family of disjoint node subsets of V
V_{g_i}	subset of V in which nodes use gateway g_i
$d(u,v)$	length of the shortest path between v and u
$\hat{G}(v)$	set of the closest gateways of node v
$\hat{d}_v$	hop distance to the closest gateways of node v
$P(v)$	candidate parents of v
$S(V,E_S)$	shortest path spanning forest of N
E_S	set of links in the forest S
$T_{g_i}(V_{g_i},E_{g_i})$	tree in S rooted in gateway g_i
$T_{g,u}(V_{g_i,u},E_{g_i,u})$	subtree of T_g rooted at node u
$ch(v)$	channel assigned to node v
$\lambda = 1$	traffic generated by each node
$t(e_{uv})$	traffic carried the link e_{uv} in both directions
$l_S(g_i)$	load of the tree rooted at gateway g_i
$\hat{l}(g_i)$	minimum load of the tree rooted at gateway g_i
$\hat{l}$	minimum load on the network
$l_S(v)$	load of the subtree $T_{g,u}$ rooted at node v
$R1^N$	set of nodes on gateways neighborhood (1^{st} ring)
$R1^N_{g_i}$	set of unassigned nodes on the neighborhood of g_i
$R1^S_{g_i}$	set of assigned nodes on the neighborhood of g_i
V_H	set of links in the network (same as E)
$H(V_H,E_H)$	hidden links graph of the network N
$H^{R1}(V_H,E_H^{R1})$	1^{st} ring hidden graph
$M(e_{ab})$	set of links that are hidden from link $e_{ab} \in E_{H,S}$
$m(e_{ab})$	miss ratio of link $e_{ab} \in E_{H,S}$
m	miss ratio of the network
m_{R1}	miss ratio of the gateways neighborhood

Table 5.1: Notations used on the problem formalization.

5.1.1 Network, interference and traffic model

We consider a WMN with fixed located wireless nodes, which are equipped with a single-radio interface. We model the network as a simple graph $N(V,E)$ where V is the set of nodes in the network, E is the set of wireless links where $E = \{e_{uv} : u,v \in V \wedge dist(u,v) \leq \varrho\}$, $dist(u,v)$ is the Euclidean distance between u and v, and ϱ is the radio receiving range. e_{uv} represents a link from node u to node v. Nodes u and v are neighbors if $e_{uv} \in E$. There are $\kappa = |G|$ gateway nodes which are simultaneously connected to the infra-structured network through a wired network interface and to the WMN through a single-radio wireless interface, where $G = \{g_1, g_2, ..., g_\kappa\} \subset V$. Each node $v \in V \backslash G$ communicates with the infra-structured network through a single gateway $g_i \in G$. In a network N there is at least a family of sets $\mathcal{V} = \{V_{g_i} : g_i \in G\}$, where $V_{g_i} \subset V$ is a set of nodes using a gateway g_i including the gateway g_i, where $\bigcap_{g_i \in G} V_{g_i} = \emptyset$ and $\bigcup_{g_i \in G} V_{g_i} = V$

The distance $d(u,v)$ is defined as the number of edges in the shortest path between u and v. For each node $v \in V$, it is possible to characterize the set of closest gateways $\hat{G}(v)$ defined in Eq. 5.1, where $\hat{d}_v$=$min(\{d(v,g_j) : g_j \in G\})$ is the hop distance between node v and the closest gateways.

$$\hat{G}(v) = \{g_i : d(v,g_i) = \hat{d}_v \ \wedge \ g_i \in G\} \tag{5.1}$$

If v immediately precedes node u on the shortest path between u and a gateway $g_i \in \hat{G}(u)$, then the node v is the parent of u on this path. The children of v are all nodes whose path to the gateway include node v. For each node $u \in V$ it is possible to define the set of candidate parents $P(u)$ given by Eq. 5.2, which is the set of nodes that are parents of node u on all possible shortest paths between u and each of the gateways $g_i \in \hat{G}(u)$

$$P(u) = \{v : e_{uv} \in E \ \wedge \ \hat{d}_v = \hat{d}_u - 1 \ \wedge \ g_i \in \hat{G}(u)\} \tag{5.2}$$

We assume that communication flows in the stub WMN exist between each node $v \in V \backslash G$ and one of its closest gateways $g_i \in \hat{G}(v)$ or

vice-versa. We also assume that the path used by an upstream flow includes exactly the same nodes as the path used by downstream flows; therefore, each node uses its parent as next hop to forward data to the gateway and expects to receive data from the gateway through the same parent. Consider the network in Figure 5.1(a). The path of the upstream flow between node n_4 and the gateway g_1 is the ordered list (n_4, n_3, n_2, g_1) and the path of the downstream flow is the ordered list (g_1, n_2, n_3, n_4), which includes the same set of nodes; in this example, node n_3 is the parent of node n_4. The paths used by these flows form a shortest path spanning forest S of N, where $S(V, E_S) = \bigcup_{i \in G} T_i$, and T_i is a shortest path spanning tree of the subgraph of N that contains all the vertexes $v \in V_{g_i}$ communicating through g_i. The forest of the flows on the network shown in Figure 5.1(a) is represented in Figure 5.1(b). Each tree $T_i(V_{g_i}, E_{g_i})$ is rooted at a gateway $g_i \in G$. The edge set E_S is the disjoint union of the edges set $E_{g_i} \subset E$ of each tree T_i. We define $T_{g_i,v}(V_{T_{g_i,v}}, E_{T_{g_i,v}})$ as the subtree of tree T_{g_i} with root at node v, where $V_{T_{g_i,v}}$ contains the node v and its children. Figure 5.1(b) highlights the tree T_{g_2,n_6}, in this case, $V_{T_{g_2,n_6}} = \{n_6, n_7, n_8\}$

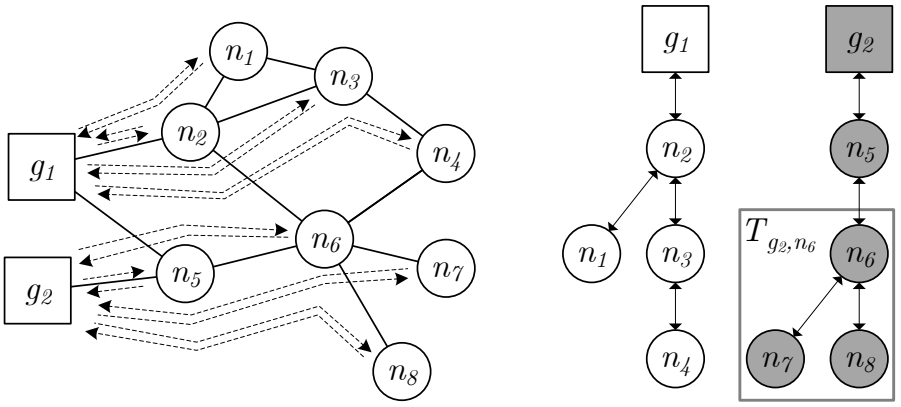

(a) Network N (b) Forest S of N

Figure 5.1: Sample network and shortest path spanning forest that illustrate the models used in this work. In the network presented in (a), solid lines represent links in the network, and dashed lines represent flows. (b) is a shortest path spanning forest S of the network in (a).

When at least one node has multiple gateways at minimum distance, there are multiple vertex set families $\mathcal{V}$, each capable of creat-

ing a different shortest path spanning forest. $S^{\mathcal{V}_i}$ is a shortest path spanning forest of N that uses the vertex set family $\mathcal{V}_i$. When a node v is assigned to a tree T_{g_i} that do not correspond to a gateway in its set of closest gateways, $g_i \notin \hat{G}(v)$, the spanning forest resultant from this assignment is not shortest path.

Multiple channels will be used to improve the network capacity. There are κ channels available in the network, as many as the number of gateways and trees in the spanning forest. We assume orthogonal radio channels that do not interfere with each other. A static and unique channel is assigned to each gateway $g_i \in G$. Due to this $(gateway, channel)$ unique static assignment, the terms gateway and channel will be used interchangeably throughout this chapter; for clarity we assume that G is also the set of available channels. Each node $v \in V$ in the network has its unique radio interface configured on a single channel g_i. This assignment is static or quasi-static since it is expected to be changed only when there are significant changes to the network topology. Two nodes u and v can successfully communicate if $ch(u) = ch(v)$, where $ch(v)$ is the radio channel assigned to node v. When a node v is assigned to channel $ch(v) = g_i$ the flows of node v traverse gateway $g_i \in G$.

Communications between two wireless nodes through a wireless link will interfere with other communication links in the network due to the broadcast nature of wireless links. Interference is caused by active nodes on the vicinity of both the sender or the receiver of a link. The interference model [13] [43] defines the set of pairs of links in a network that interfere with each other. We assume the interference model as a binary interference model where two links either interfere or not.

5.1.2 Load model

As mentioned earlier, we assume that a traffic flow in the network is generated by a gateway $g_i \in G$ and consumed by a node $v \in V \backslash G$, or vice-versa. We also assume that each node generates and receives a mean bit rate of $\lambda = \lambda_d + \lambda_u$ bit/s, where λ_d is the bit rate of the downstream flow generated by the gateway towards a node v, and λ_u is the bit rate of upstream flow generated by node v towards the

gateway. We assume that all nodes v generate and receive the same amount of traffic λ. This uniform traffic assumption is reasonable on stub WMN of mesh access points (MAPs) since the amount of clients is expected to be statistically the same among the MAPs over the time.

Only the links $e \in E_S$ carry traffic. We define $t(e_{uv}) = t(e_{vu})$ as the traffic carried by the upstream link between u and v plus the traffic carried by the downstream link between v and u, where v is the parent of u. The traffic $t(e_{uv})$ is the traffic generated by u and by all the children of u. In fact, $t(e_{uv}) = |V_{g_i,u}|\lambda$, where $V_{g_i,u}$ is the set of vertexes of the subtree $T_{g_i,u}$ containing u and its children. In the sample topology presented in Figure 5.1(b), $t(e_{n_6n_5}) = |V_{g_2,n_6}|\lambda = 3\lambda$.

We assume that nodes are placed dense enough so that most of the paths to the closest gateway are short in terms of number of hops, such as 3 or 4 hops; similar assumptions are made by other works [22]. Thus, there is little chance of spatial reuse within a route tree. When the depth of a route tree becomes large, spatial reuse must be considered to the load estimation, but we consider it as topic for future work.

The traffic generated by or to node $v \in V$ will be transmitted through $d(v, g_i)$ hops inside the WMN until it reaches the destination (g_i for upstream, and v for downstream). Therefore the load imposed to the tree rooted at g_i by a node v is $\lambda d(v, g_i)$ and the total load on the tree rooted at gateway g_i is $\lambda \sum_{v \in V_{g_i}} d(v, g_i)$. Since we assume λ, the mean bit rate, is a constant value and equal for all nodes, we can ignore this factor and let the load on a channel $l_S(g_i)$ be completely defined by the relationships between links, nodes and gateways on the network N as given in Eq. 5.3. Note that $l_S(g_i)$ depends on the family $\mathcal{V}_i$ used to form S, thus

$$l_S(g_i) = \sum_{v \in V_{g_i}} d(v, g_i) \tag{5.3}$$

The minimum load on the tree rooted at g_i can be defined as $\hat{l}(g_i) = \sum\{\hat{d}_v : g_i \in \hat{G}(v), \forall v \in V_{g_i}\}$. The minimum total load in the network is the sum of the minimum load on all trees in the network

given by Eq. 5.4.

$$\hat{l} = \sum_{g_i \in G} \left(\sum_{v \in V_{g_i}} \hat{d}_v \right) = \sum_{v \in V} \hat{d}_v \tag{5.4}$$

Generalizing, we can obtain the load of the subtree rooted at any node $v \in V$ by considering that each node has to forward its traffic and also its children traffic; therefore the total load on the subtree $T_{g,v} \subset S$ rooted at v is $l_S(v)$ given by Eq. 5.5.

$$l_S(v) = \sum_{a \in V_{T_{k,v}}} d(a, v) \tag{5.5}$$

5.1.3 1st ring - gateway neighborhood

We define the 1st ring of a network $R1^N$ in Eq. 5.6 as the set of nodes directly connected to at least one of the gateways, including the gateways; $R1^N$ is also called gateways neighborhood of a WMN.

$$R1^N = \{v : v \in V \wedge d(v, g_i) \leq 1, \forall g_i \in G\} \tag{5.6}$$

The 1st ring of a gateway $R1^N_{g_i} = \{v : v \in V \wedge d(v, g_i) \leq 1\}$ is the set of nodes directly connected to g_i including g_i, where $\bigcup_{g_i \in G} R1^N_{g_i} = R1^N$. Note that $\left| \bigcup_{g_i, g_j \in G} \left(R1^N_{g_i} \cap R1^N_{g_j} \right) \right| \geq 0$, since one or more nodes $v \in V$ may belong to the 1st ring of multiple gateways. On the sample network of Figure 5.1(a), $R1^N_{g_1} = \{g_1, n_2, n_5\}$, $R1^N_{g_2} = \{g_2, n_5\}$, and $R1^N = \{g_1, g_2, n_2, n_5\}$.

When channels are assigned to nodes and a shortest path spanning forest S of N is formed, we can define the assigned 1st ring of a gateway $R1^S_{g_i}$ in Eq. 5.7 as the set of nodes directly connected to gateway g_i which are assigned to the channel correspondent to g_i. In this case, $\left| \bigcup_{g_i, g_j \in G} \left(R1^S_{g_i} \cap R1^S_{g_j} \right) \right| = 0$ since after assignment a node v does not belong to multiple trees. On the sample network of Figure 5.1(b), $R1^S_{g_1} = \{g_1, n_2\}$ and $R1^S_{g_2} = \{g_2, n_5\}$.

$$R1^S_{g_i} = \{v : v \in V_{g_i} \wedge d(v, g_i) \leq 1\} \tag{5.7}$$

The connectivity degree of a gateway is the number of nodes directly connected to gateway g_i and consequently assigned to the

channel correspondent to g_i ($|R1^S_{g_i}|$).

5.1.4 Hidden nodes

The hidden node problem is defined in [65] using a set of graphs that capture the interferences and the carrier sensing constraints between links in a network: if-graph, tc-graph, and rc-graph. These graphs are defined over the vertex set V_H, where $V_H = \{e_{uv} : e_{uv} \in E\}$. Please note that an edge in E becomes a vertex in the hidden node model described in this section. On this discussion about the hidden node problem we consider directional links, therefore $e_{uv} \neq e_{vu}$ and the set V_H can be used to reason about bi-directional flows. The if-graph captures the physical interference constraints; an s-graph edge between vertex 1 and vertex 2 indicates that, in order to prevent future collisions, link 1 must be capable of forewarning link 2 not to transmit after link 1 initiates a transmission. The tc-graph models the transmitter-side carrier-sensing; an edge in tc-graph between vertex e_{uv} and vertex e_{ab} means that e_{uv} can and will forewarn e_{ab} not to transmit when e_{uv} is transmitting. The rc-graph models the receiver-side carrier-sensing; an edge in rc-graph between vertex e_{uv} and vertex e_{ab} indicates that node b will ignore node a transmission when node b already senses a transmission on link e_{uv}. All links $e_{uv} \in E$ are considered to create the edges in s-graph, tc-graph, and rc-graph, however links operating on different channels or not carrying traffic are unable to interfere with others.

It is possible to obtain the hidden graph $H(V_H, E_H)$, where $E_H = \overline{TC} \cap (IF \cup RC)$ and IF and RC are respectively the set of edges on s-graph and rc-graph, and $\overline{TC}$ represents the set of edges that are not on the tc-graph. If a tc-edge does not exist from e_{uv} to e_{ab}, a transmission on e_{uv} will not be sensed by node a. But if a rc-edge or a if-edge exists between e_{uv} and e_{ab}, it indicates that node b will ignore node a transmission when node b senses a transmission on e_{uv} (rc-edge), or that there is physical interference from link 1 to link 2 (if-edge). In both cases, node a will interpret it as a collision and we can say that e_{uv} is hidden from e_{ab}. The 1st ring hidden graph $H^{R1}(V_H, E^{R1}_H)$ is the graph formed by all vertices V_H on the hidden graph H and the edges E^{R1}_H, defined in Eq. 5.8, which are edges

between the links hidden from links on the gateway neighborhood,

$$E_H^{R1} = \{(e_{uv}, e_{ab}) : (e_{uv}, e_{ab}) \in E_H \ \wedge \ e_{uv} \in V_H^{R1}\} \tag{5.8}$$

where V_H^{R1} in Eq. 5.9 is the set of links on the gateway neighborhood.

$$V_{H,S}^{R1} = \{e_{uv} : e_{uv} \in V_H \ \wedge \ (u \in G \vee v \in G)\} \tag{5.9}$$

After the channel assignment, we assume that only links $e_{uv} \in E_S$ are carrying data flows. In that case, the vertex set of if-graph, tc-graph, rc-graph and hidden links graphs is $V_{H,S}$, where $V_{H,S} = \{e_{uv} : e_{uv} \in E_S\}$. The interference of other links $e_{ab} \in E \backslash E_S$ is insignificant because they are either unfeasible if $ch(a) \neq ch(b)$ or do not carry traffic if $ch(a) = ch(b)$. After the channel assignment, the set of edges in the if-graph, tc-graph, rc-graph, and hidden links graphs are respectively IF_S, TC_S, RC_S, and $E_{H,S}$; in this case, edges (e_{uv}, e_{ab}) between links operating on different channels $ch(u) = ch(v) \neq ch(a) = ch(b)$ do not interfere with each other and are not included in IF_S, TC_S, RC_S, and $E_{H,S}$.

We define $M(e_{ab})$ in Eq. 5.10 as the set of vertexes in $V_{H,S}$ that are hidden from link e_{ab}.

$$M(e_{ab}) = \{e_{uv} : (e_{uv}, e_{ab}) \in E_{H,S} \ \wedge \ e_{ab}, e_{uv} \in V_{H,S}\} \tag{5.10}$$

The miss ratio $m(e_{ab})$ given by Eq. 5.11 is a measure of the hidden node problem on a link e_{ab}, where $I(e_{ab}) = \{e_{uv} : (e_{uv}, e_{ab}) \in (IF_S \cup RC_S) \ \wedge \ e_{ab}, e_{uv} \in V_{H,S}\}$ is the set of links that interfere with link e_{ab}.

$$m(e_{ab}) = \frac{|M(e_{ab})|}{|I(e_{ab})|} \tag{5.11}$$

The network wide miss ratio $m = |E_{H,S}| \ / \ |IF_S \cup RC_S|$ is a measure of the hidden node problem on the overall network.

The miss ratio on the gateways neighborhood m_{R1} given by Eq. 5.12, is a measure of the hidden node problem on links to and from the gateways, where $E_{H,S}^{R1}$ is the set of edges that correspond to links hidden from links on the gateway neighborhood after the channel assignment, IF_S^{R1} and RC_S^{R1} are respectively the sets of edges on if-graph and rc-graph that affect links on the gateway neighborhood,

E_H^{R1} is given by Eq. 5.8, and V_H^{R1} is given by Eq. 5.9.

$$
\begin{aligned}
m_{R1} &= \frac{\left|E_{H,S}^{R1}\right|}{|IF_S^{R1} \cup RC_S^{R1}|} \qquad (5.12)\\
E_{H,S}^{R1} &= \{(e_{uv}, e_{ab}) : (e_{uv}, e_{ab}) \in E_H^{R1} \ \wedge \ e_{uv}, e_{ab} \in E_{H,S}\}\\
IF_S^{R1} &= \{(e_{uv}, e_{ab}) : (e_{uv}, e_{ab}) \in IF_S \ \wedge \ e_{uv} \in V_H^{R1}\}\\
RC_S^{R1} &= \{(e_{uv}, e_{ab}) : (e_{uv}, e_{ab}) \in RC_S \ \wedge \ e_{uv} \in V_H^{R1}\}
\end{aligned}
$$

For the network of Figure 5.1(a), the tc-graph, rc-graph, if-graph, and hidden links graph are presented respectively in Figure 5.2(a), Figure 5.2(b), Figure 5.2(c), and Figure 5.2(d). On the hidden graph (Figure 5.2(d)) an arrow from link e_{uv} towards link e_{ab} means that e_{uv} is hidden from e_{ab}. Edges on E_H^{R1}, TC^{R1} and RC^{R1} which correspond to 1$^{\text{st}}$ ring are highlighted in red. In the graphs of Figure 5.2 we assume the protocol interference model of IEEE 802.11 [43], where the transmission range and interference range are equal and RTS and CTS control messages are used. After the channel assignment represented in Figure 5.1(b), the links $e_{n_5g_1}$, $e_{g_1n_5}$, $e_{n_6n_2}$, $e_{n_2n_6}$, $e_{n_6n_4}$, and $e_{n_4n_6}$ are unfeasible because their endpoints are assigned to different channels, therefore they are not considered to calculate the miss ratio and are represented in light gray in the graphs of Figure 5.2. Despite $ch(n_1) = ch(n_3)$ in the forest S represented in Figure 5.1(b), the links $e_{n_1n_3}$ and $e_{n_3n_1}$ do not belong to E_S because they do not carry data flows; the interference of these links on links belonging to the forest S is inexistent and they are not considered to calculate the miss ratio and are also represented in light gray in the graphs of Figure 5.2. However, if links $e_{n_1n_3}$ and $e_{n_3n_1}$ do not exist in the network represented in Figure 5.1(a), the hidden graph would include more edges, and for instance, links $e_{n_4n_3}$ and $e_{n_3n_4}$ would become hidden from $e_{n_1n_2}$. Edges between links operating on different channels are also represented in light gray because they do not interfere with each other after the channel assignment and are not considered to calculate the miss ratio.

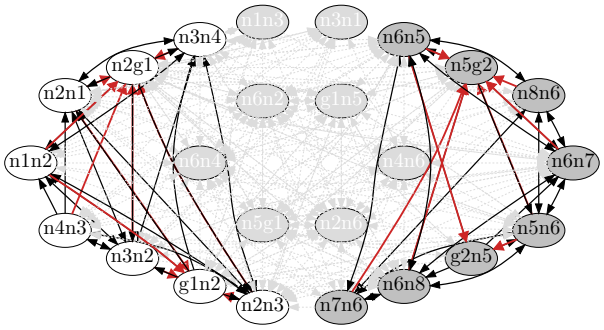

(a) tc-graph

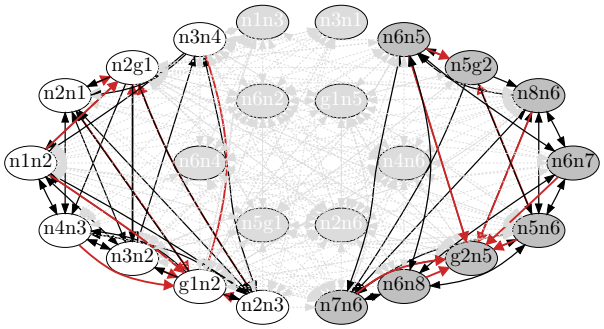

(b) rc-graph

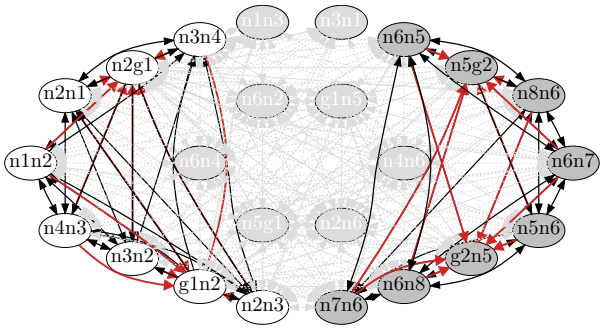

(c) if-graph

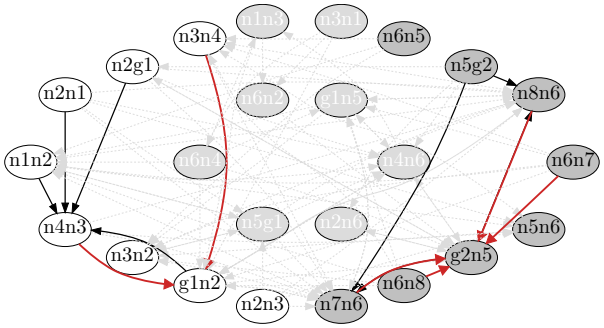

(d) hidden graph

Figure 5.2: For the network represented in Figure 5.1, (a) is the tc-graph, (b) is the rc-graph, (c) is the if-graph, and (d) represents the hidden graph.

5.2 Problem formulation

The overall goal of using multiple channels on WMN is to reduce interference, which results in improving the overall network capacity and consequent network performance. However, when multiple channels are assigned to single-radio nodes, the network connectivity will be sacrificed what bring additional difficulties such as (1) higher loads caused by long paths, (2) gateway neighborhood vulnerability caused by a reduced number of links to the gateways, and (3) hidden nodes problems that become more serious on low connected networks.

In this section, we first discuss the impact that topology characteristics have on the performance of a network, then we formulate the channel assignment problem as a multi-objective optimization model describing each of its components, and finally discuss the problem complexity.

5.2.1 Background

The performance of a WMN can be characterized using parameters such as throughput, delay, and packet loss. Here we focus on node throughput and delay. Firstly, we want to maximize the total throughput, given by the sum of flow's bit rates received by all the destinations. Secondly, we aim to maximize fairness among node's throughput, so that each node can offer an effective connection of its stations towards the infra-structured network. Thirdly, we want to minimize the end-to-end delay experienced by packets transmitted between WMN nodes and the gateways.

The natural formulation for this problem would be to directly optimize the throughput, fairness and delay of the network by means of, for instance, some utility function. There have been some attempts [19, 21, 43] to formulate and solve the problem in this way but they inevitably lead to scheduling solutions that assume a time slotted MAC, and the solutions are not easily implemented over the standard and widely disseminated IEEE 802.11 wireless cards. In this work we followed a different approach that, we believe, has value namely for telecommunication operators. We defined as objective of

this work to efficiently assign channels to nodes solely considering the topology characteristics of the WMN.

In order to achieve our goal we characterized in Chapter 3 the impact that the network topology characteristics (e.g. path hop count, node density and hidden nodes) have on the performance of a WMN. We defined a set of experiments with 18 arbitrary channel assignment scenarios in a 6x6 lattice topology network and with 8000 random scenarios. Simulations using ns-2 were preformed and, based on the results obtained, the relevant topology characteristics that have impact on the throughput of the WMN were identified as being: (1) the mean hop count, (2) the neighbor node density, (3) the number of nodes in the 1st ring, (4) the overall *miss ratio*, and (5) the 1st ring *miss ratio*. We concluded in that work that the performance of the WMN can be correlated to its topology characteristics.

In the work presented in Chapter 4, we rank the relative importance of network topology characteristics on the performance of a single-radio multi-channel IEEE 802.11 WMN. A set of 3500 topologies with 36 randomly positioned nodes were created using the network simulator ns-2 [93]. Two channel assignment strategies were then applied to each of the 3500 topologies, assigning one of two possible channels to each node. Each of the 7000 networks was simulated four times using ns-2 with two possible traffic loads (low load and high load) and two different simulation seeds. The topological and performance metrics from the 28000 network simulations were used to train a data mining model. The considered topological metrics were (1) the number of nodes per sub-network, (2) the mean hop count, (3) the neighbor node density, (4) the number of nodes in the 1st ring, (5) the overall *miss ratio*, and (6) the 1st ring *miss ratio*. The input parameters of the models are six topology metrics enumerated above and the output of each model was the three performance metrics: network aggregate throughput, fairness, and delay. Using fitted data mining models, the effect of topology metrics on performance was quantified using a sensitivity analysis procedure which revealed the relative importance of each topology metric for each model.The results suggest that the topology metric that has the greatest impact on the performance of a WMN is the

number of nodes that are directly connected to the gateway: a larger 1st ring results in increased data throughput, increased throughput fairness, and lower delay. Hop distance of nodes to the gateway and the difference of number of nodes between sub-networks also impact network performance, but mostly in provisioning of fairness. That study also suggests that throughput and delay could be improved by avoiding hidden nodes, in particular on links to the gateway. Other topology metrics are considered to have little influence on the models output.

The load on a channel presented in Eq. 5.3 is a topology metric that combines the hop distance of nodes to the gateway and the number of nodes using the channel. This combined metric was found to be more simple and to have more impact on fairness than the two simple metrics (hop distance of nodes to the gateway and the number of nodes using the channel) used separately.

The formulation of our channel assignment problem stands on the results obtained in Chapter 4. We aim to optimize four criteria: (1) maximize the connectivity degree of each gateway, (2) minimize the number of hidden nodes on the gateways neighborhood, (3) minimize the load on the network and (4) distribute fairly the load among the channels. It is difficult to find a solution that is optimal in all criteria, because optimizing one criterion will affect the other criteria. Thus, we define this problem using a multi-objective approach as in [100], exploiting the trade-offs between topology characteristics that have impact on the WMN performance.

5.2.2 Channel assignment problem

The channel assignment problem can be informally described as follows: given a WMN consisting of single-radio nodes, how to assign a unique channel to each node in the network so that the load on the assigned network is minimum (load is made independent of λ), the load on channels are as similar as possible, the connectivity degree on gateways neighborhood are as balanced as possible, and the number of hidden links on the gateway neighborhood is minimum.

Formally, the channel assignment problem is formulated by defining the mapping function $f : V \rightarrow G$, that minimizes the *total load*

(Eq. 5.13), maximizes the *load balancing* (Eq. 5.14), maximizes the *1st ring balance* (Eq. 5.15), and minimizes the *1st ring hidden links* (Eq. 5.16).

min $l(f)$

$$l(f) = \sum_{v \in V} d(v, f(v)) \tag{5.13}$$

max $lb(f)$

$$lb(f) = min\left\{\left(\sum_{v \in V_{g_i}} d(v, f(v))\right) : g_i \in G\right\} \tag{5.14}$$
$$V_{g_i} = \{v : v \in V \wedge f(v) = g_i\}$$

max $rb(f)$

$$rb(f) = min\{|R1_{g_i}^S| : g_i \in G\} \tag{5.15}$$
$$R1_{g_i}^S = \{v : f(v) = g_i \ \wedge \ d(v, g_i) \leq 1\}$$

min $h(f)$

$$h(f) = |\{(e_{uv}, e_{ab}) : (e_{uv}, e_{ab}) \in E_H^{R1} \ \wedge \ f(u) = f(v) = f(a) = f(b)\}| \tag{5.16}$$

5.2.2.1 Total load

The *total load* (Eq. 5.13) is the sum of the load carried by each channel. In order to minimize the interference, the load in the links should be minimum, since interference depends on the traffic on the network links [18]. Each node v in the network N should be assigned to the channel corresponding to one of the gateways in the set of its closest gateways $\hat{G}(v)$, what will make the total load close to the minimum load for that network given by $\hat{l}$ (Eq. 5.4).

The *total load* problem is a shortest path problem that could be solved using a classical algorithm such as the Dijkstra's algorithm

if a single channel was involved. In the presence of multiple channels, it is expected that the complexity for of this problem does not increase.

5.2.2.2 Load balancing (Eq. 5.14)

Load should be equally balanced among channels [22]. Unbalanced load causes unfairness among nodes assigned to different channels. The function $lb(f)$ is actually the load carried by the least loaded channel. By maximizing $lb(f)$, the load balancing among channels is also maximized. This is a standard max min formulation.

Our *load balancing* problem is basically the Max Balanced Connected κ-Partition problem [101], which aims to find a partition of the vertex set V, of a graph $N(V, E)$, into κ classes such that the weight of the lightest class is as large as possible and each class $V_i : i \in [1 : \kappa]$ has to induce a connected subgraph of N; in the *load balancing* problem we view the load imposed by each node $d(v, g_i)$ as the weight of the vertices. Since Max Balanced Connected κ-Partition problem is known to be a NP-hard problem [101], the load balancing problem can also be classified as NP-hard.

5.2.2.3 1st ring balancing (Eq. 5.15)

Interference problems on links to the gateways affect the network performance more seriously than links farther from gateways because gateways neighborhoods are the network bottleneck in stub WMN. The study on Chapter 4 showed that networks with higher connectivity degree at gateways have better performance in terms of throughput, fairness and delay. If the *total load* function (Eq. 5.13) is minimized, the connectivity degree of gateways is automatically set to its maximum value. However, when the 1st ring of each of the gateways have nodes in common, i.e. $\bigcup_{g_i,g_j \in G} R1_{g_i}^N \cap R1_{g_j}^N \neq \emptyset$, the connectivity degree of the gateways may be unbalanced. The $rb(f)$ is actually the connectivity degree of the gateway with smallest 1st ring. By maximizing $rb(f)$, the 1st ring balancing among channels is also maximized.

The 1st ring balancing problem is basically the Max Balanced Connected κ-Partition problem where vertices weights are unitary

and the network to be partitioned includes solely the nodes on the network 1st ring $R1^N$ (Eq. 5.6). Since Max Balanced Connected κ-Partition problem is known to be a NP-hard problem [101], the 1st ring balancing problem can also be classified as NP-hard.

5.2.2.4 1st ring hidden links (Eq. 5.16)

The decrease of the network connectivity, caused by the channel assignment, augments the hidden node problem as shown in Chapter 3. The study on Chapter 4 showed that the avoidance of the hidden node problem on the gateway neighborhood increases the network throughput and reduces the delay. The number of hidden links on the 1st ring (*1st ring hidden links*) is just the number of edges in the 1st ring hidden graph E_H^{R1} defined in Eq. 5.8, in which all nodes involved are assigned to the same channel.

Given a graph H, the Max κ-cut problem [102] is defined as the partition the vertices of H into κ partitions in order to maximize the number of edges whose endpoints lie in different partitions. In our channel assignment problem, if we view vertices of the hidden graph assigned to a particular channel as belonging to one partition, then, the *1st ring hidden links* function is actually the number of edges in the hidden graph that have endpoints in same partition. Thus, the hidden node avoidance problem is similar to the Max κ-cut problem with the variation that coloring is performed at the network graph N which causes the coloring of the H^{R1} where the cut is measured. Since Max κ-cut problem is known to be a NP-hard problem [102], our hidden node avoidance problem can also be classified as NP-hard.

5.2.3 Discussion

We define our channel assignment problem as a multi-objective optimization problem. For most multi-objective problems, it is not possible to identify a single solution that simultaneously optimizes all objectives; the set of solutions for such problems are called the Pareto optimal set. A solution belongs to the Pareto optimal set if there is no feasible solution which would improve some criterion

without causing a simultaneous worsening in at least one other criterion. Three out of the four objective functions are NP-hard problems. Therefore, finding each of the Pareto set solutions is not possible in polynomial time.

5.3 TILIA algorithm

In this section we present TILIA, a centralized algorithm for solving the channel assignment problem. Centralized algorithms are very useful in managed WMNs, and a natural solution for stub WMNs, where there is a set of gateways owned by a central entity such as a telecom operator. Centralized approaches have been proposed in recent works [15].

TILIA aims at assigning channels to nodes and defines paths for WMN nodes optimizing topology metrics by the order of importance found on our previous studies [26, 27] discussed in Section 5.2.1. TILIA uses a breadth-first tree growing technique, but instead of growing a single tree, TILIA grows a forest $S = \bigcup_{i \in G} T_i$ of κ trees rooted at each gateway $g_i \in G$. All the trees grow simultaneously and their union spans the network. TILIA solves more than the channel assignment problem; the tree growing technique also (1) enables the selection of paths between each node and the gateway that has minimum number of hops and hidden nodes, and (2) it helps finding balanced 1^{st} ring sizes. Nodes in the network are assigned to the least used channel and, within that channel, to the least used parent who forwards the traffic towards the gateway. When different channels and parents are equally loaded, the tie-break is made in two stages: first by the distance to the gateway, and then by the number of hidden nodes.

5.3.1 Algorithm description

TILIA is introduced in Algorithm 1. The TILIA input is the network graph N of a WMN and the set of gateways G. The outcome of the algorithm is a spanning forest S of N. The trees T_{g_i} of a forest S are initialized with the gateways $g_i \in G$, and $\mathcal{X}$ is initialized as an empty set of forests. The function $TiliaMainCycle()$ is

the core of TILIA algorithm. The output of $TiliaMainCycle()$ may provide one or more forests which are stored in $\mathcal{X}$. When the racing rules established for assigning channels to nodes on the gateway neighborhood result on a tie, this function is called recursively to exploit alternative forests. The $BestForest()$ function selects the forest in $\mathcal{X}$ that has the topology characteristics that fits better the channel assignment problem defined in Eq. 5.13, Eq. 5.14, Eq. 5.15, and Eq. 5.16.

Algorithm 1 TILIA algorithm

Require: $N(V,E)$, G
Ensure: spanning forest $S = \bigcup_{i \in G} T_i$ with roots in G
  Initialize trees $T_{g_i} \subset S$ as vertex $g_i \in G$
  Initialize $\mathcal{X}$ as an empty set of forests
  $TiliaMainCycle(N, S, \mathcal{X})$
  return $S := BestForest(\mathcal{X})$

In the $TiliaMainCycle()$ function, described in Algorithm 2 each node is visited once. The next node v to be visited is selected by the $NextVertex()$ function. For the selected node v, the function $BestChannels()$ returns a set $C \subset G$ (Eq. 5.1) of closest gateways to node v that currently have the minimum load. The function $BestParents()$ selects the set P of best parents of node v. Finally, the forest S and the set of selected forests $\mathcal{X}$ are updated in the $UpdateForest()$ function.

Algorithm 2 $TiliaMainCycle(N, S, \mathcal{X})$

1: **while** $V_S \neq V$ **do**
2: $v := NextVertex(N, S)$
3: $C := BestChannels(N, S, v)$
4: $P := BestParents(N, S, v, C)$
5: $UpdateForest(N, S, \mathcal{X}, v, P)$
6: **end while**

5.3.2 Select the next node to be visited

The $NextVertex()$ function, in Algorithm 3, selects the next node to be visited. Nodes are visited in increasing order of (1) hop count, (2) available nearby channels, (3) available nearby parents, and (4) hidden nodes on links to those parents.

$NextVertex()$ starts by visiting the nodes that are closer to the gateways. This strategy avoids loops and allows a better control on the gateway neighborhood which is the network bottleneck.

Algorithm 3 $NextVertex(N, S)$

1: $F := \{v : (e_{uv} \in E) \wedge (u \in V_S) \wedge (v \notin V_S)\}$
2: $min_{hc} := min(\{\hat{d}_v : v \in F\})$
3: $X = \{v : (v \in F) \wedge (\hat{d}_v = min_{hc})\}$
4: $min_{gw} := min(\{|\hat{G}(v)|, \forall v \in X\})$
5: $Y := \{v : (v \in X) \wedge (|\hat{G}(v)| = min_{gw})\}$
6: $min_P := min(\{|P(v)| : v \in Y\})$
7: $Z := \{v : (v \in Y) \wedge (|P(v)| = min_P)\}$
8: $M'(v) = \bigcup_{p \in P(v)} M(e_{pv}), \forall v \in Z$
9: $min_{hidden} := min(\{|M'(v)|, \forall v \in Z\})$
10: $A := \{v : (v \in Z) \wedge (|M'(v)| = min_{hidden})\}$
11: Let r be one node from A selected randomly
12: **return** r

The next node to be assigned is selected from $F \subset V$ of the frontier nodes of the forest S being grown from the network N. A frontier node $v \in F$ is a node in the network $v \in V$ that has not yet been added to the set of nodes V_S in the forest, but has at least a neighbor $u : e_{uv}, e_{vu} \in E$ that was previously included in V_S. The minimum distance min_{hc} of a closest frontier node $v \in F$ to a gateway is calculated in line 2. Then, the set nodes F is cropped to the subset X (line 3), containing the nodes with smallest hop count to the closest gateway.

The cardinal of the set of the closest gateways of each node $\hat{G}(v)$ (Eq. 5.1) is calculated in line 4 as the minimum number of channels min_{gw} available on each frontier node $v \in X$. The set Y, found in line 5, is a subset of X having the smallest number of nearby channels min_{gw}. The minimum number of candidate parents min_P of each frontier node $v \in Y$ is calculated in line 6. The set Z (line 7) is a subset of Y in which nodes have the smallest number of candidate parents given by $P(v)$ defined in Eq. 5.2.

At line 8, we obtain for each node $v \in Z$ the set $M'(v)$ of hidden links as the union of the sets of links $M(e_{pv})$ (Eq. 5.10) that are hidden from the link between nodes $v \in Z$ and each of their candidate parents $p \in P(v)$. The minimum cardinality min_{hidden} among the sets of links hidden from a node is calculated in line 9. Finally, the

set A, found in line 10, is a subset of Z in which nodes have the smallest number min_{hidden} of links hidden from links to the candidate parents . It is common to have $|A| \approx 1$ because each node $v \in A$ has to satisfy the four conditions described above. If more than a node is eligible, then it is selected randomly.

5.3.3 Select channels and parents

The function $BestChannels()$ shown in Algorithm 4 selects the candidate less loaded channels to be assigned to the node v returned by $NextVertex()$ function. The set of nearby channels C_{near} is found at line 1. The set C_{near} contains the channels that were previously assigned to all neighbors of v, instead of considering only the channels correspondent to the set of closer gateways of v given by $\hat{G}(v)$. At line 2, we calculate the minimum load min_l which is the load $l_S(g_i)$ (Eq. 5.3) of the less loaded tree $T_{g_i} \subset S$. At line 3, $BestChannels()$ returns a set containing all nearby channels that carry exactly min_l load.

Algorithm 4 $BestChannels(N, S, v)$

1: Let $C_{near} := \{ch(u) : e_{vu} \in E_S \ \vee \ e_{uv} \in E_S\}$
2: Let $min_l := min(\{l_S(g_i) : g_i \in C_{near}\})$
3: **return** $\{g_i \in C_{near} : l_S(g_i) = min_l\}$

By considering the channels of all the neighbors of v, including those nodes $u \notin P(v)$, the paths between v and the gateway are enabled to have more hops than the optimum distance $\hat{d}_v$, what means that the total load on the forest may be higher than the minimum load $\hat{l}$ of the network. In some scenarios this relaxation may be useful to guarantee load balancing between channels.

Consider for instance the topology represented in the Figure 5.3(a), with 25 nodes including 2 gateways. The distance of each node to the closest gateways is presented in the first line of Table 5.2 and the minimum load for this network $\hat{l} = 43$. By assigning nodes to channels in order to get the minimum load and the best possible load balance, we obtain the forest in Figure 5.3(b); this channel assignment has obvious low load balance since the load on gateway g_1 ($l(g_1) = 15$) is much smaller than the load on gateway g_2 ($l(g_2) = 28$),

as shown in the second line of Table 5.2. Another channel assignment scheme could be the forest represented in Figure 5.3(c); this channel assignment has non optimal total load $l(g_1)+l(g_2) = 45 > \hat{l} = 43$, but the load balance between channels is near optimal since $l(g_1) \approx l(g_2)$ (3^{rd} line of Table 5.2).

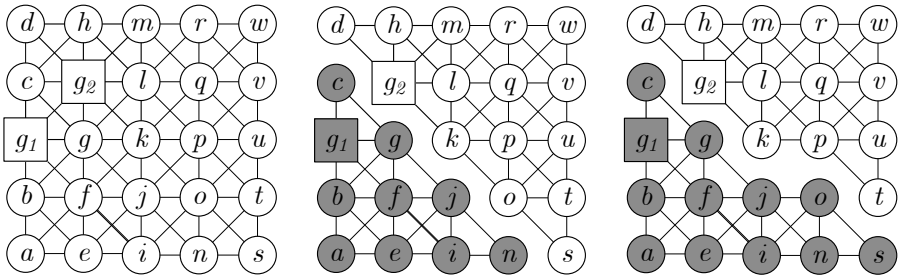

(a) Network topology before channel assignment. (b) Forest that minimizes the total load. (c) Forest that maximizes the load balancing.

Figure 5.3: Illustration of the trade-off between minimizing the total load and have load balancing.

Figure	Load from each node					$l(g_1)$	$l(g_2)$	Total load
	b c d f g h k l m	a e i j p q r	n t u v w	o	s			
5.3(a)	1	2	3	2	3	-	-	$\hat{l}$=43
5.3(b)	1	2	3	2	3	15	28	43
5.3(c)	1	2	3	3	4	22	23	45

Table 5.2: Loads for the network and forests presented in Figures 5.3(a), 5.3(b), and 5.3(c).

The function *BestParents*() shown in Algorithm 5 selects the best parent u of node v by considering three conditions: minimum distance to the gateway, minimum load, and minimum number of hidden nodes. The *BestParents*() function returns a set P of parents, if multiple parents are equally good on the gateway neighborhood, considering the hop count, the load, and the hidden nodes.

In line 1 we obtain the set of candidate parents P_{all} of node v which are the parents that are operating on the channels on set C returned by *BestChannels*(). In line 2 we calculate the *ring* of the candidate parent that is closer to its gateway. In line 3 we obtain the set of candidate parents P_{ring} that are at *ring* hops from their

gateways. At line 4, we calculate the minimum load min_{load} among candidate parents. In line 5 the set of candidate parents is cropped to P_{load} keeping only the candidate parents that have the minimum load min_{load}. In line 6 the minimum miss ratio min_m is calculated; for all links between v and each candidate parent $u \in P_{load}$, we calculate the link miss ratio as given by Eq. 5.11, min_m being the minimum value found. In line 7 we obtain the final set of candidate parents $P_{candidates}$ that present less problems with hidden nodes, that is, those whose miss ratio of links between v and each parent $u \in P_{candidates}$ is min_m.

Algorithm 5 $BestParents(N, S, v, C)$

```
 1: P_all := {u : (ch(u) ∈ C) ∧ (e_uv ∈ V)}
 2: ring := min({d(u, ch(u)) : u ∈ P_all})
 3: P_ring := {u ∈ X : d(u, ch(u)) = ring}
 4: min_load := min({l_S(u) : u ∈ P_ring})
 5: P_load := {u ∈ P_ring : l_S(u) = min_load}
 6: min_m := min({m(e_uv) : u ∈ P_load})
 7: P_candidates := {u ∈ P_load : m(u) = z}
 8: if |P_candidates| = 1 then
 9:     return P := P_candidates
10: end if
11: if ring > 1 then
12:     p := node on P_candidates selected randomly
13:     return P := {p}
14: else
15:     return P := P_candidates
16: end if
```

It is common to have $|P_{candidates}| \approx 1$ because each node $v \in P_{candidates}$ has to satisfy the tree conditions described above. When $|P_{candidates}| = 1$, the $BestParents()$ function returns $P_{candidates}$ as shown in lines 8 and 9. If multiple candidate parents are found, the returned candidate parent set depends of the distance to the gateway of the nodes being assigned. The channel assignment on the gateway neighborhood should be done carefully since (1) the topology of this part of the network has a great impact on the performance of the network [26, 27], and (2) it affects the output forest dramatically. If the parents on the $P_{candidates}$ set are located beyond the 1st ring (line 11), the $BestParents()$ function returns one random element of $P_{candidates}$ as shown in lines 12 and 13. If the

parents on the $P_{candidates}$ set are gateways or are located on the 1st ring (line 14), the $BestParents()$ function returns the $P_{candidates}$ set with all its elements as shown in line 15.

5.3.4 $UpdateForest()$ and recursiveness

After the selection of the best parent of our node v, the function $UpdateForest()$, shown in Algorithm 6, is called in order to update the forest S that is being built on the $TiliaMainCycle()$. Node v is added to V_S and the edge e_{uv} is added to E_S on line 2, where u is the first element of P (line 1) and P is the set returned by the $BestParents()$ function. When appending v causes V_S to be complete (line 3), i.e. containing all nodes in the network N, then the spanning forest S is appended to the set of forests $\mathcal{X}$ in line 4.

Algorithm 6 $UpdateForest(N, S, \mathcal{X}, v, P)$

```
1: Let u := first element of set P
2: Append v to V_S and edge e_uv to the tree T_ch(u) ⊂ S
3: if V_S = V then
4:     Append S to the set of forests X
5: end if
6: for all other p ∈ P do
7:     Initialize S' := S
8:     Delete e_uv from the tree T'_ch(p) ⊂ S'
9:     Append e_pv to the tree T'_ch(p) ⊂ S'
10:    if V_S' = V then
11:        Append S' to the forests set X
12:    else
13:        TiliaMainCycle(N, S', X)
14:    end if
15: end for
```

If the $BestParents()$ function returns a set P with multiple parents, we start to grow a new forest S' for each candidate parent $p \in P$ (line 6). Each new forest S' is a clone of the forest S grown so far (line 7). The forests S and each of the new forests S', are distinguishable only by the edge that links node v to the forest (lines 8 and 9).

Here again, if $V_{S'}$ is complete (line 10) then the spanning forest S' is also appended to the set of forests $\mathcal{X}$ (line 11). It is not expectable that $V_{S'}$ is complete in this situation, because the $BestParents()$

function returns a set P with multiple parents only on the gateway neighborhood and it is expectable that there are nodes on the network farther from the gateways; this line was added to the algorithm to keep it robust. If S' is not yet complete when appending v (line 12), then the $TiliaMainCycle()$ is called (line 13) to continue growing the forest S' recently cloned from S.

Calling the $TiliaMainCycle()$ inside the $UpdateForest()$, which in turn is called inside $TiliaMainCycle()$, transforms the later in a recursive function. However, the recursiveness is used only to overcome ties on the assignment of nodes on the gateway neighborhood. Assigning first the nodes with less channel and parent options ($NextVertex$ function) avoids most of the ties because nodes that have connectivity through a single channel are assigned first and their contribution on the channel load is taken into account when assigning nodes that are equally distant to several gateways. By avoiding ties, the recursiveness is also avoided and the complexity of TILIA reduced.

5.3.5 Select the best forest

The $BestForest()$ function shown on Algorithm 7 returns the forest that better fits as a solution to our channel assignment problem. Each forest $S \in \mathcal{X}$ is evaluated using the composed topology metric *tmet* defined as θ in Eq. 5.17 (lines 1 and 2). The forest with highest *tmet* is returned by $BestForest()$ as the solution for the network N (line 4).

Algorithm 7 $BestForest(\mathcal{X})$

```
1: for all S ∈ 𝒳 do
2:     Calculate tmet for forest S
3: end for
4: return forest S with highest tmet
```

tmet has five components corresponding to measures of (1) the total load θ_l given by Eq. 5.18, (2) the load balancing between trees in different channels θ_{lb} given by Eq. 5.19, (3) the total number of nodes on the 1st ring θ_{r1} given by Eq. 5.20, (4) the balance between the size of 1st ring around each gateway θ_{r1b} given by Eq. 5.21, and (5) the 1st ring miss ratio θ_m given by Eq. 5.22. The highest values

of each of the components *tmet* are found on the forest S that better fits our channel assignment problem formulated earlier. All components of *tmet* (Eq. 5.18 to Eq. 5.22) are in the interval $]0,1]$.

$$\theta = k_l\theta_l + k_{lb}\theta_{Lb} + k_{r1}\theta_{r1} + k_{r1b}\theta_{r1b} + k_m\theta_m \tag{5.17}$$

$$\theta_l = \frac{\hat{l}}{\sum_{g_i \in G} l_S(g_i)} \tag{5.18}$$

$$\theta_{lb} = \frac{\left(\sum_{g_i \in G} l(g_i)\right)^2}{|G| \sum_{g_i \in G} l(g_i)^2} \tag{5.19}$$

$$\theta_{r1} = \frac{\sum_{g_i \in G} |R1^S_{g_i}|}{|R1^N|} \tag{5.20}$$

$$\theta_{r1b} = \frac{\left(\sum_{g_i \in G} |R1^S_{g_i}|\right)^2}{|G| \sum_{g_i \in G} |R1^S_{g_i}|^2} \tag{5.21}$$

$$\theta_m = (1 - m_{R1}) \tag{5.22}$$

The total load component θ_l, on Eq. 5.18, is the ratio between the minimum load $\hat{l}$ of the network N given by Eq. 5.4 and the sum of loads $l_S(g_i)$ (Eq. 5.3) of trees in the forest S. In the best case $\theta_l = 1$, which occurs when the load on the forest S equals the minimum load $\hat{l}$; if the load on the forest S is much higher than $\hat{l}$, then θ_l approaches 0.

The load balancing component θ_{lb}, in Eq. 5.19, is calculated using the by Jain fairness index [97], and represents how fair load is distributed among channels. In the best case $\theta_{lb} = 1$, which occurs when the load on trees of the forest S is equally distributed; if the loads on trees of the forest S have significant differences, then θ_{lb} approaches 0.

The total number of nodes on the 1st ring component θ_{r1}, in Eq. 5.20, is the ratio between the sum of the connectivity degree of the trees in the forest S, and the cardinal of the set $R1^N$ of nodes neighbors to gateways in the original network N. In the best case $\theta_{r1} = 1$, which occurs when all nodes in the neighborhood of gateways of the original network are assigned to one of their closest gateways; if several nodes are assigned to channels correspondent to

gateways that originally were not on their neighborhood, then θ_{r1} approaches 0.

The 1st ring balance component θ_{r1b}, in Eq. 5.21, is calculated using the Jain fairness index and measures how fair are distributed the 1st ring nodes among the gateways. In the best case $\theta_{r1b} = 1$, which occurs when the sizes of the 1st ring of each of the trees in the forest S are equally distributed; if the 1st ring sizes of trees in forest S have significant differences, then θ_{r1b} approaches 0.

The 1st ring miss ratio component θ_m, in Eq. 5.22, measures the hidden node problem on the gateways neighborhood using the miss ratio defined in Eq. 5.12. In the best case, $\theta_m = 1$ which occurs when the number of hidden nodes in the gateways neighborhood is 0 and the 1st ring miss ratio is 0; if there is a substantial number of hidden nodes in the gateways neighborhood, when compared to links that interfere with each other on the 1st ring, then the 1st ring miss ratio becomes higher and θ_m approaches 0.

We introduced weights on the calculation of topology metric θ, because it may be difficult to find a forest S that maximizes all components. Each of the components contribute with different weights (k_l, k_{lb}, k_{r1}, k_{r1b}, k_m) to the topology metric θ according to the impact these topology characteristic have on the network performance studied in previously published work [27]. We propose for our algorithm $k_l = 0.5$, $k_{lb} = 0.15$, $k_{r1} = 0.1$, $k_{r1b} = 0.1$ and $k_m = 0.15$. These values were found to be optimal to the set of 200 scenarios in which we tested TILIA.

5.4 Evaluation

In this section, we evaluate TILIA. Our experiments try to answer two questions: (1) What are the performance gains of the TILIA channel assignment algorithm when compared with state-of-the-art approaches under TCP and UDP traffic? (2) How accurate is the topology metric *tmet* to predict the performance of a WMN?

5.4.1 Methodology

In order to answer the questions we benchmarked TILIA against two alternative solutions: LB-MCP [22] and a random channel assignment. The other static channel assignment solutions identified in Chapter 2 were not considered for this study because the protocol presented in [23] does not consider the existence of multiple gateways and the approach in [24] was not designed for stub WMN, which we aim to address.

We tested the performance of the three channel assignment strategies using the network simulator ns-2.29 with HTTP and UDP traffic independently. Four performance metrics were evaluated and compared: throughput, throughput fairness, packet loss, and delay. In order to compare TILIA with the other strategies we defined $gain^{\eta}_{\lambda,s}$ as the gain of TILIA over the assignment strategy s with respect to the performance metric η for a data rate λ bit/s, as shown in Eq. 5.23,

$$gain^{\eta}_{\lambda,s} = k\frac{a^{\eta}_{\lambda,\text{TILIA}} - a^{\eta}_{\lambda,s}}{a^{\eta}_{\lambda,s}} \tag{5.23}$$

where $\eta \in \{\text{throughput, fairness, packet loss, delay}\}$, $s \in \{\text{LB-MCP, random}\}$, $a^{\eta}_{\lambda,\text{TILIA}}$ and $a^{\eta}_{\lambda,s}$ are the average values of metric η for the forests created respectively by TILIA and strategy s when each node in the network generates a data rate of λ bit/s. $k = 1$ for throughput and fairness, and $k = -1$ for delay and packet loss.

5.4.1.1 Network generation and channel assignment

A set of 200 random network topologies was analyzed. Each network has 36 nodes, including the gateways, spread in an area of 1000 m×1000 m. The position of each node, defined by its (x,y) coordinates, was generated using two independent uniform distributions. Random positions locating two nodes at a distance smaller than 50 m were rejected and another position generated. After generating the 36 positions, the connectivity of the network is tested. If a node does not have at least one neighbor located at a distance less than $RXThreshold = 350\,m$, meaning that the node is isolated, the network is rejected and a new network is generated. The first two generated positions are selected to be the gateways. A TCL script

developed inside ns-2 was used to generate and store the network topologies using the dot (http://www.graphviz.org/) graph description language.

The channel assignment is performed by a python script that reads the network graph N description and returns three graphs corresponding to three possible forests S: a forest build using TILIA, other using the LB-MCP [22], and the third by assigning channels to nodes randomly. The information about the parent of each node is included in the forest graph descriptions.

5.4.1.2 Simulator parameters

Each generated network was simulated using the network simulator ns-2.29. The parameters used in simulation are presented on the Table 5.3. The simulation tool ns-2 was used with two-ray ground reflection propagation model, IEEE 802.11 DCF MAC protocol in the link layer, and a modified version of HWMP)[1] was used to establish routes. Each simulation ran with 3 different seeds.

Parameter	Value
Propagation Model	two ray ground reflection
Channel data rate	54 Mbit/s
Receiving threshold	-70.2 dBm, 350 m
Carrier Sense threshold	-70.2 dBm, 350 m
RTS/CTS	ON
Packet size	1500 bytes
Web page size	300 kbytes (3 files with 100 kbytes each)

Table 5.3: Parameters used in ns-2.29 simulations of network topologies resultant from channel assignment with TILIA and other strategies.

The duration of each simulation was configured to give time to generate 10^4 packets on each flow; the exact duration depends on the flow data rate. During the first 10 seconds a warm up flow takes place between each node and the gateway; this flow enables the ARP tables of each node to be filled. Warm up flows are not considered to calculate the network performance metrics.

5.4.1.3 TCP traffic

Experiments with TCP traffic simulate web traffic. Each mesh node behaves like an access point with one client (web browser) attached. Each client generates page requests at five different rates. The "reading" time between two page requests is an exponentially distributed random variable with average values of 5 s, 5.5 s, 6 s, 7 s, and 8 s. These values of "reading" time were selected in order to load the network below the saturation. Each web page has 3 files with 100 kByte each.

The performance metrics are page throughput, page throughput fairness, web page latency, and page loss. The page throughput is the total number of pages received by all clients on the WMN over the simulation time. Page throughput fairness is measured using the Jain's Fairness index [97] calculated with page throughputs per node. The web page latency is the delay between the transmission of a page request by the client and the reception of the last TCP acknowledgment segment after file reception. Page loss is the ratio between the number of complete pages received and acknowledged, and the number of pages requested; pages are considered lost if they were not received by the end of the simulation.

5.4.1.4 UDP traffic

Each node, except the gateways, generates an UDP traffic flow whose packets are generated by a Poisson process; in the uplink flow, packets are destined to a node in the Internet through the serving gateway. Simultaneously, a node outside the WMN generates one downlink flow destined to each node in the network, except the gateways. Flows for each node are configured with similar parameters, which are fixed for each simulation. We tested the networks with several node data rates.

For UDP, the performance metrics are throughput, throughput fairness, packet delay, and packet loss. The throughput is the total number of packets received by flows destinations over the simulation time. Throughput fairness is measured using the Jain's Fairness index [97] calculated with throughputs per node. The packet delay is the time difference between the transmission of a packet and its

reception by the flow's destination. Packet loss is the ratio between the number of packets generated but not received by flow destinations, and the number of packets generated by flow sources.

The experiments with UDP traffic simulate a video surveillance scenario, where most of the traffic is uplink. For each simulated data rate the downlink represents 10% of the total data rate of each node. Different ratios of downlink and uplink traffic were also studied.

5.4.2 TILIA performance evaluation

Figure 5.4 represent the performance metrics averaged over the 200 tested topologies simulated with 3 different seeds. Plots show the performance metrics average values and their 90% confidence interval on the left axis and the gain of TILIA over the other assignment strategies on the right axis. The performance comparison between TILIA and the state-of-the-art channel assignment strategies under TCP traffic is shown in Figure 5.4(a), 5.4(b), 5.4(c) and 5.4(d), and the comparison under UDP traffic is shown in Figure 5.4(e), 5.4(f), 5.4(g) and 5.4(h).

Figure 5.4(a) represents the page throughput results for TCP traffic and shows that TILIA has the highest page throughput with 4.35 page/s for a rate of 400 kbit/s/node. LB-MCP's highest page throughput is 4.1 page/s for a rate of 340 kbit/s/node. When channels are assigned randomly, the highest page throughput is 3.7 page/s achieved with a data rate (343 kbit/s/node). The gain of TILIA over LB-MCP is up to 8.2% but over random assignment can be up to 24.5%.

Figure 5.4(e) represents the throughput results under UDP traffic and shows that the highest throughput obtained by TILIA is 23.8 Mbit/s. LB-MCP highest throughput is 21.9 kbit/s, and when channels are assigned randomly the highest throughput is 20.5 kbit/s. The gain of TILIA over LB-MCP is up to 8.5% but over random assignment can be up to 15.4%. For data rates higher than 900 kbit/s, the throughput and the gain are higher than represented in Figure 5.4(e), however in those situations the packet loss is too high to support applications such as video surveillance.

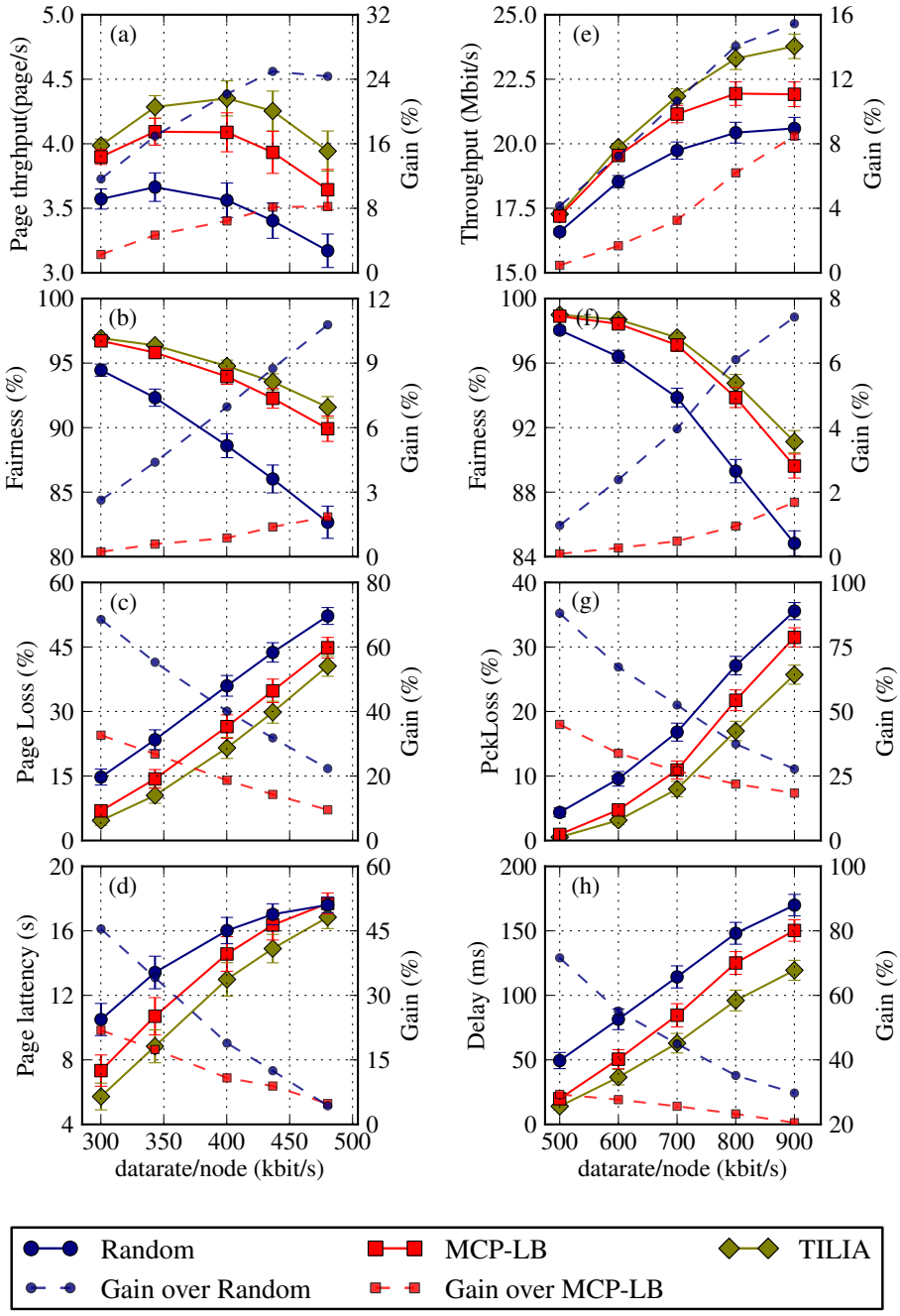

Figure 5.4: Performance comparison between TILIA and the state-of-the-art channel assignment strategies under TCP and UDP traffic.

Fairness results are shown in Figure 5.4(b) and Figure 5.4(f) for TCP and UDP experiments. Fairness is high on all channel assignment strategies evaluated, since all values are above 80%, therefore the gains of TILIA over the other channel assignment strategies is less than 10%.

Figure 5.4(c) represents the page loss results under TCP traffic. Figure 5.4(g) represents the packet loss results under UDP traffic. The page loss and packet loss increases with the data rates imposed to the network with all strategies; however the increase is influenced by the topology of the forest generated by the channel assignment strategy. TILIA page loss varies between 4.6% and 40.6% when data rates caused by page requests are respectively 300 kbit/s and 480 kbit/s; for these data rates, the page loss observed in forests generated by LB-MCP varies between 6.9% and 44.8%, while for random assignment varies between 14.8% and 52.2%. TILIA packet loss varies between 0.5% and 25.7% when the data rates of the UDP flows are respectively 500 kbit/s and 900 kbit/s; for these data rates, the packet loss observed in forests generated by LB-MCP varies between 0.9% and 31.5% while for random assignment varies between 4.3% and 35.6%. For the page loss, the gain of TILIA is higher on low data rates. TILIA performs better than the other strategies with a maximum gain of 32% over LB-MCP and 68% over the random assignment regarding page loss, and an a maximum observed gain of 45% over LB-MCP and 88% over the random assignment regarding the packet loss.

Figure 5.4(d) represents the page latency results under TCP traffic and Figure 5.4(h) represents the packet delay results under UDP traffic. The page latency and packet delay increases with the data rates imposed to the network in all strategies. However the increase is influenced by the topology of the forest generated by the channel assignment strategy. TILIA page latency varies between 5.7 s and 16.8 s when data rates caused by page requests are respectively 300 kbit/s and 480 kbit/s; for these data rates, the page latency observed in forests generated by LB-MCP varies between 7.3 s and 17.7 s while by the random assignment varies between 10.5 s and 17.6 s. TILIA packet delay varies between 14.0 ms and 119.4 ms when the data rates of the UDP flows are respectively 500 kbit/s and 900 kbit/s; for these data rates, the packet delay observed in forests generated by LB-MCP varies between 19.9 ms and 150.2 ms while by the random assignment varies between 49.4 ms and 169.9 ms. The gain of TILIA is higher on low data rates. For page latency TILIA performs better than other strategies with a maximum observed

gain of 22% over LB-MCP and 45% over the random assignment. For the packet delay, the maximum gain observed over LB-MCP is 29% and over the random assignment is 72%.

Page loss, packet loss, page latency and packet delay gains decrease when the network becomes more loaded; however, for high data rates the losses and delay are too high for web browsing purposes or video surveillance. In the graph of Figure 5.5 we present the mean data rate supported by each type of experiment for a given percentage of losses. For the same loss ratio UDP experiments support higher data rates than TCP experiments. The lower performance of TCP experiments can be partially explained by the higher overhead caused by the TCP handshake, acknowledgment and the larger packet headers. In both cases (TCP and UDP), TILIA improves significantly the performance of the network when compared with other strategies for channel assignment.

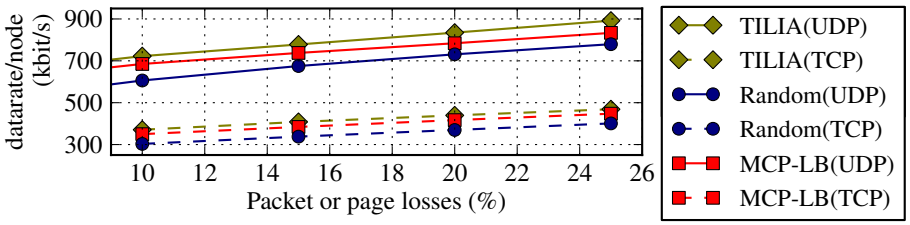

Figure 5.5: The mean data rate supported by each type of experiment for a given percentage of losses for experiments with TCP and UDP traffic.

The ratio between downlink and uplink traffic is also a cause of this result. Using UDP traffic, two other downlink versus uplink ratios were simulated with total data rate per node of 500 kbit/s: 50% for both uplink and downlink, and 10% uplink and 90% downlink. Figure 5.6 shows the results of these experiments regarding packet loss and delay. In all channel assignment strategies, less downlink and more uplink traffic lead to higher delays but lower packet loss ratio. However, even when most of the UDP traffic is downlink, TILIA has gains over the other strategies.

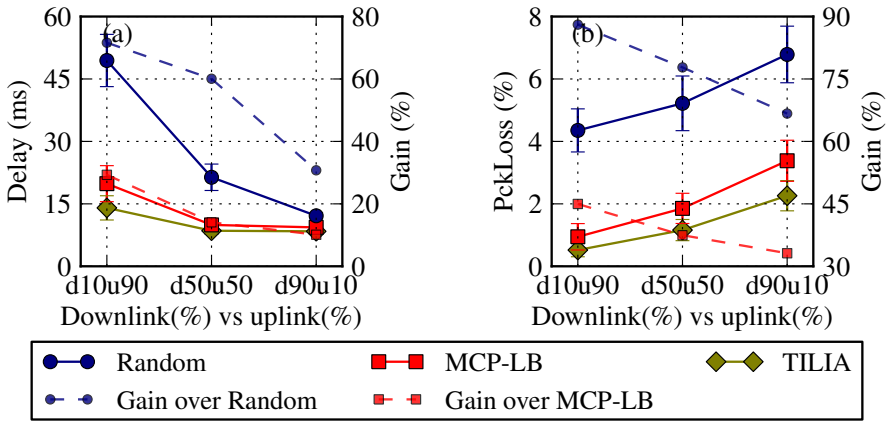

Figure 5.6: Delay and packet loss results with different ratios of downlink and uplink UDP traffic.

5.4.3 Accuracy of composed topology metric *tmet*

In order to evaluate the accuracy of the composed network topology metric *tmet*, we used the UDP simulations described above. We defined the accuracy of *tmet*, introduced in Eq. 5.17, as the percentage of cases in which a better *tmet* corresponds to better network performance. We compared the behavior of *tmet* with the behavior of the four studied performance metrics (throughput, fairness, packet loss and delay). The accuracy of *tmet* regarding the performance metric $\eta \in \{\text{throughput, fairness, packet loss, packet delay}\}$ when each node is generating a data rate of λbit/s is given by Eq. 5.24,

$$Accuracy_{\lambda}^{\eta} = \frac{1}{|T| \times |\mathcal{S}|} \sum_{t \in T} \sum_{(i,j) \in \mathcal{S}} \mathbb{1}_{\Theta_{ij}^{t} \leftrightarrow A_{ij}^{\eta t \lambda}} \tag{5.24}$$

$$\Theta_{ij}^{t} = \begin{cases} 1, & \theta_i^t - \theta_j^t > 0 \\ 0, & \text{otherwise} \end{cases} \tag{5.25}$$

$$A_{ij}^{\eta t \lambda} = \begin{cases} 1, & k \cdot a_{\lambda,i}^{\eta,t} - k \cdot a_{\lambda,j}^{\eta,t} > 0 \\ 0, & \text{otherwise} \end{cases} \tag{5.26}$$

$$\mathbb{1}_x = \begin{cases} 1, & x \text{ is true} \\ 0, & x \text{ is false} \end{cases} \tag{5.27}$$

where T is the set of the 200 simulated random topologies, and $\mathcal{S} = \binom{S}{2}$ is the set of all 2-combinations out of the set S={TILIA,

MCP-LB, random} of the considered channel assignment strategies.

The boolean function Θ_{ij}^{t} in Eq. 5.25 compares the *tmet* θ_i^t and θ_j^t of the two forests derived by the channel assignment strategies i and j for the topology t. The Θ_{ij}^{t} is 1 if the forest resultant from strategy i has a *tmet* higher than the *tmet* associated to the strategy j; otherwise, it is zero.

The boolean function $A_{ij}^{\eta t\lambda}$ in Eq. 5.26 compares the mean values of performance metric η, $a_{\lambda,i}^{\eta,t}$ and $a_{\lambda,j}^{\eta,t}$ when simulating the two forests derived by the channel assignment strategies i and j for the topology t with a data rate of λ bit/s per node. $A_{ij}^{\eta t\lambda}$ is 1 if the forest resultant from strategy i leads to a performance metric η better than the one associated to the strategy j; otherwise, it is zero. $k = 1$ for throughput and fairness, and $k = -1$ for delay and packet loss.

The indicator function $\mathbb{1}_x$ in Eq. 5.27 is 1 if the event x is true; otherwise, it is zero. In Eq. 5.24 the indicator function returns 1 if the functions Θ_{ij}^{t} and $A_{ij}^{\eta t\lambda}$ are both true or both false which occurs when the forest of topology t resultant from strategy i has simultaneously a higher *tmet* and a better performance η, or a lower *tmet* and a worse performance η.

The results of the *tmet* accuracy are shown in Figure 5.7 for throughput, fairness, packet loss, and delay. Figure 5.7 shows that the *tmet* accuracy is above 94% for all the performance metrics. The accuracy of *tmet* is higher for lower data rates because, near saturations, the network performance turns to be more chaotic and, therefore, less predictable.

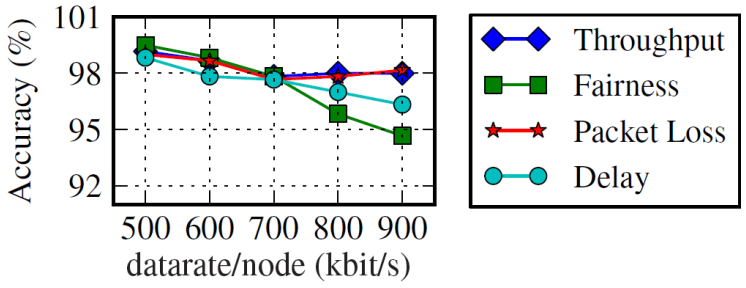

Figure 5.7: Accuracy of the network topology metric *tmet*.

5.5 Summary

We presented TILIA, a centralized channel assignment algorithm used to improve the performance of single-radio WMN using multiple channels. Our goal is to improve the performance of a multi-channel WMN by controlling solely the channel in which each node operates. We ended at enhancing the gateway neighborhood by increasing its size and avoiding hidden nodes on links around the gateway, while keeping the load balanced between channels. TILIA uses a breadth-first tree growing technique, but instead of growing a single tree, TILIA grows a forest of κ trees each of which rooted at a different gateway; all the trees grow simultaneously and their union spans the network. TILIA solves more than the channel assignment problem since it also defines the paths between each node and the gateway. Our experimental evaluation based in ns-2 simulations shows that the gains of TILIA are visible on packet loss, page loss, and packet delay, respectively with gains of 45% 33% and 29% when compared with the state-of-the-art proposal [22], and 88%, 69% and 72% when compared with random channel assignment. We also introduced the composed topology metric *tmet* used by TILIA to select the forest with best topology characteristics. The accuracy of the proposed composed topology metric is over 94%.

Chapter 6

Conclusions

6.1 Work review

In this thesis we addressed the problem of improving the capacity of stub WMNs consisting of nodes equipped with a single radio off-the-shelf 802.11 interface, by statically assigning channels to nodes. We posed the hypothesis of using solely the topology information about the WMN to solve the problem, instead of using also traffic information as done by state of the art works. To test this hypothesis we conducted an large set of experiments in which we simulated thousands of different network topologies.

In Chapter 2 we studied the DCF which is the CSMA/CA MAC protocol used in IEEE 802.11 standard. We surveyed the most important works addressing the capacity of wireless networks and WMN in particular. We described three interference models which are valuable tools for determining interference between pairs of links in a wireless network. We presented a survey of existing channel assignment methods, particularly those available for single-radio WMNs. Multi-channel MAC and routing protocols were presented as well as algorithms for channel assignment. State-of-the art works that relate the network performance with network topology metrics such as the mean hop count, the neighbor node density, the mean number of hidden nodes, and the $missratio$ were also reviewed.

Chapter 3 characterized the impact that the network topology characteristics have on the performance of a WMN. A set of metrics that characterize the gateways neighborhood were introduced: the

size of the 1st ring, the mean number of hidden nodes on the 1st ring, and the *missratio* on the 1st ring. We defined a set of experiments with 18 arbitrary channel assignment scenarios in a 6x6 lattice topology network. Simulations using ns-2 were carried out and, based on the results obtained, the topology characteristics that have impact on the throughput of the WMN were identified as being the following: the *mean hop count* calculated between nodes and the respective gateway; the *number of nodes in the 1st ring* that is the number of nodes directly connected to gateways; the *neighbor node density* that is the mean number of neighbors of a mesh node; the *miss ratio* that synthesizes the number of hidden nodes on the network; the *1st ring miss ratio* that synthesizes the number of hidden nodes on the gateway neighborhood. The main conclusion of Chapter 3 is that the performance of the WMN is highly related to these topology metrics.

In Chapter 4 we ranked the network topology characteristics by their order of influence on the performance of a single-radio multi-channel IEEE 802.11 WMN. A set of 3500 topologies with 36 randomly positioned nodes was created using the network simulator ns-2 [93]. Two channel assignment strategies were then applied to each of the 3500 topologies, by assigning one of two possible channels to each node. Each of the 7000 networks was simulated four times using ns-2 with two possible traffic loads and two different simulation seeds; low load and high load scenarios were simulated. The topological and performance metrics from the 28000 network simulations were used to train a data mining model based on support vector machines. The considered topological metrics were those identified on Chapter 3 plus the number of nodes sharing a radio channel. This metric has brought by the use of random network topologies. The new set of metrics is composed by (1) the number of nodes per subnetwork, (2) the mean hop count, (3) the number of nodes in the 1st ring, (4) the neighbor node density, (5) the *miss ratio*, and (6) the 1st ring *miss ratio*. The input parameters of the models are the six topology metrics enumerated above and the output of each model are the three performance metrics: network aggregate throughput, fairness, and delay. Using fitted data mining models, the effect of topology metrics on performance was quantified using a sensitivity

analysis procedure which revealed the relative importance of each topology metric for each model. The results obtained suggest that the topology metric that has the greatest impact on the performance of a WMN is the number of nodes that are directly connected to the gateway: a larger 1^{st} ring results in increased data throughput, increased throughput fairness, and lower delay. Hop distance of nodes to the gateway and the difference between the number of nodes in sub-networks also have impact on the network performance, but mostly in the provisioning of fairness. That study also suggests that throughput and delay could be improved by avoiding hidden nodes, in particular on links to the gateway. Other topology metrics are considered to have little influence on the models output.

In Chapter 5 we presented TILIA, a centralized channel assignment algorithm used to improve the performance of single-radio WMN using multiple channels. Our goal is to improve the performance of a multi-channel WMN by controlling solely the channel in which each node operates. We ended at enhancing the gateway neighborhood by increasing its size and avoiding hidden nodes on links around the gateway, while keeping the load balanced between channels. TILIA uses a breadth-first tree growing technique but, instead of growing a single tree, TILIA grows a forest of κ trees each of which rooted at a different gateway; all the trees grow simultaneously and their union spans the network. Each gateway operates at a different channel. All nodes associated with a tree share the same radio channel of the gateway that is the root of that tree. TILIA solves more than the channel assignment problem since it also defines the paths between each node and the gateway. Our experimental evaluation based in ns-2 simulations shows that the gains of TILIA are visible on packet loss, page loss, and packet delay, respectively with gains of 45% 33% and 29% when compared with the state-of-the-art proposal [22], and 88%, 69% and 72% when compared with random channel assignment. We also introduced the composed topology metric *tmet* used by TILIA to select the forest with best topology characteristics. The metrics considered to *tmet* are more sophisticated than those identified in Chapter 3 and ranked in Chapter 4; they are the following: *expected load on the WMN*, which is synthesized by the sum of the hop count between all nodes

and the gateway; *load balancing between channels*, which measures discrepancies between sums of the hop count of nodes sharing each channel using the fairness Jain index [97]; *number of nodes in the 1st ring*, which are the nodes directly connected to gateways; *balancing on the 1st ring*, which measures discrepancies between the number of nodes directly connected to each gateway using the fairness Jain index [97]; *1st ring miss ratio*, which synthesizes the number of hidden nodes on the gateway neighborhood. The accuracy of *tmet* is over 94%.

6.2 Contributions

This thesis provides the following original contributions:

1. **Identification and ranking of network topology metrics by their order of influence on the performance of a single-radio multi-channel IEEE 802.11 WMN**, which are by order of importance: *expected load on the WMN*, which is synthesized by the sum of the hop count between all nodes and the gateway; *load balancing between channels*, which measures discrepancies between sums of the hop count of nodes sharing each channel; *1st ring miss ratio*, which synthesizes the number of hidden nodes on the gateway neighborhood; *number of nodes in the 1st ring*, which are the nodes directly connected to gateways; *balancing on the 1st ring*, which measures discrepancies between the number of nodes directly connected to each gateway; *miss ratio*, which synthesizes the number of hidden nodes on the network; *neighbor node density*, which is the mean number of neighbors of a mesh node;

2. **A centralized joint routing and channel assignment algorithm for single-radio WMN**. We propose TILIA, an algorithm that reduces frame collisions while providing very good load balancing. The novelty of TILIA when compared with the state-of-the-art proposals [19], [23],[24] is that TILIA reduces interference caused by hidden nodes [19], it considers the existence of multiple gateways [23], and it was designed for

stub WMN [24]. Experimental evaluations based in ns-2 simulations show that the gains of TILIA are visible on packet loss, HTML page loss, and packet delay, respectively with gains of 45%, 33%, and 29% when compared with a state-of-the-art proposal [22], and with gains of 88%, 69% and 72% when compared with random channel assignment.

3. **A joint topology metric that considers relevant topology characteristics**. The characteristics considered to the *tmet* metric are the expected load on the WMN, the load balancing between channels, the 1st ring $missratio$, the number of nodes in the 1st ring, and the balancing on the 1st ring. The metric *tmet*, defined in Eq. 5.17, can predict the network performance with an accuracy of 94% and can be used to rank different channel assignment schemes generated by TILIA for a given network topology. To the best of our knowledge this is the first composed metric for CSMA/CA based WMNs using network wide topological information.

6.3 Future work

The topics for future work presented in this section are both new research ideas building upon the work presented in this thesis, applications of this work, and working issues to help improving our work.

Design a dynamic WMN radio planning tool. A management system that dynamically selects the number of channels in the network considering traffic load and the density of nodes in the network could be used to plan WMN. The idea is that a higher number of channels could be used on denser and loaded networks, while sparse or less loaded networks could use a lower number of channels. The TILIA algorithm could also be used to assign channels to nodes when the number of available radio channels changes.

Design a distributed channel assignment algorithm. Using the knowledge about the topology metrics that have impact on the WMN performance, a distributed channel assignment algorithm for single-radio stub WMN nodes could be designed. Distributed algorithms could be applied to scenarios such as disaster recovery.

Adapt TILIA to WSN. WSNs have constraints that were not considered on the design of TILIA such as nodes operating on low power, radios with short ranges, and variants of CSMA/CA MAC protocols. Evaluating TILIA for WSN would rise new research issues.

Evaluate *tmet* and TILIA in broader scenarios. The simulation scenarios that are used to evaluate *tmet* and TILIA could be generalized: (1) use topologies with a variable number of nodes; (2) use a variable number of channels; (3) use different traffic patterns and traffic loads.

Test TILIA in a WMN testbed. During the PhD research work a proof-of-concept experiment of gathering topology information in a multi-channel single-radio WMN was carried out and an architecture was designed to integrate TILIA into a testbed. The usage of TILIA with real traffic and interference conditions would clarify the value of our work.

Generalize our WMN model and design an improved algorithm. The simplifications considered in our WMN model could be removed in order to define a more generic model. These generalizations could be applied to design a new channel assignment algorithm, considering the following:

- The nodes in the network communication graph may generate different amounts of traffic. Thus, the load could be weighted considering these differences.

- When nodes inside the WMN are required to communicate peer-to-peer, the traffic patterns assumed on our model become inappropriate and must be reconsidered.

- Path loss effects can influence the degree of interference between links, thus the model could consider fractional interference between links.
- When the depth of a route tree becomes large, spatial reuse must be considered in the load estimation.
- Even when radio channels are orthogonal in theory, they do interfere due to device imperfections (e.g., radio leakage and improper shielding). Thus, modeling of nonorthogonal (i.e., interfering) channels seems to be a good idea. In addition, this also allows us to explicitly utilize nonorthogonal channels.

References

[1] IEEE standard for information technology–telecommunications and information exchange between systems local and metropolitan area networks–specific requirements part 11: Wireless lan medium access control (MAC) and physical layer (PHY) specifications. *IEEE Std 802.11-2012 (Revision of IEEE Std 802.11-2007)*, pages 1 –2793, 2012.

[2] Ian F. Akyildiz and Xudong Wang. *Wireless mesh networks*. John Wiley & Sons, 2009.

[3] Eva Gustafsson and Annika Jonsson. Always best connected. *IEEE Wireless Communications*, 10(1):49 – 55, February 2003.

[4] Raffaele Bruno, Marco Conti, and Enrico Gregori. Mesh networks: commodity multihop ad hoc networks. *IEEE Communications Magazine*, 43(3):123 – 131, March 2005.

[5] John Jubin and Janet D. Tornow. The darpa packet radio network protocols. *Proceedings of the IEEE*, 75(1):21 – 32, January 1987.

[6] Imrich Chlamtac, Marco Conti, and Jennifer J.-N. Liu. Mobile ad hoc networking: imperatives and challenges. *Ad Hoc Networks*, 1(1):13 – 64, July 2003.

[7] Tania Calcada and Manuel Ricardo. Extending the coverage of a 4g telecom network using hybrid ad-hoc networks: a case study. In *Mediterranean Ad Hoc Networking Workshop (Med-HocNet'05)*, France, June 2005.

[8] Tania Calcada and Manuel Ricardo. Extending the coverage of a 4g telecom network using hybrid ad-hoc networks: a case study. In K. Al Agha, I. Guérin Lassous, and G. Pujolle, editors, *Challenges in Ad Hoc Networking*, pages 367–376. Springer, July 2006.

[9] Susana Sargento, Tania Calcada, João Paulo Barraca, Sérgio Crisóstomo, João Girão, Marek Natkaniec, Norbert Vicari, Francisco J. Galera, Manuel Ricardo, and Andrzej Glowacz. Mobile ad-hoc networks integration in the daidalos architecture. In *IST Mobile & Wireless Communications Summit*, Germany, June 2005.

[10] Roger Karrer, Ashu Sabharwal, and Ed Knightly. Enabling large–scale wireless broadband: The case for tap. *ACM SIGCOMM Computer Communication Review*, 34(1):27–34, January 2004.

[11] Pradeep Kyasanur and Nitin H. Vaidya. Capacity of multi-channel wireless networks: impact of number of channels and interfaces. In *International Conference on Mobile Computing and Networking (MobiCom'05)*, pages 43–57, Germany, September 2005.

[12] Murali Kodialam and Thyaga Nandagopal. Characterizing the capacity region in multi-radio multi-channel wireless mesh networks. In *International Conference on Mobile Computing and Networking (MobiCom'05)*, pages 73–87, Germany, September 2005.

[13] Piyush Gupta and Panganamala R. Kumar. The capacity of wireless networks. *IEEE Transactions on Information Theory*, 46(2):388–404, March 2000.

[14] Ozlem Durmaz Incel. A survey on multi-channel communication in wireless sensor networks. *Computer Networks*, 55(13):3081 – 3099, September 2011.

[15] Jorge Crichigno, Min-You Wu, and Wei Shu. Protocols and architectures for channel assignment in wireless mesh networks. *Ad Hoc Networks*, 6(7):1051–1077, September 2008.

[16] Aditya Dhananjay, Hui Zhang, Jinyang Li, and Lakshminarayanan Subramanian. Practical, distributed channel assignment and routing in dual-radio mesh networks. *ACM SIGCOMM Computer Communication Review*, 39(4):99–110, October 2009.

[17] Mahesh K. Marina, Samir R. Das, and Anand Prabhu Subramanian. A topology control approach for utilizing multiple channels in multi-radio wireless mesh networks. *Computer Networks*, 54(2):241 – 256, February 2010.

[18] Anand Prabhu Subramanian, Himanshu Gupta, Samir R. Das, and Jing Cao. Minimum interference channel assignment in

multiradio wireless mesh networks. *IEEE Transactions on Mobile Computing*, 7(12):1459–1473, December 2008.

[19] Jungmin So and Nitin H. Vaidya. Multi-channel mac for ad hoc networks: handling multi-channel hidden terminals using a single transceiver. In *International Symposium on Mobile Ad Hoc Networking and Computing (MobiHoc'04)*, pages 222–233, Japan, May 2004.

[20] R. Maheshwari, H. Gupta, and S.R. Das. Multichannel mac protocols for wireless networks. In *IEEE Sensor and Ad Hoc Communications and Networks (SECON '06)*, volume 2, pages 393 – 401, USA, September 2006.

[21] Paramvir Bahl, Ranveer Chandra, and John Dunagan. SSCH: slotted seeded channel hopping for capacity improvement in IEEE 802.11 ad-hoc wireless networks. In *International Conference on Mobile Computing and Networking (MobiCom'04)*, pages 216–230, USA, September 2004.

[22] Jungmin So and Nitin H. Vaidya. Load-balancing routing in multichannel hybrid wireless networks with single network interface. *IEEE Transactions on Vehicular Technology*, 55(3):806–812, May 2006.

[23] Yafeng Wu, J.A. Stankovic, Tian He, and Shan Lin. Realistic and efficient multi-channel communications in wireless sensor networks. In *IEEE International Conference on Computer Communications (Infocom'08)*, pages 1193 –1201, April 2008.

[24] Ramanuja Vedantham, Sandeep Kakumanu, Sriram Lakshmanan, and Raghupathy Sivakumar. Component based channel assignment in single radio, multi-channel ad hoc networks. In *International Conference on Mobile Computing and Networking (MobiCom'06)*, pages 378–389, USA, 2006.

[25] T. Calcada and M. Ricardo. Topology aware channel assignment for single-radio stub WMN. *IEEE Transactions on Mobile Computing*, 2012. Under revision.

[26] Tania Calcada and Manuel Ricardo. Characterization of network topology impact on the performance single-radio wireless mesh networks. *Telecommunication Systems*, 2012.

[27] Tania Calcada, Paulo Cortez, and Manuel Ricardo. Using data mining to study the impact of topology characteristics on the performance of wireless mesh networks. In *IEEE Wireless Communications and Networking Conference (WCNC'12)*, pages 1725–1730, France, April 2012.

[28] Tania Calcada and Manuel Ricardo. The impact of network topology on the performance of multi-channel single-radio mesh networks. In *Networking and Electronic Commerce Research Conference (NAEC'11)*, pages 183–195, Italy, October 2011.

[29] Filipe Teixeira, Tania Calcada, and Manuel Ricardo. Protocol for channel assignment in single-radio mesh networks. In *Conference on Mobile Networks and Management (MONAMI'11)*, Portugal, September 2011.

[30] Filipe Teixeira, Tania Calcada, and Manuel Ricardo. Protocol for channel assignment in single-radio mesh networks. In Kostas Pentikousis, Rui Aguiar, Susana Sargento, and Ramón Agüero, editors, *Lecture Notes of the Institute for Computer Sciences, Social Informatics and Telecommunications Engineering*, pages 17–30. Springer, May 2012.

[31] Filipe Teixeira, Tania Calcada, and Manuel Ricardo. Single-radio stub wireless mesh networks - architecture for a channel assignment subsystem. In *Networking and Electronic Commerce Research Conference (NAEC'12)*, Italy, October 2012.

[32] C. Perkins, E. Belding-Royer, and S. Das. Ad hoc On-Demand Distance Vector (AODV) Routing. RFC 3561, 2003.

[33] IEEE802.11s. IEEE wireless LAN medium access control (MAC) and physical layer (PHY) specifications draft on mesh networking v2.0. April 2008.

[34] Kaixin Xu, Mario Gerla, and Sang Bae. Effectiveness of rts/cts handshake in ieee 802.11 based ad hoc networks. *Ad Hoc Networks*, 1(1):107 – 123, July 2003.

[35] Shugong Xu and Tarek Saadawi. Does the ieee 802.11 mac protocol work well in multihop wireless ad hoc networks? *IEEE Communications Magazine*, 39(6):130 –137, June 2001.

[36] Matthias Grossglauser and David N. C. Tse. Mobility increases the capacity of ad hoc wireless networks. *IEEE/ACM Transactions on Networking*, 10(4):477–486, August 2002.

[37] Michael Gastpar and Martin Vetterli. On the capacity of wireless networks: the relay case. In *IEEE International Conference on Computer Communications (Infocom'02)*, volume 3, pages 1577–1586, USA, June 2002.

[38] Jangeun Jun and M.L. Sichitiu. The nominal capacity of wireless mesh networks. *IEEE Wireless Communications*, 10(5):8–14, October 2003.

[39] Parth H. Pathak and Rudra Dutta. Impact of power control on capacity of large scale wireless mesh networks. In *IEEE International Symposium on Advanced Networks and Telecommunication Systems (ANTS'09)*, pages 1–3, India, December 2009.

[40] Vartika Bhandari and Nitin H. Vaidya. Connectivity and capacity of multi-channel wireless networks with channel switching constraints. In *IEEE International Conference on Computer Communications (Infocom'07)*, pages 785 –793, USA, May 2007.

[41] Enrique J. Duarte-Melo and Mingyan Liu. Data-gathering wireless sensor networks: organization and capacity. *Computer Networks*, 43(4):519–537, November 2003.

[42] Jimmi Gronkvist and Anders Hansson. Comparison between graph-based and interference-based STDMA scheduling. In *International Symposium on Mobile Ad Hoc Networking and Computing (MobiHoc'01)*, pages 255–258, USA, October 2001.

[43] Mansoor Alicherry, Randeep Bhatia, and Li Erran Li. Joint channel assignment and routing for throughput optimization in multi-radio wireless mesh networks. In *International Conference on Mobile Computing and Networking (MobiCom'05)*, pages 58–72, Germany, August 2005.

[44] Thomas Moscibroda, Roger Wattenhofer, and Yves Weber. Protocol design beyond graph-based models. In *Workshop on Hot Topics in Networks (HotNets'06)*, USA, November 2006.

[45] Gaurav Sharma, Ravi R. Mazumdar, and Ness B. Shroff. On the complexity of scheduling in wireless networks. In *International Conference on Mobile Computing and Networking (MobiCom'06)*, pages 227–238, USA, September 2006. ACM.

[46] Nachum Shacham and Peter King. Architectures and performance of multichannel multihop packet radio networks. *IEEE Journal on Selected Areas in Communications*, 5(6):1013 – 1025, July 1987.

[47] Robert E. Kahn, Steven A.Gronemeyer, Jerry Burchfiel, and Ronald C. Kunzelman. Advances in packet ratio technology. *Proceedings of the IEEE*, 66(11):1468 – 1496, November 1978.

[48] Habiba Skalli, Samik Ghosh, Sajal K. Das, Luciano Lenzini, and Marco Conti. Channel assignment strategies for multiradio wireless mesh networks: Issues and solutions. *IEEE Communications Magazine*, 45(11):86–95, November 2007.

[49] Yong Ding and Li Xiao. Channel allocation in multi-channel wireless mesh networks. *Computer Communications*, 34(7):803 – 815, May 2011.

[50] Weisheng Si, Selvadurai Selvakennedy, and Albert Y. Zomaya. An overview of channel assignment methods for multi-radio multi-channel wireless mesh networks. *Journal of Parallel and Distributed Computing*, 70(5):505–524, May 2010.

[51] Survey of multi-channel mac protocols for ieee 802.11-based wireless mesh networks. *The Journal of China Universities of Posts and Telecommunications*, 18(2):33 – 44, April 2011.

[52] Mingfei Wang, Linlin Ci, Ping Zhan, and Yongjun Xu. Multi-channel mac protocols in wireless ad hoc and sensor networks. In *ISECS International Colloquium on on Computing, Communication, Control, and Management (CCCM '08)*, volume 2, pages 562 –566, China, August 2008.

[53] Roberto Riggio, Tinku Rasheed, Stefano Testi, Fabrizio Granelli, and Imrich Chlamtac. Interference and traffic aware channel assignment in wifi-based wireless mesh networks. *Ad Hoc Networks*, 9(5):864 –875, July 2011.

[54] Nitin Jain, Samir R. Das, and Asis Nasipuri. A multichannel csma mac protocol with receiver-based channel selection for multihop wireless networks. In *International Conference on Computer Communications and Networks (ICCCN'01)*, pages 432–439, USA, October 2001.

[55] Jiandong Li, Z.J. Haas, Min Sheng, and Yanhui Chen. Performance evaluation of modified ieee 802.11 mac for multi-channel multi-hop ad hoc network. In *International Conference Advanced Information Networking and Applications (AINA'03)*, pages 312 – 317, China, March 2003.

[56] Asimakis Tzamaloukas and J.J. Garcia-Luna-Aceves. Channel-hopping multiple access. In *International Conference on Communications (ICC'2000)*, volume 1, pages 415 –419, USA, June 2000.

[57] Z. Tang and J.J. Garcia-Luna-Aceves. Hop reservation multiple access for multichannel packet radio networks. *Computer Communications*, 23(10):877 – 886, May 2000.

[58] Hoi-Sheung, Wilson So, Jean Walrand, and Jeonghoon Mo. Mcmac: A parallel rendezvous multi-channel mac protocol. In *IEEE Wireless Communications and Networking Conference (WCNC'07)*, pages 334 –339, Hong Kong, March 2007.

[59] Jenhui Chen, Shiann-Tsong Sheu, and Chin-An Yang. A new multichannel access protocol for ieee 802.11 ad hoc wireless lans. In *IEEE International Symposium on Personal, Indoor and Mobile Radio Communications (PIMRC'03)*, volume 3, pages 2291 – 2296, China, September 2003.

[60] Jingbin Zhang, Gang Zhou, Chengdu Huang, S.H. Son, and J.A. Stankovic. Tmmac: An energy efficient multi-channel mac protocol for ad hoc networks. In *International Conference on Communications (ICC'07)*, pages 3554 –3561, Scotland, June 2007.

[61] Jeonghoon Mo, H.-S.W. So, and J. Walrand. Comparison of multichannel mac protocols. *IEEE Transactions on Mobile Computing*, 7(1):50 –65, January 2008.

[62] Ping Chung Ng and Soung Chang Liew. Throughput analysis of IEEE802.11 multi-hop ad hoc networks. *IEEE/ACM Transactions on Networking*, 15(2):309–322, April 2007.

[63] Jinyang Li, Charles Blake, Douglas S.J. De Couto, Hu Imm Lee, and Robert Morris. Capacity of ad hoc wireless networks. In *International Conference on Mobile Computing and Networking (MobiCom'01)*, pages 61–69, Italy, July 2001.

[64] Jia-Chun Kuo, Wanjiun Liao, and Ting-Chao Hou. Impact of node density on throughput and delay scaling in multi-hop wireless networks. *IEEE Transactions on Wireless Communications*, 8(10):5103–5111, October 2009.

[65] Li Bin Jiang and Soung Chang Liew. Improving throughput and fairness by reducing exposed and hidden nodes in 802.11 networks. *IEEE Transactions on Mobile Computing*, 7(1):34–49, January 2008.

[66] Ahmad Ali Abdullah, Fayez Gebali, and Lin Cai. Modeling the throughput and delay in wireless multihop ad hoc networks. In *IEEE Global Telecom. Conference (GLOBECOM'09)*, pages 1–6, USA, November 2009.

[67] Jin Yang, Jae Kwon, Ho Hwang, and Dan Sung. Goodput analysis of a WLAN with hidden nodes under a non-saturated condition. *IEEE Transactions on Wireless Communications*, 8(5):2259–2264, May 2009.

[68] Kaixin Xu, Mario Gerla, and Sang Bae. How effective is the IEEE 802.11 RTS/CTS handshake in ad hoc networks. In *IEEE Global Telecom. Conference (GLOBECOM'02)*, volume 1, pages 72–76, Taiwan, November 2002.

[69] Abdelmalik Bachir, Dominique Barthel, Martin Heusse, and Andrzej Duda. Hidden nodes avoidance in wireless sensor networks. In *International Conference Wireless Networks, Communications and Mobile Computing (WirelessCom'05)*, volume 1, pages 612–617, USA, June 2005.

[70] Sumit Khurana, Anurag Kahol, and Anura P. Jayasumana. Effect of hidden terminals on the performance of IEEE 802.11 MAC protocol. In *IEEE Conference on Local Computer Networks (LCN'98)*, pages 12–20, USA, June 1998.

[71] Michel Bahr. Update on the hybrid wireless mesh protocol of ieee 802.11s. In *IEEE International Conference on Mobile Adhoc and Sensor Systems (MASS'07).*, pages 1 –6, Italy, October 2007.

[72] Usman Ashraf, Slim Abdellatif, and Guy Juanole. Route selection in IEEE 802.11 wireless mesh networks. *Telecommunication Systems*, pages 1–19, June 2011.

[73] Bang Wang, Hock Beng Lim, Di Ma, and Cheng Fu. The hop count shift problem and its impacts on protocol design in wireless ad hoc networks. *Telecommunication Systems*, 44(1-2):49–60, June 2010.

[74] Jangeun Jun and M.L. Sichitiu. Fairness and QoS in multihop wireless networks. *IEEE Vehicular Technology Conference (VTC-2003-Fall)*, pages 2936–2940, October 2003.

[75] Nagesh S. Nandiraju, Deepti S. Nandiraju, Dave Cavalcanti, and Dharma P. Agrawal. A novel queue management mechanism for improving performance of multihop flows in IEEE 802.11 s based mesh networks. In *International Conference Performance, Computing, and Communications (IPCCC'06)*, pages 162–168, USA, April 2006.

[76] Jangeun Jun, Pushkin Peddabachagari, and M.L. Sichitiu. Theoretical maximum throughput of IEEE 802.11 and its applications. In *International Symposium Network Computing and Applications (NCA'03)*, pages 249–256, USA, July 2003.

[77] Chi Pan Chan, Soung Chang Liew, and An Chan. Many-to-One throughput capacity of IEEE 802.11 multihop wireless networks. *IEEE Transactions on Mobile Computing*, 8(4):514–527, April 2009.

[78] T. Hastie, R. Tibshirani, and J. H Friedman. *The elements of statistical learning: data mining, inference, and prediction.* Springer Verlag, February 2009.

[79] R. H Kewley, M. J Embrechts, and C. Breneman. Data strip mining for the virtual design of pharmaceuticals with neural networks. *IEEE Transactions on Neural Networks*, 11(3):668–679, May 2000.

[80] Enrique Castillo, José Manuel Gutiérrez, Ali S Hadi, and Beatriz Lacruz. Some applications of functional networks in statistics and engineering. *Technometrics*, 43(1):10–24, February 2001.

[81] Emad A. El-Sebakhy. Software reliability identification using functional networks: A comparative study. *Expert systems with applications*, 35:4013–4020, March 2009.

[82] E. Castillo, A. S Hadi, B. Lacruz, and R. Pruneda. Semiparametric nonlinear regression and transformation using functional network. *Computational Statistics and Data Analysis*, pages 2129–2157, 2008.

[83] Betanzos, A. Alonso, E. Castillo, F. Romero, and N. Marono. Shear strength prediction using dimensional analysis and functional networks. In *European Symposium on Artificial Neural Networks*, pages 251–256, April 2004.

[84] Paulo Cortez, Miguel Rio, Miguel Rocha, and Pedro Sousa. Internet traffic forecasting using neural networks. In *International Joint Conference on Neural Networks (IJCNN'06)*, page 2635–2642, Canada, July 2006.

[85] Corinna Cortes and Vladimir Vapnik. Support-vector networks. *Machine learning*, 20(3):273–297, September 1995.

[86] Alex J Smola and Bernhard Schölkopf. A tutorial on support vector regression. *Statistics and computing*, 14(3):199–222, August 2004.

[87] Xia Wang, Johnny S. Wong, Fred Stanley, and Samik Basu. Cross-layer based anomaly detection in wireless mesh networks. In *International Symposium on Applications and the Internet (SAINT'09)*, pages 9–15, USA, July 2009.

[88] Claudina Rattaro and Pablo Belzarena. Throughput prediction in wireless networks using statistical learning. In *Latin-American Workshop on Dynamic Networks (LAWDN'10)*, Argentina, November 2010.

[89] Youssef Iraqi. Topology effect on the capacity of wireless mesh networks. In *IEEE GCC Conference and Exhibition (IEEE-GCC'11)*, pages 311–314, United Arab Emirates, February 2011.

[90] Jkob Hoydis, Marina Petrova, and Petri Mahonen. Effects of topology on local throughput-capacity of ad hoc networks. In *IEEE International Symposium on Personal, Indoor and Mobile Radio Communications (PIMRC'08)*, pages 1–5, France, September 2008.

[91] Joshua Robinson and Edward Knightly. A performance study of deployment factors in wireless mesh networks. In *IEEE International Conference on Computer Communications (Infocom'07)*, pages 2054–2062, USA, May 2007.

[92] Paulo Cortez and Mark J. Embrechts. Opening black box data mining models using sensitivity analysis. In *IEEE Symposium on Computational Intelligence and Data Mining (CIDM'11)*, France, April 2011.

[93] The network simulator ns-2. http://www.isi.edu/nsnam/ns/.

[94] Yang Xiao and Jon Rosdahl. Throughput and delay limits of IEEE 802.11. *IEEE Communications Letters*, 6(8):355– 357, August 2002.

[95] Vladimir Cherkassky and Yunqian Ma. Practical selection of SVM parameters and noise estimation for SVM regression. *Neural Networks*, 17(1):113–126, January 2004.

[96] Paulo Cortez. Data mining with neural networks and support vector machines using the r/rminer tool. *Industrial Conference on Advances in Data Mining: Applications and Theoretical Aspects (ICDM'10)*, pages 572–583, July 2010.

[97] Rajendra Jain, Dah-Ming Chiu, and William R. Hawe. A quantitative measure of fairness and discrimination for resource allocation in shared systems. Technical Report 301, Digital Equipment Corporation, September 1984.

[98] Chih-Yu Lin, Shu-Hsien Lu, and Yu-Chee Tseng. A channel management protocol for multi-channel, single-radio 802.11-based wireless mesh networks. In *IEEE International Workshop on Computer Aided Modeling and Design of Communication Links and Networks (CAMAD'11)*, pages 26–30, Japan, June 2011.

[99] Jonathan Gross and Jay Yellen. *Graph Theory*. Chapman, 2006.

[100] Djohara Benyamina, Abdelhakim Hafid, and Michel Gendreau. Design of scalable and efficient multi-radio wireless networks. *Wireless Networks*, 18(1):75–94, 2012.

[101] Liliane R.B. Salgado and Yoshiko Wakabayashi. Approximation results on balanced connected partitions of graphs. *Electronic Notes in Discrete Mathematics*, 18:207–212, December 2004.

[102] A. Frieze and M. Jerrum. Improved approximation algorithms for max k-cut and max bisection. *Algorithmica*, 18:67–81, May 1997.